Molecular and cellular investigation of the endothelial-mesenchymal transition

Ummarino, Dario

Awarding institution:
King's College London

Molecular and Cellular Investigation of the Endothelial-Mesenchymal Transition

A thesis submitted to King's College London for the degree of Doctor of Philosophy

Dario Ummarino

July 2015

Abstract

Recent biomedical literature has proposed that the Endothelial-Mesenchymal Transition (EndMT) is a critical cellular process involved in the pathophysiology of a number of diseases, including cardiovascular conditions such as atherosclerosis and cardiac fibrosis. Classified as a subtype of Epithelial-Mesenchymal Transition (EMT) due to similarities in molecular events, EndMT is characterized by endothelial cells (ECs) turning into a different cell lineage through suppression of endothelial-specific genes and activation of mesenchymal-specific ones. Members of the Transforming Growth Factor β (TGFβ) superfamily have been shown to play a major role in the initiation of this process.

HDAC3α, an alternative splicing isoform of the mouse gene HDAC3, has been previously found to be involved in the EndMT. Through the overexpression of HDAC3α in human ECs and a pressure-overload mouse model, the present research project aimed at characterizing the molecular mechanisms underlying the function of HDAC3α in EndMT and its role in cardiac fibrosis. Results indicate that HDAC3α induces an EndMT phenotype through the upstream activation of TGFβ signalling, a mechanism that is potentially mediated by increased secretion of proteases. Furthermore, HDAC3α expression is increased in fibrotic hearts but its direct role in EndMT *in vivo* needs further investigation.

Subsequently, experiments aiming at modelling the EndMT *in vitro* in human ECs revealed that EndMT-like responses (morphological changes, altered gene/protein expression) were induced by inflammatory cytokines, with little evidence of the typical endothelial markers-DOWN/mesenchymal markers-UP molecular pattern triggered by TGFβ ligands. Further cellular and molecular data led to interpret the phenotypic changes of ECs *in vitro* as inflammatory-induced responses such as vascular leakage and angiogenic-healing, rather than a differentiation into a distinct cell type. Taken together, these results challenge the EndMT concept in adult tissues.

Declaration

I declare that the work undertaken in this thesis was conducted by myself, except where indicated.

Dario Ummarino
King's College London

Acknowledgments

First of all, I would like to thank the British Heart Foundation for providing the funding for my PhD project. The generous salary allowed me to settle in this country and live a great life outside the lab. I hope my commitment to my work has met the expectations of those people who believed in Science and spent their money on research.

I wish to thank my supervisor Lingfang Zeng for letting me open my eyes about scientific research and Prof Catherine Shanahan for supporting me during the PhD project.

I am also very grateful to Dr Claire Potter and Dr Ka Hou (Raymond) Lao for providing useful feedbacks and corrections for this thesis. Special thanks also go to Mrs Sherrie King, whose exceptional goodness and dedication to work were fundamental throughout my PhD, and to Mr Zhongy Zhang, another good soul of the lab, for the technical assistance in slicing the hearts of the poor mice.
Furthermore, I would like to thank all colleagues in the Zeng and Xu labs who helped me during my project and the TTT Sca1+ group; our laughs and our Philosophy of Academic Bullshit made the lab a better place.

Finally, I would like to thank Dr Flavia Autore and Mr Ruben (Bebbo) Ummarino for their patience, understating and encouragement during the writing of this thesis. I owe them everything.

Table of Contents

List of Figures

List of Tables

Abbreviations

Ad	adenovirus
ALK	activin receptor-like kinase
BSA	bovine serum albumin
CAF	cancer-associated fibroblasts
CAM	cell adhesion molecules
CD31	cluster of differentiation 31
cDNA	complementary DNA
DNA	deoxyribonucleic acid
DPX	di-n-butyle phthalate in xylene
ECM	extracellular matrix
EGF	epidermal growth factor
EGFR	epidermal growth factor receptor
EMT	epithelial-mesenchymal transition
EndMT	endothelial-mesenchymal transition
eNOS	endothelial nitric oxide synthase
ESAM	endothelial selective adhesion molecule
ESC	embryonic stem cell
F-actin	filamentous actin
FBS	fetal bovine serum
FSP1	fibroblast specific protein
GFP	green fluorescent protein
HAEC	human aortic endothelial cells
HCMEC	human coetaneous microvascular endothelial cells
HDAC	histone deacetylase
HDMEC	human dermal microvascular endothelial cells
HMEC	human immortalized endothelial cell
HUVEC	human umbilical vein endothelial cells
IGF	insulin-like growth factor

IL1	interleukin 1
IPF	idiopathic pulmonary fibrosis
JAG1	jagged 1
JAM	junction adhesion molecules
kDa	kilodalton
MET	mesenchymal to epithelial transition
MLCK	myosin light chain kinase
MOI	multiplicity of infection
mRNA	Messenger RNA
NO	nitric oxide
NOS	nitric oxide synthase
NuRD	nucleosome remodelling deacetylase
PBS	phosphate-buffered saline
PCR	polymerase chain reaction
PDGF	platelet-derived growth factor
PECAM	platelet endothelial cell adhesion molecule
PFA	paraformaldehyde
PGF	placental growth factor
qPCR	quantitative PCR
RIPA	radio-immunoprecipitation assay
RNA	ribonucleic acid
RT-PCR	reverse transcription polymerase chain reaction
SFM	serum free medium
siRNA	small interfering RNA
SM22	smooth muscle 22
SMA	smooth muscle actin
SMC	smooth muscle cells
TAC	transverse aortic constriction
TF	tissue factor
TGF	transforming growth factor

TJ	tight junctions
TNF	tumour necrosis factor
TSA	trichostatin A
VCAM	vascular cell adhesion molecule
VEGF	vascular endothelial growth factor
vWF	Von Willebrand factor
WB	Western blot

Chapter I - Introduction

1.1 The Endothelium

1.1.1 Evolution of the endothelium

All complex metazoans share an internal system for pumping fluids throughout the body and its general organization varies greatly across different species. This difference ranges from the open and low-pressure circulation of invertebrates to the closed, high-pressure systems of vertebrates. The key selective pressures that determine the evolution of these systems are the physico-chemical properties of oxygen diffusion into the cells and the removal of waste (1). The complex cardiovascular systems of vertebrates thus evolve in response to increasing animal size and metabolic demand. Less intuitive is why the endothelial cells (ECs) evolved. Different hypotheses have been put forward in this regard. One possibility is that an endothelial lining serves as a barrier to prevent the loss of plasma proteins, which are necessary to maintain a balance between the osmotic and the hydrostatic pressures (2). Another suggestion is that the ECs are derived from a specialized type of blood cell found in invertebrates, the *amoebocyte*. Through a process of "epithelialization", this mobile cell could have formed a proto-endothelial cell whose primary functions, consistent with this origin, would have been immunological cooperation and regulation of vascular growth (3). Nevertheless, speculations about the evolution of the endothelium are difficult to formulate because ECs have evolved a number of different functions. It is likely that multiple and concurrent explanations account for its evolutionary history. Answering these questions will provide important insight into not only the function of endothelium but also its physiological interplay with other systems and its vulnerability to disease (4).

1.1.2 Development of the endothelium

The endothelial lineage derives from mesodermal progenitors called angioblasts or hemangioblasts, since these precursors have also been shown to give rise to the hematopoietic cells (5). During early development, these progenitor cells migrate throughout the embryo to give rise the both intraembryonic vasculature and the extraembryonic endothelium of the yolk sac, which together will be part of the vitelline circulation.

In the yolk sac the angioblasts form cell aggregates called blood islands. The outer layer of these structures will subsequently differentiate into ECs while internal cells will form hematopoietic cells. On the other hand, during the intraembryonic vascular development the angioblasts follow a different differentiation pathway as they give rise to both endothelial and cardiac lineages (6). The endocardial tubes, the precursors of the heart, are indeed formed by both ECs and myocytes (see section 1.3.1).

The de-novo formation of blood vessels involves the migration and coalescence of angioblasts, a process termed vasculogenesis. In vertebrate development, the dorsal aorta and the cardinal vein are the first blood vessels to be formed (7). Following vasculogenesis, the expansion and definition of the vascular network proceed through the "angiogenesis", i.e., the growth of new blood vessels from pre-existing ones (Figure 1) (8). Angiogenesis is a multistep process that requires coordinated cellular activities by ECs such as migration, cell division, survival and lumen formation. The early events that characterise the initiation of angiogenesis have been described by the "tip-stalk" cellular model (9), which identifies two distinct EC phenotypes in a nascent angiogenic sprout (Figure 2). Tip cells are polarized and migratory cells that emerge from a quiescent endothelial monolayer and guide the formation of a new vessel branch. Increased filopodia formation and secretion of proteases allow tip cells to degrade the surrounding basement membrane and to explore the extracellular space. On the other hand, stalk cells trail behind tip cells in a nascent endothelial sprout. They proliferate in order to extend the vessel and form the vascular lumen. Importantly, the emergence of tip and stalk phenotypes is not pre-determined; ECs can in fact dynamically compete for either positions as a consequence of several genetic and environmental cues (10). Once formed, sprouts of different vessels can then fuse together (anastomosis) and will establish a continuous lumen to allow blood flow circulation. Subsequently, the nascent vasculature requires maturations steps involving the production of a basement membrane and the

recruitment of supporting mural cells (e.g. smooth muscle cells and pericytes) (11).

Several signalling pathways such as Angiopoietin-Tie and Notch have been shown to control different aspects of vascular development (12, 13). However, the most characterised master regulators of both vasculogenesis and angiogenesis are the Vascular Endothelial Growth Factors (VEGFs) (14). VEGF family includes five different members: VEGF-A, VEGF-B, VEGF-C, VEGF-D and PGF (placental growth factor). VEGFs bind to two tyrosine-kinase receptors, VEGFR-1 (flt-1) and VEGFR-2 (KDR/flk-1) and activate multiple downstream signals that regulate different behaviours of ECs during angiogenesis. The ability of VEGFs to induce diverse responses is not only due to the presence of multiple genes but also to the different isoforms generated by alternative splicing (15). The production and secretion of VEGFs, and thus the initial activation of vasculogenesis and angiogenesis, are induced by hypoxia: in low oxygen concentrations, cells of different tissues produce the Hypoxia-inducible factor (HIF), a transcription factor that induce the expression of VEGF (16). Therefore, in both development and disease, this general mechanism directs the angiogenic growth towards oxygen-deficient tissues in order to restore the appropriate blood circulation.
Further details on the molecular mechanisms of angiogenesis can be found in the following paragraphs (1.4.2 Roles of HDACs in endothelial cells).

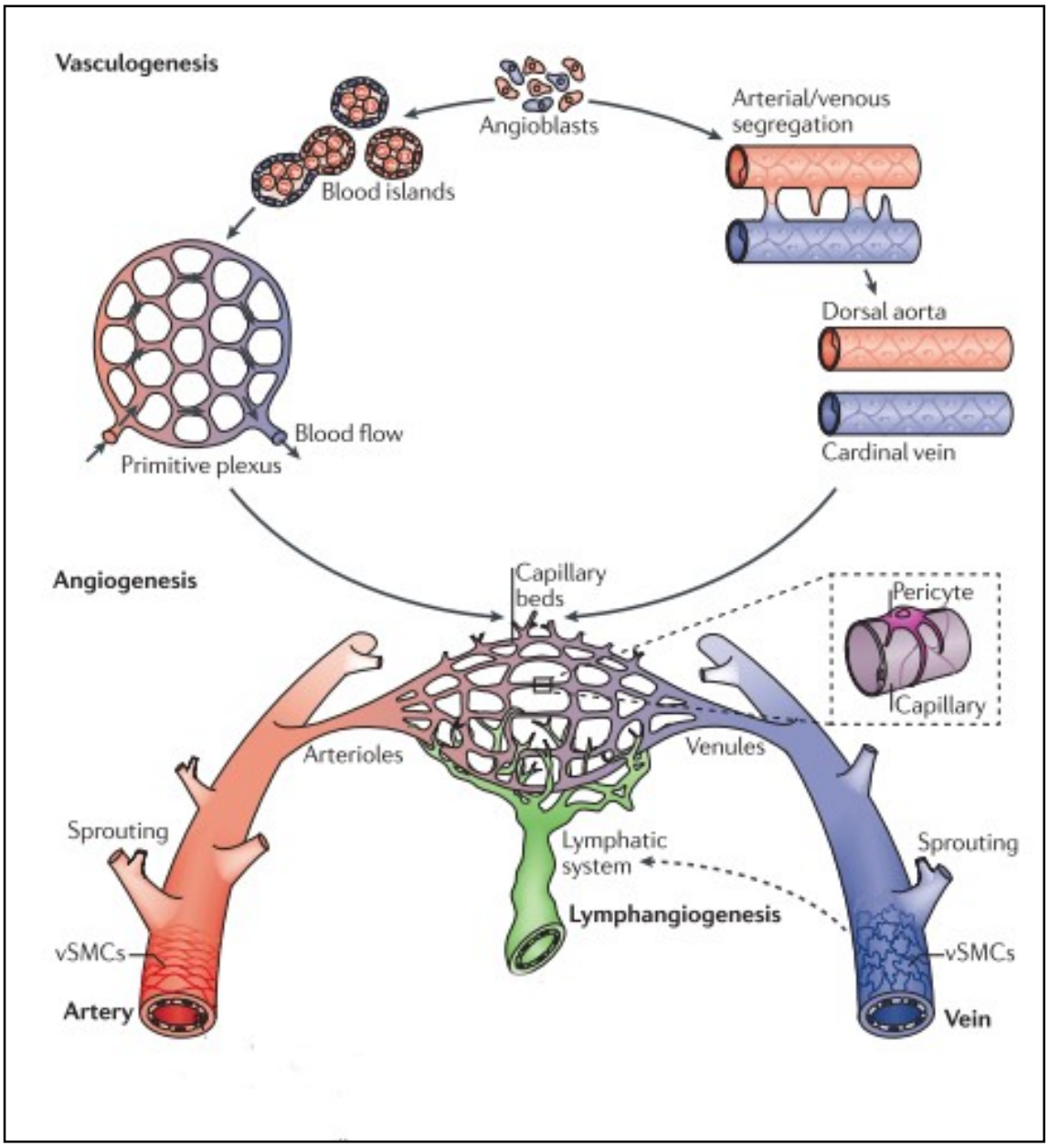

Figure 1: Vasculogenesis and angiogenesis during vascular development. The figure illustrates the sequential steps of vascular development. During vasculogenesis, angioblasts can either assemble into blood islands and a primitive plexus, or form the first intraembryonic vessels: dorsal aorta and cardinal vein. Subsequently, angiogenesis expands these primitive structures forming an intricate vessel network. The figure is adapted from Herbert et al. (8).

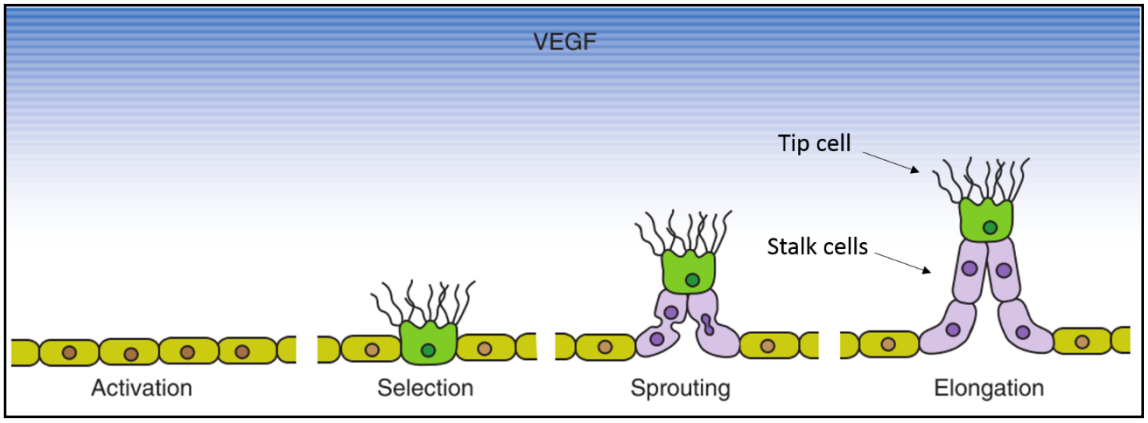

Figure 2: Tip and Stalk endothelial cells in angiogenesis. Pro-angiogenic factors such as VEGF induces the sprouting of quiescent blood vessels. Two different endothelial phenotypes will emerge during this process: the tip cell is the exploratory and migratory the guide the sprout whereas stalk cells proliferate to increase its length. The figure is adapted from Gaudens et al. (9).

1.1.3 Functions of the endothelium

There are five general types of blood vessels in the human body, according to their size: arteries, arterioles, capillaries, venules and veins. Arteries are strong and elastic vessels that carry oxygenated blood away from the heart at high pressure. The arteries branch into thinner arterioles which in turn are connected to the capillaries, the smallest type of blood vessel, where there is the exchange of gases and nutrients to the surrounding tissues. Venules link the capillaries to veins, which carry blood back to the heart. Each blood vessel type presents a different composition of cellular layers beyond the endothelium. Arteries and arterioles are characterised by multiple layers of connective and muscular tissue (e.g. fibroblasts and smooth muscle cells), which are necessary to withstand and regulate high pressured blood flow. Venules and veins are also surrounded by these cellular layers, although to a lesser extent given the much lower blood pressure in these vessels. On the other hand, capillaries are composed almost exclusively of ECs. This feature maximizes their permeability to gases and fluids.

The histological diversity of the blood vessels results in an high heterogeneity of endothelial cell structure and function (17). For instance, the endothelium can be structurally classified as continuous or discontinuous. In continuous endothelium, which characterises most of the arteries and veins as well as the capillaries of certain tissues, ECs are tightly connected and associated with a continuous layer of basement membrane. Continuous endothelium can be fenestrated or non-fenestrated. Fenestrae are circular transcellular pores of about 70nm in diameter and are mainly located in endothelia with active filtration and transport functions, such as glands and gastrointestinal mucosa. Discontinuous or sinusoidal endothelium, mainly found in organs like liver and bone marrow, lacks a basement membrane and presents larger fenestrae (18). The structural diversity of endothelium in different blood vessels reflects the multiple roles that ECs play within the cardiovascular system. These functions can be schematically grouped into i) barrier function, ii) vasodilation/blood flow regulation, iii) coagulation/haemostasis, iv) innate/adaptive immunity.

1.1.3.1 Barrier function

The endothelium has a central role in regulating tissue homeostasis. It is often described as a semi-permeable barrier, for it selectively allows certain molecules, e.g. plasma proteins, solutes, immune cells, to pass through it. The semi-permeable barrier function is actively regulated by ECs through different mechanisms. In general, two types of endothelial transport have been described: paracellular and transcellular pathways (19). The paracellular route is controlled by the junctional structures that maintain the tight cell-cell contacts in the endothelial monolayers. Examples of these intercellular junctions are adherens (AJs) and tight junctions (TJs). The AJs' main component is vascular endothelial (VE-) cadherin. VE-cadherin is a transmembrane calcium-dependent glycoprotein characterised by homophilic binding. VE-cadherin is essential for regulating the integrity of adherens junction and thus endothelial permeability. It also plays an indispensable role in the correct development of the vascular system (20). TJs are cellular structures which include adhesive proteins such as occludins, claudins and JAMs (junction adhesion molecules). TJs help regulating paracellular permeability, although their role seems to be secondary to AJs (21). In normal conditions, AJs and TJs restrict the passage of solutes larger than 3 nm in radius. Their function is nevertheless very dynamic. Different external stimuli, such as inflammatory cytokines, can in fact promptly increase endothelial permeability through biochemical regulation of intercellular junctions (22).

Transcellular pathways involve the selective transport of macromolecules (e.g. albumin, insulin and lipids) through the cell cytoplasm, a process termed transcytosis. This type of transport is characterised by energy-dependent vesicle trafficking and is receptor-mediated. Caveolae, plasma membrane invaginations 50 to 100 nm in diameter, are the main cellular structures that mediate transcytosis in ECs (23).

In conclusion, regulation of the endothelial barrier function is achieved through both transcellular and paracellular pathways. These transport mechanisms are finely regulated through structural and molecular processes and respond specifically according to the different vascular regions. A functioning endothelial barrier has a key role in homeostatic physiology but also has important implications for the development of various cardiovascular disorders.

1.1.3.2 Vasodilation/blood flow regulation

To meet the metabolic demands of different tissues, the cardiovascular system adjusts blood flow through the relaxation/constriction of smooth muscle cells that surround blood vessels. The endothelium, being in direct contact with circulating blood, is the first tissue that "senses" the physical forces generated by blood flow. This hemodynamic force acts on the endothelium as shear stress and tensile strain, which are converted by ECs into molecular signals towards the vessel wall. This phenomenon is collectively known as mechanotransduction. A multiplicity of molecular mechanisms account for this type of response and current opinion is that the entire endothelial cytoskeleton functions as a mechanotransducer rather than signalling through the actions of individual membrane receptors. Downstream of these "sensing" mechanisms, several biochemical signals are generated by the endothelium to relax blood vessels. An example of a well-established vasodilation factor is nitric oxide (NO), a signalling molecule that mediates several cellular processes in both animals and plants (24). NO is synthesized in ECs from L-arginine by the enzyme NOS3, also known as eNOS (endothelial nitric oxide synthase), which is one of the three tissue-specific NOS isoforms together with NOS1 (nNOS; neuronal) and NOS2 (iNOS; inducible, involved in immune responses). With respect to endothelium-mediated vascular relaxation, the general signalling function of NO is to bind and activate its receptor present on smooth muscle cells (SMCs), soluble guanylyl cyclase (sGC). sCG activation leads to the synthesis of cyclic guanosine monophosphate (cGMP) which in turn functions as a second messenger, activating ion channels and intracellular protein kinases. When triggered in SMCs this signalling cascade has the overall function of relaxing the sarcomere, leading to vasodilation.

1.1.3.3 Blood coagulation/haemostasis

Another illustrative example of how blood and endothelium functionally interact is haemostasis, namely the primary defence process that prevents vascular bleeding. This response has been divided into two sequential steps. Primary events include the recruitment of platelets and their aggregation, while the secondary processes comprise blood coagulation or fibrin formation (25). A pivotal ligand in primary haemostasis is Von Willebrand factor (vWF), a multimeric glycoprotein stored in endothelial-specific organelles called Weibel–Palade bodies (26). The peculiar length and domain architecture of vWF are indicative of its function. It is able to bind different proteins thus providing an adhesive bridge between platelets and the subendothelial collagen proteins that become exposed to blood flow upon vascular injury. The formation of an initial platelet plug is soon followed by blood coagulation, which characterises the secondary response (27). The coagulation cascade involves a complex series of enzymatic reactions among 13 different coagulation factors. Following endothelial damage, coagulation is first triggered by the binding between tissue factor (TF) and Factor VII, which are located in the subendothelial space and plasma, respectively. In the penultimate stage of the coagulation cascade the protease thrombin converts fibrin from fibrinogen. Fibrin is then cross-linked to the platelet plug, leading to its stabilization.

1.1.3.4 Innate/adaptive immunity

Similarly to the blood coagulation cascade, at the onset of inflammation the endothelium orchestrates a series of molecular signalling events that facilitate the recruitment and migration of immune cells towards the injured or infected tissue. From a general perspective, the response of the endothelium during inflammation has been termed "activation" and it has been schematically divided into two phases (28). Phase I activation involves rapid signalling events that do not involve *de novo* transcription of inflammatory genes. During this phase ECs mediate the increase of blood pressure, the initial attachment of leukocytes and the opening of gaps in the monolayer. Central to these processes are the ligands of G protein-coupled receptors such as histamine and the signalling pathways mediated by intracellular Ca^{2+}. Phase II activation involves the same processes as Phase I but the stimulation is predominantly provided by inflammatory cytokines, such as Tumour Necrosis Factor (TNF) and interleukin-1 (IL-1), which are mainly secreted by activated leukocytes. The signalling pathways promoted by these cytokines induce the expression of multiple genes whose function is to sustain and resolve the inflammation (28).

Throughout the inflammatory response, the interaction between the ECs and leukocytes is coordinated by several molecular mechanisms. The traditional working model consists of a sequential three-step cascade: rolling, arrest and transmigration (29). Leukocyte rolling is mediated by single-chain transmembrane glycoproteins known as selectins, a family of cell adhesion molecules (CAM). L-selectin is expressed by leukocytes while P- and E-selectin are expressed by ECs. The interaction of these proteins with their ligands is responsible for the initial capture of leukocytes by ECs. The characteristic rolling is due to the low-affinity transitory nature of these bonds. The arrest of leukocytes is largely mediated by integrins, another family of transmembrane receptors, which are present on their surface. Integrins bind to immunoglobulin proteins expressed on activated ECs, such as VCAM-1 and ICAM-1. Several chemokines (e.g. CXC and CC families) modulate the binding affinity of integrins for their ligands and are essential for triggering leukocyte arrest. The final steps of leukocyte interaction involve transmigration through the endothelial layer (diapedesis), which can be achieved by both transcellular and paracellular routes (see section 1.1.3.1). In addition to the major component proteins of adherens and tight junctions, other proteins have been shown to mediate leukocyte migration, including PECAM1 (Platelet endothelial cell adhesion molecule), JAMs and

ESAM (endothelial selective adhesion molecule) (30).

1.2 Epithelial Mesenchymal transition (EMT)

1.2.1 Epithelial and Mesenchymal dichotomy

"Epithelial" and "mesenchymal" refer to the two possible arrangements of cells in multicellular organisms. These arrangements are largely the result of the adhesive properties of individual cells. In an epithelium, cells develop complex cell-cell junctions and adhere firmly to each other (see section 1.1.3.1). As a result, epithelial cells form contiguous sheets characterised by two fundamental functional aspects: i) a barrier between "interior" and "exterior" biological compartments, ii) vectorial transport of molecules across this barrier (31). These properties emerge as a direct consequence of their membrane domain organization; besides the already mentioned cell-cell junctions, epithelial cells present an apical (the free surface facing the external space) and a basal domain (the point of contact with internal tissues) that together determine their defining characteristic: "apico-basal polarity" (32). Furthermore, this polarization involves other cellular elements such as the cytoskeleton and several cytoplasmic organelles (33).

Mesenchymal cells are characterised by a contrasting organization; they do not display a compacted and regular arrangement as they lack strong cell-cell junctions. Rather than epithelial apico-basal polarity, mesenchymal cells present a "front-back" polarity that allows them to migrate (34).

Overall, the definitions provided above describe a general organization of cells. Epithelial and mesenchymal can in fact be viewed as "cellular states" and these terms can encompass several types of differentiated cells. In light of these definitions, the ECs that cover blood vessels and the epithelial cells, rich in microvilli, that line the small intestine are both specialized types of epithelial tissues. On the other hand, fibroblasts, cells of the connective tissue that provide structural support to the surrounding tissues, are examples of specialized mesenchymal cells.

1.2.2 Interconversion of epithelial and mesenchymal phenotypes: the EMT

In embryonic development, epithelial and mesenchymal cells are not fixed cell types that differentiate into the same kind of cell. Instead, they can dynamically change from one configuration to the other. This conversion is called epithelial-mesenchymal transition (EMT) (35). During development EMT is necessary for the formation of the three embryonic germ layers. As embryonic development starts with a single epithelial sheet, the epiblast, EMT allows cells to detach and migrate away from the parental tissue and subsequently, to form new layers. The mesoderm is considered the first mesenchymal tissue, or the *primary mesenchyme*, for it maintains a relatively stable mesenchymal phenotype compared to the other two germ layers, ectoderm and endoderm (36). Subsequently, the mesoderm will differentiate into different types of tissues (e.g. bone, muscle, circulatory system) through the inverse process of mesenchymal to epithelial transition (MET). In general, several cycles of EMT and MET are responsible for the formation of different organs and tissues during embryonic morphogenesis (37). Other examples of well characterised EMTs during embryogenesis are the formation of neural crest cells and the development of endocardial cushions in the heart (see section 1.3.1).
Earlier studies into the mechanism of EMT recognized the interplay of both internal genetic programs and the environmental signals acting upon cells. One of the first molecular events found to play a central role in embryonic EMT was the modulation of E-Cadherin, the prototypic cell-cell adhesion protein whose protein family appeared early in the evolution of multicellular organisms (38, 39). Both ectopic expression and gene knockdown experiments demonstrated the role of E-Cadherin as a master gene of EMT (40).

1.2.3 EMT in cancer

The EMT attracted increasing attention from the research community when this process was first linked to diseases such as cancer and fibrosis. Elizabeth Hay, a pioneer of the field, was the first to prefigure the involvement of EMT in tumour biology. In a paper published in 1982, Greenburg and Hay demonstrated that both embryonic and adult epithelial tissues, when embedded in collagen gels, gave rise to mesenchymal cells that migrated away from the explants (41). These cells presented pseudopodia and filopodia and resembled normal mesenchymal cells *in vivo* in terms of morphology and ultrastructure. The authors noted that the EMT was induced only when explants were suspended within the gel, but not when they were placed on top of it. The authors also noted that mesenchymal cells formed in areas where the apical surface of the epithelium was in close contact with the collagen gel, thus highlighting the importance of the extracellular environment as a physical inducer of EMT. This study showed that even adult epithelial cells possess the intrinsic ability to undergo EMT and sparked interest to further understand the underlying molecular mechanisms and the possible involvement in diseases.

Later in the 80s, Jean Paul Thiery's group showed that rat bladder carcinoma cell lines changed their epithelial arrangement to acquire a fibroblastic morphology when cultured in a specific medium (42), thus suggesting a link between EMT and cancer. Increased motility and invasiveness, as well as cytoskeletal rearrangements involving the expression of the intermediate filament vimentin, were some of the most prominent features that characterised these cancer cells. The factor responsible for the induction of EMT was later identified as FGF1 (acidic fibroblast growth factor). The role of growth factor signalling in the alteration of cell morphology had been suggested a few years earlier when the first epithelial "scattering factor" was discovered (later identified as hepatocyte growth factor, HGF (43)) (44). Since then, a growing list of growth factor ligands, such as insulin-like growth factor (IGF), epidermal growth factor (EGF) and transforming growth factor beta (TGFβ) has been shown to induce EMT in several cancer cell lines (45).

Further influential insights into the mechanisms controlling the EMT in tumour progression came with studies that showed that the E-Cadherin gene could be transcriptionally downregulated in epithelial cells by the transcription factors Snail and

Twist (46-48). Snail, a zinc finger protein, and Twist, a basic-helix-loop-helix (bHLH) transcription factor, were originally identified in Drosophila as two essential genes for mesoderm formation during gastrulation (49).

1.2.4 EMT in tissue fibrosis

Another important step in the growth of EMT research was the link between EMT and fibrosis. In a series of papers published from 2002 onwards, Eric Neilson's laboratory has advanced the hypothesis that EMT is responsible for converting epithelial cells of the kidney into fibroblasts during fibrosis. Fibroblasts of the connective tissue are a heterogeneous cell population that becomes activated in tissue fibrosis and secretes large amounts of collagens. In order to characterise unique markers of fibroblasts, Neilson's lab initially isolated a gene that they called FSP1 (fibroblast-specific protein, also known as S100A4) which they showed to induce the acquisition of a fibroblastic phenotype when over-expressed in an epithelial cell line. FSP1 was also stained *in vivo* in tissue sections of mouse fibrotic kidneys (50). The occurrence of EMT *in vivo* was later confirmed in a mouse lineage-tracing model. FSP1+ fibroblasts accumulating in fibrotic kidneys were found to be derived from epithelial cells (51). This finding established the idea that EMT, in addition to development and cancer, was also a crucial process involved in chronic conditions of adult tissues, sparking much interest in this research field over the following years (52).

1.3 Endothelial-mesenchymal transition (EndMT)

1.3.1 Origin of the EndMT concept

The first evidence of ECs transforming into mesenchymal cells was provided by Markwald et al. in 1977 (53). Their study aimed to investigate the cellular composition of specific areas of the developing vertebrate heart called cardiac cushions. These structures eventually form the atrioventricular and semilunar cardiac valves. During early embryogenesis, the heart develops as a single tube composed of two layers, the myocardium and the endocardium. Cardiac cushions in this primitive tube appear as swellings between the two layers and are composed of mesenchymal cells and extracellular matrix. Using histological, cytological and ultrastructural techniques in both chick and mouse embryos, Markwald et al. set out to investigate the origin of mesenchymal cells of the cardiac cushions. Serial heart sections showed that the first mesenchymal cells were in close contact with the endothelium, then progressively migrating towards the opposite myocardial layer. These cells were characterised by elongated structures, primitive intercellular contacts and were surrounded by matrix. Besides a migratory appearance, they were also characterised by proliferation and a secretory phenotype. At the ultrastructural level, the mesenchymal cells shared similar cytoplasm organization to ECs. From these observations Markwald et al. concluded that the mesenchymal cells of the endocardial cushions were derived from the endothelium. They proposed a model in which a small number of ECs detach from the parent endothelium to give rise to "seeded" mesenchymal cells, which in turn are able to proliferate and invade the extracellular space. The molecular mechanism underlying this process was unknown, but the authors speculated that the composition of the extracellular matrix, and specifically the active secretion of proteins such as hyaluronan and collagen, could have a determining role in guiding the migration and proliferation of mesenchymal cells. Markwald et al. coined the term "epithelial mesenchymal transformation" to describe this process. The original drawing summarizing their model is reproduced in Figure 3.

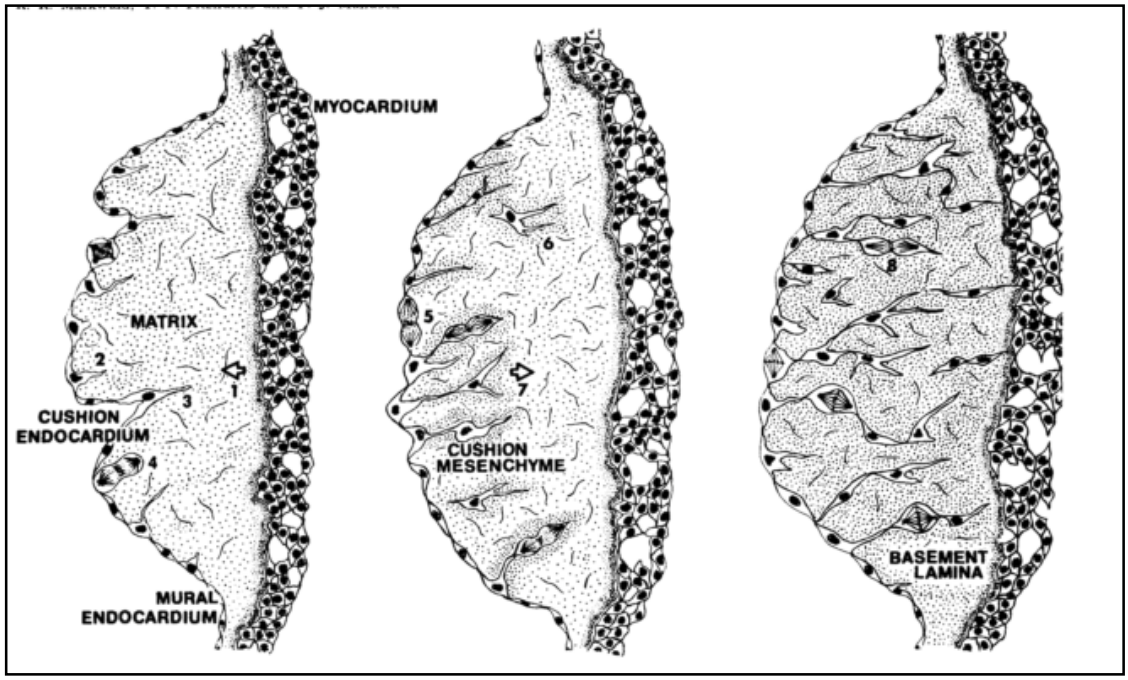

Figure 3: Original drawing of endocardial cushions development by Markwald et al. (53). The figure describes the sequential steps of ECs transforming into mesenchymal cells that populate the endocardial cushions. First, the myocardium secretes matrix components while some ECs detach from the endocardial layer and form a protrusion towards the matrix. Secondly, cells lose contact with the endothelium and acquire a mesenchymal phenotype characterised by increased proliferation, secretion and migration. Finally, the newly formed mesenchymal cells reach the myocardium and proliferate. Image reproduced from Markwald et al. (53).

1.3.2 Literature review of EndMT

1.3.2.1 EndMT literature

During the following three decades after the seminal EndMT study by Roger Markwald and co-workers in the late 70s (53), most research on this topic focused on the mechanisms underlying this developmental process. In these studies, endocardial cushion explants cultured *ex vivo* were pivotal to dissect the signalling pathways involved in EndMT (see section 1.3.2.4).

As shown in Figure 4, from 2007 onwards EndMT research has grown exponentially as this process was suggested to be involved in several pathologies. Using mouse lineage-tracing models, the laboratory of Raghu Kalluri in Harvard demonstrated the occurrence of EndMT in adult tissues during disease for the first time. In three papers, which are the most highly cited papers in the field at the time of writing, Kalluri et al. report a direct contribution of EndMT in the pathogenesis of cardiac fibrosis, kidney fibrosis and cancer (54-56), indicating EndMT as a promising therapeutic target for these conditions.

In the following subparagraphs, the relevant literature concerning EndMT will be reviewed in chronological order. Studies on cultured ECs will be first described as they provide the cellular basis used later to corroborate the experiments *in vivo*. Table 1 summarizes these *in vitro* findings, including the cell types and parameters used to assess mesenchymal transition.

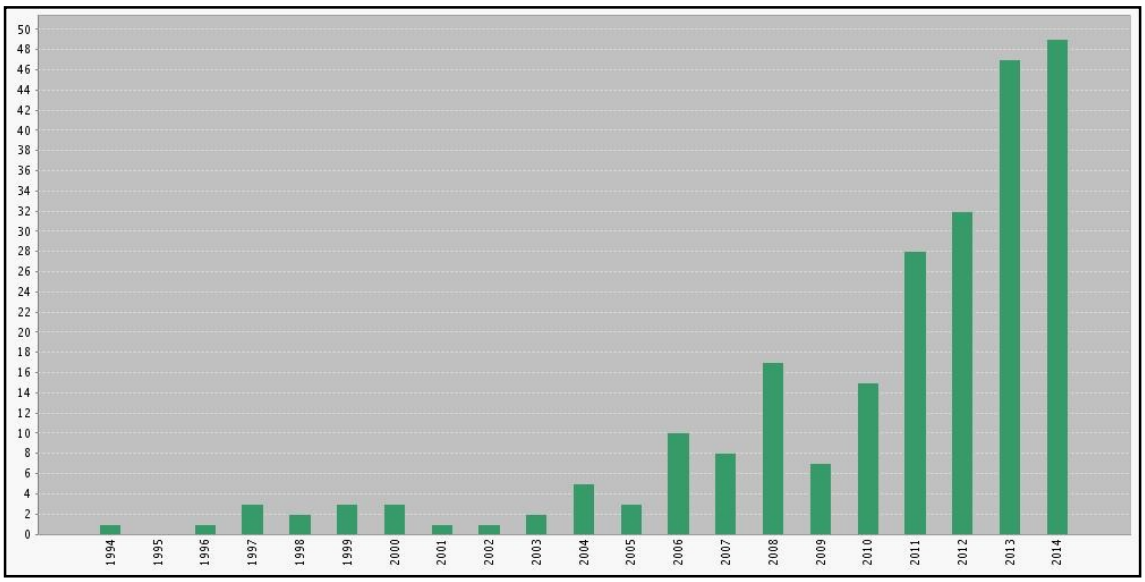

Figure 4: Research on endothelial mesenchymal transition 1994-2014. The Web Of Science database was queried with different terms related to EndMT, e.g., "[endothelial mesenchymal] transition", "transdifferentiation", "transformation", and the graph illustrating EndMT-related papers was generated by the on-line tool.

1.3.2.2 EndMT in cultured endothelial cells

Initial studies dealing with the hypothesis that ECs possess the capacity to transdifferentiate into mesenchymal cells aimed to clarify the developmental relations between ECs and smooth muscle cells (SMCs) and its implications in vascular disorders, such as atherosclerosis. The main parameter used to assess the conversion of ECs was the expression of alpha-smooth muscle actin (αSMA, HUGO gene name ACTA2), an actin isoform which had been found to be specifically expressed in vascular smooth muscle cells (57). In 1992 Arciniegas et al. reported that bovine aortic ECs express αSMA when stimulated *in vitro* with the growth factor TGFβ (58). A higher percentage of αSMA-positive cells was observed with increasing incubation time and this effect was reversible. They thus concluded that TGFβ could induce the differentiation of ECs into smooth muscle cells. Since TGFβ was known to be present in atherosclerotic lesions, the authors proposed the involvement of this cellular process in atherogenesis. In line with these findings, DeRuiter et al. (1997) analysed *in vivo* embryonic ECs of quail dorsal aorta through cell tracing techniques (59). They reported that ECs could migrate into the subendothelial space, giving rise to mesenchymal cells which lost an endothelial-specific marker and expressed αSMA. These findings added more evidence for the hypothesized interconversion between ECs and SMCs during development. Furthermore, since the study focused on fully differentiated ECs, they confirmed the hypothesis that the endothelium could potentially contribute to the disease of the vessel wall.

Subsequently, Paranya et al. (2001) showed that clonal populations of mature ECs derived from ovine aortic valves could be induced to express αSMA with or without TGFβ (60). Moreover, cells expressing αSMA also showed increased capacity to migrate towards PDGFβ. The authors therefore concluded that mature ECs could reactivate the endothelial-mesenchymal transdifferentiation program previously observed in the development of endocardial cushions. Contrary to the previous *in vitro* findings, they reported that this effect was specific to valve endothelium since ECs from other vascular sources (e.g. HDMECs (human dermal microvascular endothelial cells), HUVECs (human umbilical vein endothelial cells) or ECs derived from ovine peripheral veins) failed to express αSMA, even in the presence of TGFβ.

Further data on the mesenchymal plasticity of ECs came from Frid MG et al. (2002). Through a cell sorting FACS approach, the authors found that a small population of cells within purified bovine aortic and pulmonary endothelium presented features of

mesenchymal cells. The percentage of cells amounted to 0.01-0.03 %. The authors showed that these cells not only expressed αSMA but, over time in culture, they also stained positive for other smooth-muscle-related markers, such as Sm22, Calponin and SM-myosin. The emergence of this phenotype was dependent on TGFβ but independent of cell proliferation. The authors were among the first to suggest that this phenomena could share common mechanisms with the epithelial-mesenchymal transition (EMT). They suggested a model in which ECs give rise to mesenchymal cells via EMT and subsequently differentiate into smooth-muscle cells.

The first *in vitro* evidence that human ECs retain the ability to transdifferentiate to smooth-muscle cells was provided by Ishisaki et al. in 2003. They showed that HUVECs, when deprived of the growth factor FGF for several weeks, gave rise to enlarged cells expressing calponin and SM22. However, the expression of endothelial markers vWF and PECAM1 was not significantly changed. Furthermore, FGF-deprived HUVECs showed increased contractility in an *in vitro* assay compared to control cells. The authors also reported that activin-A signalling was involved in this phenotypic change.
Further molecular details on the induction of mesenchymal features in ECs came from the study of Noseda et al. (2004). The investigators showed that the activation of Notch signalling was necessary to induce a mesenchymal transformation. Expression of the intracellular domain of Notch in different endothelial cell types (ovine ECs, human immortalized endothelial cells (HMECs), HUVECs and human aortic endothelial cells (HAECs)) led to an increased number of cells expressing αSMA. These effects were not dependent on TGFβ and the addition of TGFβ itself was not able to induce EndMT or αSMA expression. Besides inducing αSMA, Notch expression in HMEC also down-regulated endothelial (VE-Cadherin, PECAM1, Tie1, Tie2 eNOS) and mesenchymal markers (fibronectin and PDGFR). Moreover, the authors reported that Notch-expressing HMEC cell migration towards PDGFβ was increased.

Author/Year	Summary	Phenotype analysed	Cell type	Ref.
Arciniegas E. et al. 1992	ECs differentiate into smooth muscle-like cells in the presence of TGFβ1	αSMA upregulation by IF (immunofluorescence) and WB (Western blot). FVIII downregulation by IF	Bovine Aortic ECs (BAECs)	(58)
DeRuiter M.C. et al. 1997	Embryonic ECs transdifferentiate *in vivo* into sub-endothelial mesenchymal cells	Colloidal gold EC tracing-QH1 antigen/ αSMA IHC	Quail Embryonic Aortic EC	(59)
Condorelli G. et al. 2001	ECs transdifferentiate in cardiomyocytes when co-cultured together	Co-localization of GFP (green fluorescent protein) expression (precedent retroviral infection) and αMHC/troponin I by IF	Embryonic Aortic Mouse ECs and HUVECs	(61)
Paranya G. et al. 2001	ECs undergo TGFβ-mediated transdifferentiation to a mesenchymal phenotype	Upregulation of αSMA by WB; increased migration	Ovine Aortic Valve ECs	(60)
Frid M.G. et al. 2002	ECs gives rise to smooth muscle cells via EndMT	Decreased DiI-Ac-LDL uptake by FACS;IF staining of αSMA, Sm22, SM-MHC, Calponin	Bovine Aortic ECs (BAECs)	(62)
Ishisaki A. 2003	ECs differentiate into smooth muscle-like cells upon FGF deprivation	Calponin expression by IF; calponin and SM22 mRNA upregulation by RT-PCR; increased contractility	HUVECs	(63)
Noseda M. et al. 2004	Notch activation induces endothelial-mesenchymal transformation	Cell morphology by bright-field microscopy; downregulation of VE-Cadherin, Tie1, Pecam1, eNOS and upregulation of αSMA, fibronectin, PDGFR by WB; migration	Immortalized human microvascular EC line (HMEC-1)	(64)

Liebner S. et al. 2004	β-Catenin is required for endothelial-mesenchymal transformation	αSMA staining by IF	Embryonic mouse ECs	(65)
Watanabe M. et al. 2006	TGFβ1 induce mesenchymal transdifferentiation in ECs with increased contraction reduced NO production	Upregulation of calponin, SM-MHC and αSMA by WB, actin stress fibres formation by phalloidin staining	Bovine Aortic ECs (BAECs)	(66)
Zeisberg M. et al. 2007	Human ECs gives rice to fibroblast-like cells via EndMT	Cell morphology by bright-field microscopy, VE-Cadherin, Pecam1 downregulation and FSP1(S100a4); vimentin, Col1A1 upregulation by IF; vimentin and fibronectin upregulation by ELISA	Human Coronary ECs (HCEC)	(54)
Medici D. et al. 2010	ECs gives rise to multipotent stem-like cells	Cell morphology by bright-field microscopy,; VE-cadherin, Pecam1, vWF downregulation and FSP-1, αSMA, N-cadherin upregulation by WB; FSP1 upregulation by FACS; Snail, Slug, ZEB-1, SIP-1, LEF-1 and Twist upregulation by ELISA	HUVECs and Human Coetaneous Microvascular ECs (HCMECs)	(67)

Table 1: Summary of the main publications reporting EndMT-related phenotypes in cultured endothelial cells. The studies are listed in a chronological order with information regarding the main finding, parameters used to assess EndMT and the cell type involved.

1.3.2.3 EndMT is involved in different pathologies.

The application of genetic recombination techniques in cell lineage-tracing studies offered an important opportunity to investigate the origin of different cell types in mouse disease models (68). In 2007, Zeisberg et al. put forward the hypothesis that fibroblasts accumulating in cardiac fibrosis were derived from ECs. This study followed their previous suggestion that in kidney tissue fibrosis, fibroblasts originated from the epithelium via an EMT (51) (see section 1.2.4). Zeisberg et al. used a transgenic mouse in which ECs were labelled through the Tie1 promoter, and stained mesenchymal cells for the fibroblast marker FSP1. They also used FSP1-GFP mice and Pecam1 staining as an alternative strategy. They thus determined that in fibrotic hearts the percentage of cells co-expressing mesenchymal and endothelial markers increased compared to normal hearts. They calculated that 27-35% of all fibroblasts accumulating in cardiac fibrosis were derived from ECs through an EndMT. *In vitro* experiments corroborated those findings, as human coronary ECs (HCEC) treated with TGFβ1 acquired a fibroblast-like morphology. Immunofluorescence staining of these cells showed a consistent EMT pattern: downregulation of endothelial markers (VE-Cadherin, PECAM1) and upregulation of mesenchymal proteins (FSP1, vimentin, pro-collagen I and αSMA). Overall, the study performed by Zeisberg et al. suggested for the first time that ECs could undergo an EndMT even in adult tissues, with important implications for cardiovascular disorders. Furthermore, the recapitulation *in vitro* of this phenomenon offered good opportunities to decipher the molecular mechanisms underlying the process.

Using similar *in vivo* experimental strategies, the Kalluri group further extended the relevance of EndMT to other different pathological conditions, such as kidney fibrosis and cancer. Tie2-Cre reporter mice indicated that a substantial amount of FSP1-positive fibroblasts, which accumulate in kidney fibrosis and in tumours as cancer-associated fibroblasts (CAF), originated from ECs. The authors then proposed the EndMT process as a general feature of tissue remodelling during fibrosis, including the formation of a stromal component that facilitates tumour progression.

In 2010, the Kalluri group in collaboration with Bjorn Olsen brought EndMT to a new dimension, showing that ECs could transform into multipotent stem-like cells. The authors determined that in *fibrodysplasia ossificans progressiva* (FOP), a disease in which soft tissues such as muscle or ligaments turn into bone, the ossified regions were

of an endothelial origin, thus implicating EndMT in the progression of the disease. Lineage tracing experiments with Tie2-Cre reporter mice indicated that chondrocytes and osteoblasts were in fact derived from ECs. Human ECs cultured *in vitro* retained this remarkable plasticity. In HUVECs and HCMECs both the inactivation of ALK2 (the disease-causing gene) and exogenous treatment with TGFβ2 or BMP4 induced a clear EMT pattern: endothelial markers shut down (VE-Cadherin. PECAM1, vWF) and mesenchymal genes switched on (FSP1, αSMA, N-Cadherin). Furthermore, ALK2-deficient HUVECs gave rise to mesenchymal cells which could further differentiate into chondrocytes, osteoblasts or adipocytes when cultured in specific media. These findings highlighted a remarkable and unexpected potential of EndMT; the process was now implicated not only in organ fibrosis and cancer, but also in bone fracture repair. Furthermore, the apparently easy way of turning ECs into different cell types promised valuable applications in tissue bioengineering (69).

Following the general principles and experimental designs delineated by the Kalluri group, EndMT has been subsequently implicated in other pathologies. For instance, in a mouse model of lung fibrosis induced by the drug bleomycin, which recapitulates the disease idiopathic pulmonary fibrosis (IPF), fibroblasts that were activated in the lung interstitium were reported to be derived from capillary ECs (70). Moreover, using different vein graft models, EndMT was also found to generate cells of the neointima, a tissue remodelling process underlying several cardiovascular conditions (71). These studies highlighted a causal role for TGFβ and FGF signalling in triggering the EndMT in ECs both *in vivo* and *in vitro*.

Finally, EndMT was also found to contribute to intestinal fibrosis, a condition that characterises inflammatory bowel diseases (IBD) (72). The authors reported that mesenchymal features could be induced in ECs *in vitro* by inflammatory cytokines.

1.3.2.4 Molecular mechanisms of EndMT

The first investigations into the molecular mechanisms of EndMT focused on the development of cardiac valves, a process in which endothelial transdifferentiation had been previously well characterised (see section 1.3.1). These studies used endocardial cushion explants cultured *ex vivo* as they proved to be informative tools to investigate the signalling pathways underlying the induction of EndMT (73). The general model of EndMT regulation emerging from these systems highlighted an interplay between the different tissues that form the primordial heart tube; inductive signalling factors are secreted from the myocardium and bind to specific receptors expressed by a subset of ECs, and the proteins of the extracellular matrix between the myocardium and endothelium actively participate in the progression of EndMT (74).

Mouse knockout studies subsequently complemented the initial experiments on cardiac cushion development, leading to the identification of the main EndMT factors the underlying signalling pathways: TGFβ-BMP, Wnt/β-Catenin, Notch and ErbB (75). Among these, TGFβ signalling has received particular attention given its role in developmental EndMT and, potentially, EndMT-induced fibrosis (76, 77),

TGFβ is a multifunctional cytokine that controls cell proliferation, differentiation and death depending on the cell type and cell environment. It is part of a large superfamily of factors that counts 33 members in mammals, including TGFβs, activin and inhibin, BMPs and Nodal (78). The common transduction pathway of these related factors consists of i) the binding to membrane receptors that have a cytoplasmic serine/threonine kinase domain, ii) the assembly of a receptor complex that phosphorylates proteins of the SMAD family, iii) the translocation of SMAD proteins in the nucleus where they bind DNA and regulate the transcription of target genes (Figure 5). Different combinations of receptor-Smad proteins, together with cell type-specific factors, ensure the specificity of each TGFβ -related factor (79).

Several *in vitro* and *in vivo* studies report that TGFβ ligands are the main inducers of EndMT in ECs. Among the three mammalian TGFβ isoforms (TGFβ1-3), only the knock-out of TGFβ2 abolishes the formation of heart valves in mice (80). This is consistent with an earlier study showing different temporal requirements for TGFβ2 and TGFβ3, but only TGFβ2 being necessary for the induction of EndMT in endocardial cushions (81). TGFβ2 has been shown to signal primarily through the type I receptor ALK5, which interacts with the type II TGFβ receptor and endoglin (82). Since most knockout mice for Smad

genes are embryonically lethal, little information exists regarding the intracellular mediators of EndMT *in vivo*. However, a recent study showed that the endocardial-specific deletion of Smad4 blocked EndMT resulting in acellular cardiac cushions (83).
The EMT key regulators Snail and Slug (see section 1.2.3) have also been shown to be necessary for EndMT during endocardial cushion development. A cooperation between Notch and TGFβ signalling pathways has been reported for the activation of these two transcription factors but conflicting findings are reported regarding their individual contribution (84, 85). In these studies, the function of Snail/Slug to downregulate the cell-cell junction protein VE-Cadherin, as it was previously established for E-cadherin in EMT, has been demonstrated indirectly in immortalized endothelial cell lines.
A few studies attempted to further characterise the EndMT molecular events in primary ECs culture *in vitro*. Kokudo et al. for instance used mouse ECs derived from embryonic stem cells (MESECs) and showed that Snail was responsible for TGFβ2-dependent downregulation of Claudin-5 and upregulation of mesenchymal/smooth muscle cell markers (86). Similarly, Medici et al. reported that Snail had a necessary role in the EndMT-related protein expression changes induced by TGFβ2, but its overexpression alone was not sufficient to induce the same phenotype. Furthermore, the TGFβ2 signal transduction mechanisms responsible for the activation of Snail were shown to comprise both SMAD-dependent and SMAD-independent signalling pathways (87). In SMAD-dependent pathways, the type I receptor ALK5 is involved and the signal is propagated by SMAD2 and SMAD3 (88). SMAD-independent pathways include several intracellular kinases such as extra-cellular signal-regulated kinase (ERK), c-Jun NH2-terminal kinase (JNK), and p38 MAP kinase (89). The current model of the TGFβ signal transduction pathway in EndMT is shown in Figure 5.

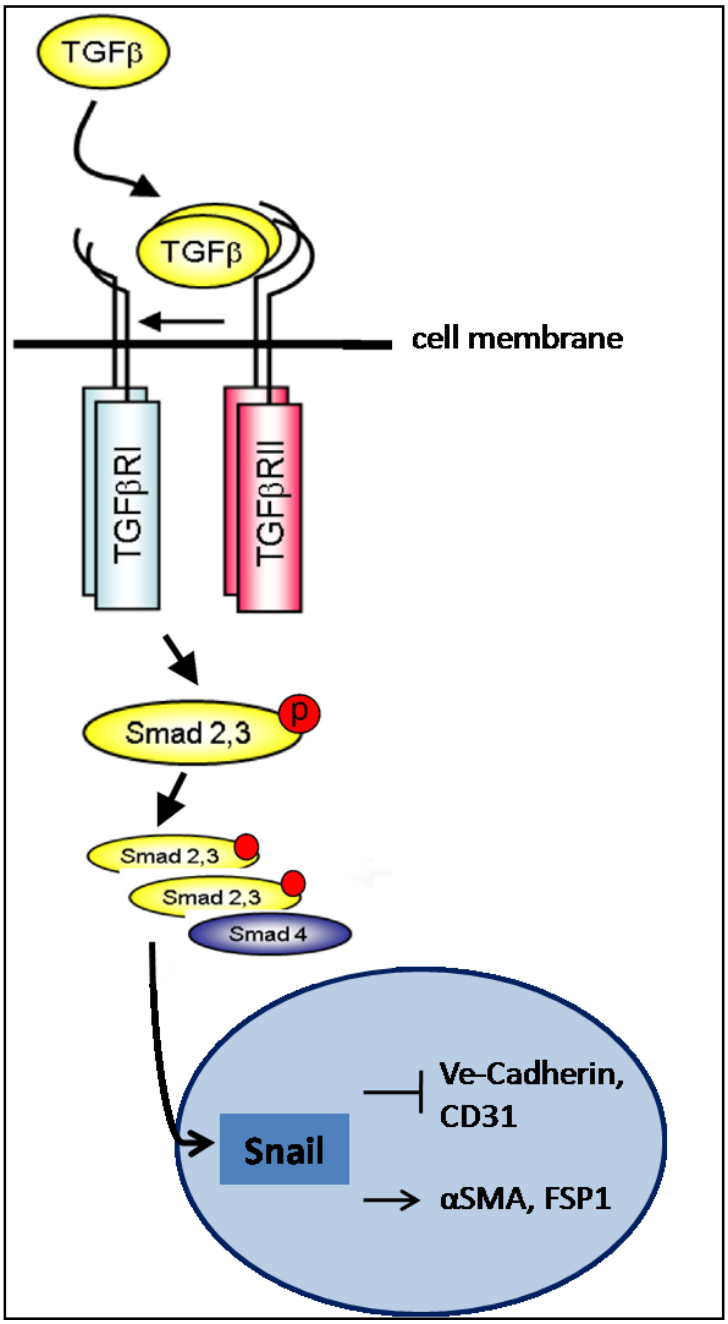

Figure 5: Currently proposed model for TGFβ signalling pathway in EndMT induction. TGFβ ligands bind to cell membrane receptors, determining the phosphorylation of Smad2 and Smad3 and their association with Smad4. The Smad complex translocates into the nucleus to activate the transcription of Snail, which in turn leads to the downregulation of endothelial markers (VE-Cadherin, CD31 (Pecam1)) and upregulation of mesenchymal markers (αSMA, FSP1).

1.4 Histone deacetylases (HDACs)

The epigenetic regulation of chromatin has long been recognized to play an important role in EMT (90). Epigenetic modifications are crucial in the signalling cascades that drive differentiation and developmental processes, since they provide a rapid and reversible way to control gene expression, without changing the DNA sequence (91). Methylation of DNA and acetylation/methylation of histone proteins are the two major forms of epigenetic regulation that ultimately alter the chromatin structure, which in turn has a profound effect on gene function.

Acetylation correlates with active gene transcription as the chromatin structure is relaxed and accessible to transcription factors and RNA polymerases. Conversely, the deacetylation of histone tails results in the compaction of chromatin which represses gene transcription, impeding the binding of the transcriptional machinery to gene promoters (92). The balance of these two counteracting mechanisms is finely regulated by two classes of enzymes, histone acetyltransferases (HATs) and histone deacetylases (HDACs).

1.4.1 HDAC protein family

The mammalian genome encodes 18 HDACs which are grouped into four classes according to their homology with yeast histone deacetylases (93). All members share a highly conserved deacetylase domain but differ in structure, subcellular localization and expression pattern, that results in different cellular functions (see Table 2). Class I members (similar to yeast Rpd3) include HDAC1, -2, -3 and -8, which are ubiquitously expressed in many human tissues and cell lines. They mainly localize to the nucleus and their lengths range from 400 to 500 amino acids. However, recent studies have revealed that both HDAC3 and HDAC8 can shuttle between the cytosol and the nucleus (94, 95). With the exception of HDAC8, whose function has been poorly characterised, Class I HDACs form large multi-subunit complexes that associate with transcription factors and other chromatin modifiers(96). In mammals, HDAC1 and -2, which display high structural similarity, can bind to each other forming the catalytic core of three different complexes: *Sin3*, nucleosome remodelling deacetylase (NuRD) and corepressor of RE1-silencing transcription factor (CoREST). HDAC3 can form two different multi-protein complexes, nuclear receptor corepressor (N-CoR) and silencing mediator of retinoic acid and thyroid hormone receptors (SMRT). Since they are mainly found in such nuclear complexes, the deacetylation of histones to repress gene transcription is the predominant function of Class I HDACs. Furthermore, their association with several different proteins indicates the complex and tight regulation of their activity, which is highly pronounced in developmental processes that require a global modulation of transcriptional programmes. With the exception of HDAC8, knockout of Class I HDACs in mice have resulted in embryonic lethality (97).

Class II HDACs are divided into two sub-classes. Class IIa members include HDAC4, -5, -7, -9, while Class IIb comprises HDAC6 and -10. Members of these two subclasses (similar to yeast Hda1) mainly differ from Class I by their tissue-specific expression pattern and their considerably lower deacetylase activity. Other differences include their length (almost double of Class I HDACs) and their cellular localization, since Class II HDACs can shuttle between the nucleus and the cytoplasm. Class IIa HDACs differ from Class IIb members by the presence of binding sites for myocyte enhancer factor-2 (MEF2) and 14-3-3 proteins on the N-terminal extension of the protein. Their nuclear-cytoplasm shuttling and the occurrence of post-translational modifications such as phosphorylation, indicates their primary role as signal transducers, coupling external stimuli to

transcriptional regulation (98). Class IIb HDAC6 is the most abundant cytoplasmic deacetylase whose main function is to deacetylate cytoskeletal proteins, while little is known about the biological function of HDAC10, which presents a leucin-rich domain at the C-terminal,. Both Class I and Class II HDACs are sensitive to the inhibitor Trichostatin A (TSA).

Class III HDACs are a group of proteins called Sirtuins (SIRT1-7). Although they possess a deacetylase domain, they diverge from classical HDACs as their enzymatic activity requires the cofactor NAD+ (Nicotinamide adenine dinucleotide). This feature suggests their involvement in metabolic functions (99).

HDAC11 is the most recently discovered and the only member of HDAC Class IV (100). It shares the properties of both Class I and Class II HDACs but very few functions have been described so far.

Table 2: Members of the HDAC protein family

Class	Name	length	location	Cellular functions
I	HDAC1	482aa	nucleus	Cell proliferation, blood cell development – forms large multiprotein nuclear repressive complexes
	HDAC2	488aa	nucleus	Functions in complex with HDAC1 to exert overlapping processes
	HDAC3	428aa	nucleus/ cytoplasm	Cell growth, apoptosis and differentiation.
	HDAC8	377aa	nucleus/ cytoplasm	Regulation of centrosome and sister chromatid cohesion in mitosis
IIa	HDAC4	1084aa	nucleus-cytoplasm shuttling	Chondrocytes differentiation and formation of neuronal synapses
	HDAC5	1122aa	nucleus-cytoplasm shuttling	Muscle cells differentiation and function
	HDAC7	855aa	nucleus-cytoplasm shuttling	Muscle cell differentiation, endothelial cell function, T lymphocytes apoptosis
	HDAC9	1011aa	nucleus-cytoplasm shuttling	Myocyte differentiation, cardiac cells growth
IIb	HDAC6	1215aa	nucleus/ cytoplasm mainly	Cell migration, autophagy
	HDAC10	669aa	nucleus/ cytoplasm	Homologous recombination
IV	HDAC11	347aa	Nucleus	Cytokines expression in T cells

1.4.2 Roles of HDACs in endothelial cells

1.4.2.1 Proliferation

Endothelial cell (EC) proliferation is the initial step in the formation of new blood vessels (angiogenesis). Quiescent ECs in an intact vessel re-enter the cell cycle, requiring the reprogramming of gene transcription profiles. Cell cycle genes are up-regulated, while cell cycle-arrest genes are shut down. As one of the major chromatin structure regulators, HDACs are undoubtedly involved in this process. So far, the direct involvement of HDACs has been documented for HDAC1 and HDAC7. Tavar-Castillo L et al. reported that HDAC1 positively regulated hypoxia-inducible factor-1 alpha (HIF-1α), leading to VEGF production and angiogenesis (101). Lee D et al. recently reported that oscillatory shear stress up-regulated HDAC1/2/3 via the PI3K/Akt (RAC-alpha serine/threonine-protein kinase) pathway, leading to the upregulation of cyclin A and downregulation of p21 (CIP1) and contributing to EC proliferation (102). These data suggest that HDAC1 may promote EC proliferation through regulation of different signal pathways.

HDAC7 is specifically expressed in ECs during embryogenesis, the disruption of which causes embryonic lethality at an early stage due to blood vessel rupture. HDAC7-null mouse embryos are characterised by enlarged but fragile blood vessels. These blood vessels have more ECs in numbers but lose cell-to-cell contact due to MMP10-mediated degradation of VE-cadherin (103). These observations indicate that HDAC7 maintains vascular integrity through preservation of EC adhesion and imply that HDAC7 may play a negative role in EC proliferation. Indeed, Wang et al. (104) reported that VEGF induced the phosphorylation of HDAC7 at three different sites via PKD kinase and the export of HDAC7 from the nuclei to release the repression of VEGF responsive genes. Margariti et al. (105) revealed that HDAC7 formed a complex with the signal transducer β-catenin, preventing its translocation to the nucleus that in turn keeps the ECs in a quiescent state. Stimulation with VEGF caused disruption of the complex and the translocation of β-catenin into the nuclei, leading to cell proliferation. Considering the opposite effects of Class I HDACs (HDAC1) and Class II HDACs (HDAC7) on EC proliferation, the balance between these two classes of HDACs may determine the EC proliferative or quiescent state.

1.4.2.2 Migration

EC migration starts with the disruption of cell-to-cell contacts, which occurs through the breakdown of adherens junction and re-arrangement and polarization of the cytoskeleton. So far, the involvement of HDACs in EC migration is only documented for Class II HDACs. As described above, disruption of HDAC7 up-regulates MMP10, leading to breakdown of VE-cadherin, which suggests that HDAC7 may play an inhibitory role in EC migration. However, Mottet et al. (106) reported that the silencing of HDAC7 through siRNA transfection inhibited EC tube formation and migration, partially due to the upregulation of platelet-derived growth factor-B (PDGF-B) and its receptor PDGFR-β, which suggests that HDAC7 may play a positive role in EC migration. In contrast to controversial reports into HDAC7 in EC migration, the roles of HDAC5, 6 and 9 seem to be concordant. HDAC5 is reported to suppress the expression of FGF2 and Slit2, which are required for sprout development (107). VEGF-induces the phosphorylation of HDAC5 by PKD (108), exports HDAC5 out of the nucleus and releases the suppression of pro-angiogenic gene expression, increasing tube formation and migration. HDAC6 is a well-established regulator of cytoskeletal dynamics (109). It has been reported that HDAC6 stimulates membrane ruffling and polarization, essential steps in cell motility, in an EB1 dependent manner (110). EB1 localizes to the growing ends of microtubules. Kaluza et al. (111) also reported that HDAC6 promotes EC migration through the deacetylation of cortactin. Inhibition of HDAC6 deacetylase activity severely impaired EC migration. Similarly to HDAC6, HDAC9 also plays a positive role in EC migration through repression of the transcription of the anti-angiogenic micro-RNA cluster miR-17-92 (112). Therefore, the balance between different members of Class II HDACs and the homeostasis between the cytoplasmic and nuclear localisation of single Class II HDACs modulate EC motility and migration.

1.4.2.3 Cell survival

The balance between apoptosis and cell survival in ECs is critical in determining the function of blood vessels (113). Apoptotic signals contribute to release of anti-angiogenic factors leading to vessel quiescence and even vessel regression, whereas the maintenance of cell survival promotes the formation of new blood vessels. The switch towards pro or anti-angiogenic signalling pathways depends on the microenvironment in which ECs reside, such as the presence of growth factors, the adhesion to extracellular matrix and mechanical forces generated by blood flow. In this aspect, Class I HDACs seem to play a major role. For instance, Zeng et al.(114) revealed that HDAC1 deacetylates the Tumour suppressor protein p53 in response to laminar flow. The activation of the HDAC1-p53 pathway arrested ECs in the G0/G1 phase, a critical cellular response that promotes vessel relaxation. Furthermore, Aurora et al.(115) showed that HDAC1 participates in an anti-angiogenic pathway driven by NF-κB. When ECs are stimulated by anti-angiogenic molecules, NF-κB increases the expression of HDAC1, which in turn decreases histone acetylation around the promoter region of the prosurvival protein cFLIP (CASP8 and FADD-like apoptosis regulator), leading to transcriptional suppression. Another key mediator of EC survival is HDAC3. HDAC3 acts as a prosurvival molecule to maintain the integrity of blood vessels through the activation of Akt1, one of the best known anti-apoptotic kinases (116). HDAC3 expression was shown to be significantly increased in vessel areas subjected to turbulent blood flow, indicating that this histone deacetylase can "sense" the physical forces acting on the vasculature and induce a protective cellular response in ECs.

1.4.2.4 Cell differentiation

Whether or not endothelial differentiation from stem/progenitor cells contributes to the formation of blood vessels is still a debated topic. Circulating endothelial progenitor cells (EPCs) in peripheral blood were found to differentiate into ECs *in vivo* and *in vitro,* providing an additional differentiation route for angiogenesis (117). However, conflicting result have been reported so far, and the identity and function of EPCs remains controversial (118). Nonetheless, the differentiation of pluripotent stem cells into ECs is an area of investigation with great therapeutic potential.

The epigenetic control of lineage-specific gene programmes has a primary role in stem cell biology (119).One of the first demonstrations of the role of HDACs in endothelial differentiation was provided through investigation into the effect of HDAC inhibitors. Impairment of deacetylase activity blocks the differentiation of adult progenitor cells into ECs and the molecular mechanism of this effect was found to be mediated through reduced expression of the homeobox transcription factor Hox-A9, which in turn regulates the expression of endothelial-specific markers such as eNOS, VEGF-R2 and VE-Cadherin (120). HDAC-dependent Hox-A9 activity was also found to be relevant *in vivo*, as it mediates the formation of EPCs and postnatal neovascularisation in ischemic tissues in mice.

Further details of the involvement of HDACs in endothelial lineage commitment were reported by Spallotta et al.(121). The investigators showed that Class II HDACs, HDAC4 and HDAC7 in particular, are specifically activated in embryonic stem cells (ESCs) exposed to nitric oxide (NO). As a result, global deacetylation of H3 histones and activation of mesoderm-specific genes were observed. NO-induced ESCs display promising therapeutic potential as they contribute to the regeneration of vascular and muscular structures in a mouse hindlimb ischemia model.

In addition to its role in EC survival, HDAC3 is reported to be involved in EC differentiation. Laminar shear stress has been demonstrated to be an important stimulus that enhances embryonic stem cell or progenitor cell differentiation to an EC lineage. During this process, Zeng et al. found that laminar flow stabilized HDAC3 protein via the VEGF receptor-PI3K–Akt pathway in a ligand independent manner, which in turn deacetylated p53 and activated p21, contributing to EC differentiation. A similar mechanism has been identified in VEGF-induced EC differentiation (122).

1.4.2.5 Mural cell recruitment

The final stages of the vasculature formation require the recruitment of mural cells (pericytes and smooth muscles cells (SMCs)) and the generation of the extracellular matrix (ECM). This maturation process confers structural and functional support to the newly formed blood vessels (11). SMCs, pericytes and ECM components may furthermore represent an important but largely unexplored source of molecular signals that regulate ECs under physiological and pathological conditions. The contribution of HDACs to the differentiation and function of SMCs provides insights into the molecular characterization of the current anti-angiogenic therapies. The presence of transcription factor MEF2 binding sites at the N-terminal of Class II HDACs (HDAC4-5-7-9) initially pointed to their crucial role in myogenesis during embryonic development (123). Further study uncovered a more complex situation in which HDACs can also regulate smooth muscle differentiation (124). HDAC5 was found to participate in the dual function of the transcription factor Myocardin, which induces the activation of the smooth muscle gene programme, and represses the transcription of skeletal muscle genes (125).

The role of HDACs is not confined to development but it is also related to the function of differentiated SMCs. Waltregny et al. (126) showed that HDAC8 is associated with the cytoskeleton of SMCs and could regulate their contractility. In another report, van der Veer et al. (127) demonstrated that NAD+ dependent deacetylase activity is necessary to induce phenotypic change to a contractile state, thus suggesting the involvement of sirtuins in blood vessel maturation.

Recently, the role of HDACs in mural cells in the context of angiogenesis has been addressed directly in human pericytes. Karen et al. (128) showed that different HDAC inhibitors impair pericyte migration, proliferation, and their differentiation towards collagen I-producing fibroblasts, indicating that HDACs keep the pericytes in a proangiogenic phenotype. This effect is accompanied by the expression of different angiogenic genes involved in the stabilization and maturation of the remodelling vessels. As noted by the investigators, these results may therefore offer additional ways to explain at cellular level how HDAC inhibitors effectively reduce Tumour angiogenesis *in vivo*. A summary of the roles of HDACs in ECs is provided in Table 3.

Table 3: Summary of the different roles of HDACs in endothelial cells

Name	Functions	Molecular target/partners	Reference
HDAC1	Cell cycle arrest, inhibition of prosurvival molecules	p53, NF-κB	(114), (115)
HDAC3	Cell survival, EC differentiation under shear stress	Akt1, p53-p21	(116), (122)
HDAC4	Hypoxia gene programme	HIF-1alpha	(129, 130)
HDAC5	Cell migration, SMCs differentiation	FGF2-Slit2 (ECs), Myocardin(SMCs)	(125), (107)
HDAC6	Cell migration, cell motility, Hypoxia gene programme	EB1, cortactin, HIF-1alpha	(110), (111)
HDAC7	Cell growth, cell proliferation, cell migration	MMP10, Beta-catenin	(103), (104), (105)
HDAC8	SMCs contractility	alpha-SMA	(126)
HDAC9	Not determined	miR-17-92	(112)

1.5 Project Background

The present PhD research project is based on previous findings of the host laboratory regarding the functional characterization of new HDAC3 isoforms. Below are summarised the most relevant results that frame the background of this thesis.

1.5.1 HDAC3 gene gives rise to multiple splicing variants

HDAC3 has been found to undergo extensive RNA processing during stem cell differentiation and mouse embryonic development. As shown in Figure 6 A, the RT-PCR on total RNA from mouse embryos and new born mice, revealed multiple transcripts of different sizes. These transcripts were isolated and sequenced, leading to the identification of four isoforms named HDAC3α, β, γ and δ. The exon-intron structure of these isoforms is illustrated in Figure 6 B. Compared to the full-length cDNA of HDAC3, an extensive sequence rearrangement occurs: intron 12 is kept as an additional exon in HDAC3α, β and δ, while in all isoforms several exons in the 5' region are spliced out. A recombination-like event seems to occur between exons 3 and 9 in HDAC3α and between exons 3 and 10 in HDAC3β.

To verify that these sequences were correctly translated into proteins, cDNAs corresponding to the four isoforms were cloned in flag-tag expression vectors, which were in turn transfected in 293 cells. As shown in Figure 6 C, Western blot with anti-flag antibodies revealed protein bands whose sizes corresponded to the ones predicted from cDNA sequences. To determine whether the protein expression of the splicing variants occurred in a physiologic cellular context, the GFP coding sequence was inserted in the intron 12 within the open reading frame of HDAC3α and β in a mouse embryonic stem cell (ESC) line. As shown in Figure 6 D, when ESCs were induced to differentiate, some cells expressed GFP. Thus, these results demonstrate that at least two splicing variants, HDAC3α and β, are physiologically translated into proteins *in vitro*.

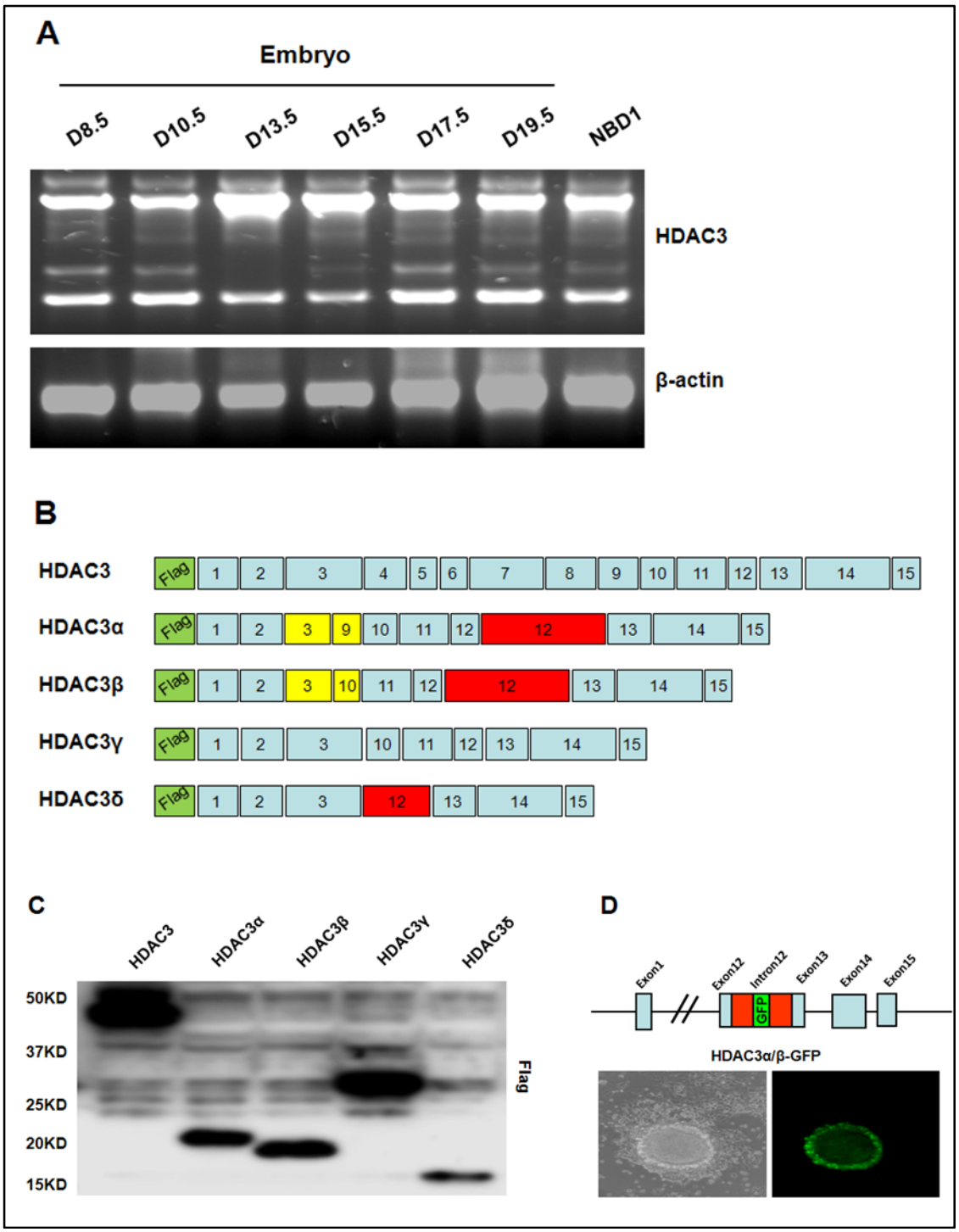

Figure 6: Characterization of HDAC3 splicing variants. A) RT-PCR analysis of HDAC3 mRNA expression performed on RNA samples extracted from mouse embryos at different stages and from newborn mice. β-actin expression represents the internal control. B) Schematic illustration of the exon-intron structure of the four HDAC3 isoforms. C) The expression of individual isoforms were analysed in 293 cells by Western blot with antibodies against Flag-tag. D) Schematic representation of GFP inserted into HDAC3 intron 12 within the open reading frame of HDACα and β isoforms (upper panel). Bottom panel: GFP expression in HDAC3 α/β-GFP transgenic mouse embryonic stem cell line.

1.5.2 HDAC3α overexpression induces the endothelial-mesenchymal transition in HAECs

The function of HDAC3α was investigated in primary ECs through an adenoviral-mediated gene overexpression system. HAECs were infected with Ad-HDAC3α or Ad-null viruses in the presence of serum-free medium. 72 hours after infection, ECs lost the characteristic round shape and acquired an elongated fibroblast-like morphology (Figure 7 A). An immunofluorescence staining was then performed to check whether this morphological change was accompanied by altered expression of EndMT markers. Cells treated with Ad-Null virus expressed high level of the endothelial-specific junction protein VE-Cadherin (Figure 7 A, bottom panels), while in the presence of Ad-HDAC3α its expression was significantly reduced. Furthermore, HDAC3α-overexpressing cells showed positive expression of the mesenchymal marker αSMA around the nucleus, which is absent in Ad-null control cells.

The induction of EndMT-associated markers was subsequently analysed through Western blot in HAECs infected with different concentrations of Ad-HDAC3α viruses (Figure 7 B). HDAC3α downregulated the endothelial marker Pecam1 and induced the expression of mesenchymal proteins N-Cadherin, αSMA and Snail2 in a dose-dependent manner.

Taken together, these results indicate that HDAC3α overexpression induces morphological and biochemical changes consistent with the endothelial-mesenchymal transition and this splicing isoform may thus play an active role in this process.

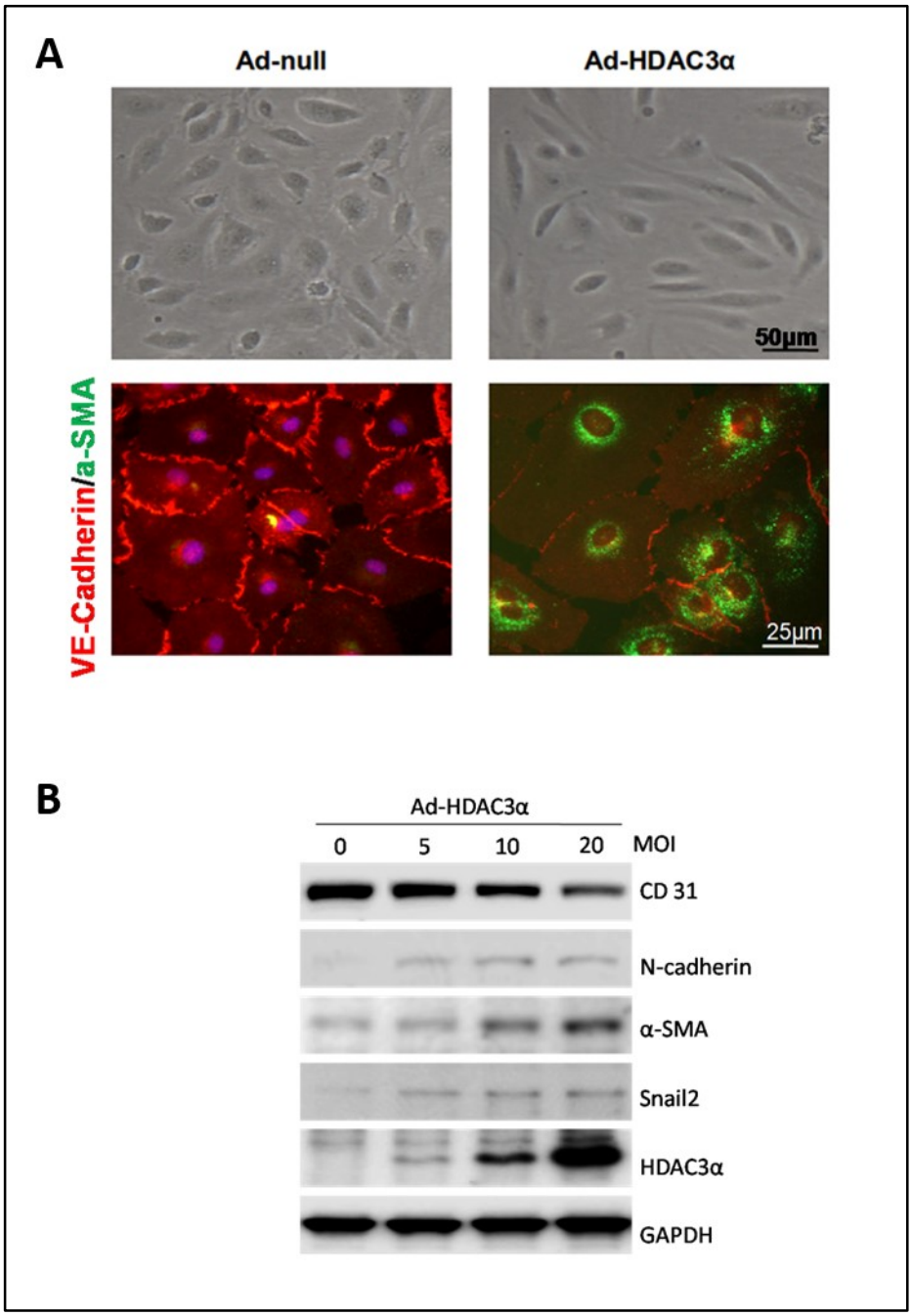

Figure 7: HDAC3α overexpression induces EndMT in HAECs. Upper panel: HAECs infected with Ad-Null or Ad-HDAC3α viruses in the presence of serum-free medium. Bright field images were taken 72 hours post infection (top panels). Immunofluorescence staining performed with antibody against VE-Cadherin and αSMA (bottom panels). Bottom panel: Western blot analysis of EndMT-related markers in HAECs infected with different concentrations of Ad-HDAC3α

Chapter II – Materials and Methods

2.1 *In vivo* methods

2.1.1 Minimal invasive transverse aortic constriction (TAC) in mice

Surgical TAC procedures were performed by Dr. Xuebin Dong (Department of Cardiology, King's College London) as described elsewhere (131). Male C57/BL6 mice weighing 20–30 g were used in the experiments. Echocardiography was performed on the day of harvesting to validate myocardial hypertrophy. After collection, hearts were quickly frozen in liquid nitrogen or immersed in 4% paraformaldehyde for subsequent experiments.

2.1.2 Protein extraction from heart tissue

Frozen heart tissues were placed in Matrix D tubes (MP Biomedicals) in the presence of 400 µl of lysis buffer. Tissues were mechanically disrupted using the FastPrep machine. Tissue lysates were then transferred in 1.5 ml sterile eppendorf tubes, sonicated with the Branson Sonifier 150 at the lowest setting for 10seconds at 4ºC and incubated for a further 30minutes on ice. The lysates were then centrifuged at 16000xg for 15minutes at 4ºC. The supernatants were transferred into new micro-centrifuge tubes and protein levels were measured using the Biorad Protein Assay on the Biorad Spectrophotometer 3000.

2.1.3 RNA extraction from heart tissue

Frozen heart tissue was placed in Matrix D tubes (MP Biomedicals) in the presence of 500µl of RNA lysis buffer from miRVANA kit (Ambion). Tissues were mechanically disrupted using the FastPrep machine. RNA from tissue lysates was extracted with acid-phenol:chloroform method following the miRVANA kit protocol. RNA was eluted in 25µl of DEPC (diethyl dicarbonate)-treated water and the concentration was measured using a NanoDrop1000 spectophotometer (ThermoScientific).

2.1.4 Picrosirius red staining of heart paraffin sections

Paraffin heart sections (10μm) were de-waxed in xylene and ethanol and rinsed in water. Sections were then immersed in 0.2% phosphomolybdic acid (Fluka), rinsed in water and immersed in 0.1% Picrosirius Red (Direct Red 80, Fluka) for 2 hours. After 2 washes in acidified water, sections were dehydrated with increasing concentration of ethanol, cleared in xylene and finally mounted with DPX (Di-N-Butyle Phthalate in Xylene) mounting medium (Sigma).

2.1.5 Immunofluorescence staining of heart frozen sections

10μm heart sections were prepared from frozen mouse hearts with the cryostat and stored at -20°C. Before immunostaining, sections were dried at RT for 30 minutes and then fixed in methanol for 15 minutes. After one wash in PBS (Phosphate-Buffered Saline) for 5 minutes, sections were permeabilized with 0.1% Triton X-100 in PBS at RT for 15 minutes and washed three times with PBS for 5 minutes. Blocking solution of secondary antibody normal host serum diluted 1:20 in PBS was then applied for 1 hour at RT. Sections were then incubated with primary antibody (anti-HDAC3α 1:50 in blocking solution, anti-CD31 (BD bioscience) 1:100 in blocking solution) at RT for 1 hour or at 4°C overnight. After washing three times with PBS, secondary antibodies (Alexa Fluor - Invitrogen) were diluted 1:1000 in blocking solution and applied to the sections for 45 minutes. Samples were then counterstained with DAPI (4',6-Diamidino-2-Phenylindole, Dihydrochloride) at RT for 5 minutes, washed three times with PBS and mounted with Fluorescent mounting medium (Dako).

2.2 Cell culture

2.2.1 Cell culture of human aortic endothelial cells

Postnatal HAECs were purchased from Sigma and cultured on gelatin-coated flasks (0.4mg/ml) in M199 medium supplemented with 1ng/ml β-endothelial cell growth factor, 3μg/ml Endothelial Cell Growth Supplement from bovine neural tissue, 10u/ml heparin, 1.25μg/ml thymidine, 10% foetal bovine serum, 100u/ml penicillin and streptomycin in a humidified incubator supplemented with 5% CO_2. Cells were passaged every three days at a ratio of 1:3. Cells were used up to passage 8. Cell supplements and culture medium were purchased from Sigma and Gibco, respectively.

2.2.2 Cell culture of HUVECs

Pooled HUVECs were purchased from Lonza and used between passage 3 and 8. HUVECs were routinely cultured on gelatin-coated flasks in EGM2 medium with Bullet Kit (2% FBS + different growth factors) in a humidified incubator supplemented with 5% CO_2. 2% stock solution of gelatin was purchased from Sigma and diluted to 0.2% for coating. Cells were split every 2/3 days and the medium changed every other day**.**

2.2.3 Cell culture of Adventitia Progenitor Cells (APCs)

APCs were provided by the laboratory of Professor Qingbo Xu (132). APCs were cultured on 2% gelatin-coated flasks in complete stem cell medium (American Type Culture Collection, Rockville, Massachusetts, USA) containing 10% FBS, leukemia inhibitory factor (10 ng/ml), 0.1mM 2-mercaptoethanol, penicillin (100 U/ml) and streptomycin (100 mg/ml)

2.2.4 Cytokines and Growth Factors

Human Recombinant TGFβ2, TNF and IL1β were purchased from Prepotech and diluted in milli-Q water following the manufacturer's instructions. All factors were used at a final concentration of 10 ng/ml.

2.2.5 Cell freezing

For long-term storage, cells were resuspended with the following solution: 50% cell culture medium, 40% FBS, 10% DMSO. After resuspension, cell solutions were transferred into 2.0 ml cryovials (Corning), put immediately on ice and stored in liquid nitrogen.

2.2.6 Chemical inhibitors

Chemical inhibitors used in cell culture experiments are listed in Table 4below:

Table 4: Chemical inhibitors used in cell culture experiments

Inhibitor	Company	Target	Concentration
LY294002	Sigma	PI3K/Akt	10μM
PD98059	Sigma	MAP kinase	10μM
SB202190	Sigma	p38	10μM
SP60005	Sigma	JNK	10μM
Y27632	Sigma	ROCK1	5 μM
ML-7	Sigma	MLCK	10μM
Cycloheximide	Sigma	60S ribosome subunit	10 μg/ml
Actinomycin-D	Sigma	GpC sites of DNA	1 μg/ml
C3 Transferase	Cytoskeleton, Inc.	RhoA, B, C	1 μg/ml
IKK Inhibitor II	Merck Millipore	IKK (inhibitor of nuclear factor kappa-B kinase)	10 μM

2.2.7 Other cell culture reagents

Calcium and magnesium-free PBS was purchased from Sigma or Gibco and supplemented with penicillin-streptomycin (LifeTechnologies). Cell splitting was performed using Trypsin-EDTA (phenol red) purchased from LifeTechnologies.

2.3 Gene expression analysis

2.3.1 RNA Extraction from cells

RNA extraction was performed using the RNeasy Mini Kit following the manufacturer's protocol. Reactions were carried out at room temperature with a centrifugal force of 10,000xg. To elute the RNA, RNeasy columns were transferred into clean 1.5 ml microcentrifuge collection tubes and 30 µl of RNase-free water was added to the RNeasy column membrane, followed by 1 minute spinning. The RNA concentration was measured using a NanoDrop1000 spectophotometer (ThermoScientific).

2.3.2 Reverse transcription of RNA

Reverse transcription was performed using the Improm-II Reverse transcription system (Promega) in a 20µl reaction as outlined in Table 5 below. Mix A was added to 1.0µg/10µl RNA and heated at 70°C for 5 minutes then chilled on ice to allow denaturation of RNA. Mix B was then added and the following programme was carried out: 22°C for 5 minutes; 42°C for 1hour 30minutes; 70°C for 15minutes. cDNAs were then diluted in 80µl of DEPC-treated water to obtain a final concentration of 10ng/µl.

Table 5: Reagents and concentrations for RNA retrotranscription

Component	Volume (µl)	Final Concentration
Mix A Improm II 5X reaction buffer Random Primer 25mM MgCl2 25mM dNTP DEPC treated water	 4 0.1 2.4 0.4 to 7µl	 1x 0.5µg 3mM 0.5mM
Mix B 2500u Rnasin ribonuclease inhibitor Improm II RT DEPC treated water Total	 0.5 1 1.5 3µl	 20u 1u

2.3.3 Quantitative real time polymerase chain reaction (qPCR)

Relative gene expression was analysed by qPCR using the Eppendorf Mastercycler® ep realplex. For each sample, 15ng of cDNA was combined with 10µl of SYBR Green (Qiagen, Cat. No. 204057) and 0.75µM of forward + reverse primer mix for the target gene. The final volume was adjusted to 20µl with DEPC water and the samples were loaded on 96 well plates (Eppendorf twintec real-time PCR plates). The qPCR conditions were as follows: 5min at 95ºC; 95ºC for 15 seconds and 60ºC for 30 seconds for 40 cycles; 10 minutes of 95ºC. For each sample, the qPCR reaction was performed in duplicate Threshold cycle (Ct) values of individual genes were then normalised against endogenous housekeeping genes (18s, GAPDH (Glyceraldehyde 3-phosphate dehydrogenase) or RPL13A). Gene expression levels were calculated using the ΔΔCt method. The primers used for qPCR were designed using the on-line tool PrimerBLAST of NCBI (http://www.ncbi.nlm.nih.gov/tools/primer-blast/) setting the following criteria: PCR product length of 120-180 bp, primer size 18-22, GC content of 40-60%. Other parameters were set automatically by the software. Alternatively, some primers were selected consulting the on-line database PrimerBank

(http://pga.mgh.harvard.edu/primerbank/). The complete lists of mouse and human primer's sequences are shown in Table 6 and Table 7, respectively.

Table 6: List of mouse primers used for qPCR analysis

Primer	Sequence (5'->3')
VE-Cadherin Forward	AGAAGAAACCGCTGATCGGC
VE-Cadherin Reverse	CACTGGTCTTGCGGATGGAG
eNOS Forward	ACCCTCCGCCATCCACAGAACC
eNOS Reverse	ACATGGGGGTAGCCGGGGGT
αSMA Forward	AGTGGAGAAGCCCAGCCAGTCG
αSMA Reverse	CCATTGTCGCACACCAGGGC
FSP1 Forward (S100A4)	AGACCCTTGGAGGAGGCCCTG
FSP1 Reverse (S100A4)	GGAAGCTAGGCAGCTCCCTGGT
Collagen I alpha I Forward	TGATGG CCAACCTGGTGCGA
Collagen I alpha I Reverse	ACCAACGTTACCAATGGGGCCG
HDAC3α Forward	AGCATTCGAGGACATGGGGAAT
HDAC3α Reverse	TGGCATCATGAAGTGGATCTTACC
GAPDH Forward	ACGGCCGCATCTTCTTGTGC
GAPDH Reverse	CGGCCAAATCCGTTCACACCGA

Table 7: List of human primers used for qPCR analysis

Primer	Sequence (5'->3')
TGFβ 1 Forward	ACCCTCCGCCATCCACAGAACC
TGFβ 1 Reverse	ACGGCCGCATCTTCTTGTGC
TGFβ 2 Forward	AGACCCTTGGAGGAGGCCCTG
TGFβ 2 Reverse	TGGCATCATGAAGTGGATCTTACC
TGFβ 3 Forward	CATCATAGAACTCATTGGGTG
TGFβ 3 Reverse	ATTGTCGCACACCAGGGCTG
ADAMTS1 Forward	GGTGACTGGACACAAATCGC
ADAMTS1 Reverse	AAAGCGGAGACCGAAGACGA
18s Forward	GGTGACTGGACACAAATCGC
18s Reverse	ATACATGCCGACGGGCGCTG
HDAC3 Forward	CATCTCTGCTGGTAGAAGAGG
HDAC3 Reverse	CATCATAGAACTCATTGGGTG
PECAM1 Forward	GACATGGCAACAAGGCTGTG
PECAM1 Reverse	AGATTCCAGTTCGGGCTTGG
VE-Cadherin Forward	TTGGAACCAGATGCACATTGAT
VE-Cadherin Reverse	TCTTGCGACTCACGCTTGAC
eNOS Forward	TGATGGCGAAGCGAGTGAAG
eNOS Reverse	ACTCATCCATACACAGGACCC
S100A4 (FSP1) Forward	TCTTGGTTTGATCCTGACTGCT
S100A4 (FSP1) Reverse	ACTTGTCACCCTCTTTGCCC
N-Cadherin Forward	TCAGGCGTCTGTAGAGGCTT
N-Cadherin Reverse	ATGCACATCCTTCGATAAGACTG
ACTA2 (αSMA) Forward	TGGCTGGCCGAGATCTCACT
ACTA2 (αSMA) Reverse	TGCGGCAGTGGCCATCTCAT
TAGLN (SM22) Forward	CCGTGGAGATCCCAACTGG
TAGLN (SM22) Reverse	CCATCTGAAGGCCAATGACAT
PDGFβ Forward	CTCGATCCGCTCCTTTGATGA
PDGFβ Reverse	CGTTGGTGCGGTCTATGAG
RND1 Forward	GATGTAAGCTCGTTCTGGTCG
RND1 Reverse	AGCAATCCTTCGCTAACACTTG
DLL4 Forward	GTCTCCACGCCGGTATTGG
DLL4 Reverse	CAGGTGAAATTGAAGGGCAGT
JAG1 Forward	GTCCATGCAGAACGTGAACG
JAG1 Reverse	GCGGGACTGATACTCCTTGA
Hey1 Forward	GTTCGGCTCTAGGTTCCATGT
Hey1 Reverse	CGTCGGCGCTTCTCAATTATTC
COL1A1 F	TAACCCCCTCCCCAGCCACAAA
COLA1 R	TGGTGGGATGTCTTCGTCTTGGC
COL1A2 Forward	GAGCGGTAACAAGGGTGAGC
COL1A2 REV	CTTCCCCATTAGGGCCTCTC
Tenascin-C Forward	TCCCAGTGTTCGGTGGATCT

Tenascin-C Reverse	TTGATGCGATGTGTGAAGACA
Elastin Forward	GCAGGAGTTAAGCCCAAGG
Elastin Reverse	TGTAGGGCAGTCCATAGCCA
COL22A1 Forward	TCCGACTTCAATGCCATCGAC
COL22A1 Reverse	TACACGAACGCTAGGACAGAG
COL16A1 Forward	CCACCAGAAGACGTGGTATCT
COL16A1 Reverse	CAGGACACAAAGTCGCCATC
COL3A1 Forward	GGAGCTGGCTACTTCTCGC
COL3A1 Reverse	GGGAACATCCTCCTTCAACAG
COL4A3	GGATTGCCAGGATTTTCTGGT
COL4A3	TGGTACACCGACAAGTCCGTA
MMP1 Forward	AAAATTACACGCCAGATTTGCC
MMP1 Reverse	GGTGTGACATTACTCCAGAGTTG
LOX (Lysyl oxidase) Forward	GCCGACCAAGATATTCCTGGG
LOX Reverse	GCAGGTCATAGTGGCTAAACTC
RPL13A Forward	CATAGGAAGCTGGGAGCAAG
RPL13A Reverse	GCCCTCCAATCAGTCTTCTG

2.4 Protein expression analysis

2.4.1 Protein collection

Cell pellets were resuspended in 50µl RIPA (Radio-Immunoprecipitation Assay) buffer (Sigma) and incubated on ice for 15 minutes. The lysates were then sonicated with the Branson Sonifier 150 at the lowest setting for 10 seconds at 4ºC and kept 30 minutes on ice. Lysates were then centrifuged at 16000xg for 15 minutes at 4ºC. The supernatants were transferred to new micro-centrifuge tubes and protein concentrations were measured using the Biorad Protein Assay on the Biorad Spectrophotometer 3000.

2.4.2 Western blot

50µg of total protein were loaded in SDS buffer and boiled for 5 minutes before loading onto a NuPage, 4-12% gel (Invitrogen). The samples were run at 160V for about 80 minutes in an XCell SureLock® Mini-Cell system from Invitrogen and transferred to a PVDF membrane (Amersham, hybond-P) at 25V for 1hour and 30minutes using an XCell II™ Blot Module (Invitrogen). Membranes were then blocked with 5% milk in PBS-Tween 0.1% (PBS-T). The antibodies against HDAC3α and β were developed by Genescript in rabbit with peptide PQGDTILTSPQNDL and diluted 1:100 in 5% milk PBS-T. The complete list of antibodies used and relative concentrations is shown in Table 8). Membranes were incubated with primary antibodies on a rotator either overnight at 4ºC or at room temperature for minimum 2 hours minimum. Secondary HRP-conjugated antibodies (Dako) were diluted in 5% milk PBS-T (1:3000) and incubated for 45 minutes. Membranes were then treated with ECL detection reagents (Amersham) and exposed on films (Amersham, Kodak) using the Compact X4 instrument (Xograph Imaging System). Alternatively, membranes were incubated with dye-conjugated IRDye® secondary antibodies (LI-COR) diluted 1:15000 in 5% milk/PBS-T. Blots were then scanned using the Odyssey® CLx instrument and digital images were obtained using the Image Studio™ software (LI-COR).

Table 8: Primary antibodies used in Western Blot analyses

Antibody	Company - code	Concentration
Rabbit anti-GAPDH	Sigma (SAB4300645)	1:1000 in 5% milk PBS-T
Rabbitanti-HDAC3α	Custom made (Genescript)	1:100 in 5% milk PBS-T
Rabbit anti-HDAC3	Sigma (H3034)	1:100 in 5% milk PBS-T
Mouse anti-αSMA	Sigma (A5228)	1:100 in 5% milk PBS-T
Mouse anti-FLAG	Sigma (F3165)	1:100 in 5% milk PBS-T
Rabbit anti-pSmad2	Sigma (SAB4300251)	1:100 in TBS-T
Rabbit anti-TGFβ1	Abcam (ab9758)	1:100 in 5% milk PBS-T
Goat anti-TGFβ2	Abcam (ab10850)	1:100 in 5% milk PBS-T
Rabbit anti-Collagen IV	Abcam (ab19808)	1:100 in 5% milk PBS-T
Rabbit anti-VE-Cadherin	Abcam (ab33168)	1:100 in 5% milk PBS-T
Rabbit anti-IκBα	Cell Signaling (4812)	1:1000 in 5% milk TBS-T
Rabbit anti-pSmad2 (Ser 465/467)	Cell Signaling (3108)	1:1000 in 5% BSA TBS-T
Mouse anti-Smad2	Cell Signaling (3103)	1:1000 in 5% milk TBS-T
Rabbit anti-pCofilin (Ser3)	Cell Signaling (3311)	1:1000 in 5% milk TBS-T
Rabbit anti-Cofilin	Cell Signaling (3318)	1:1000 in 5% milk TBS-T
Mouse anti-NOS3 (eNOS)	Santa Cruz Biotechnology (sc-376751)	1:100 in 5% milk PBS-T
Rabbit anti-Jagged1	Santa Cruz Biotechnology (sc-11376)	1:100 in 5% milk PBS-T

2.5 Gene overexpression/inhibition

2.5.1 Adenoviral-HDAC3 gene transfer

The Adenoviral-Flag-HDAC3α (Ad-HDAC3α) viruses were created from pShuttle2-Flag-HDAC3α plasmid with the Adeno-X^{TM} expression system (PT3414–1; Clontech). Viruses were produced, amplified in 293 cells, and titered (end point dilution assay) according to the protocol provided. For EndMT induction, HAECs were incubated with Ad-null or Ad- HDAC3α at 10 multiplicity of infection (MOI) for 6 hours. After removal of virus solutions, cells were cultured in human endothelial serum free medium (SFM, Invitrogen) for 48/72 hours and harvested.

2.5.2 siRNA treatment

SMARTpool siRNAs for JAG1, RND1 and non-targeting were purchased from Dharmacon and used at a final concentration of 20 nM in complete medium. Before transfection, siRNAs were complexed with Lipofectamin in opti-MEM medium (both from LifeTechnologies). In experiments with concomitant cytokine treatment, siRNA were transfected 5-7 hours before cytokine addition in HUVECs.

2.6 Immunofluorescence analysis

2.6.1 Immunofluorescence staining of HUVECs

HUVECs were plated on Millicell EZ Slides (glass chamber slides) from Millipore coated with a solution of 1μg/μl of fibronectin (Sigma). Cells were washed three times with PBS containing NaCl and $MgCl_2$ and then fixed in 3.8% PFA for 10 minutes. Subsequently, cells were permeabilized with 0.2 % Triton X-100 for 5 minutes, washed and blocked with 2% BSA in PBS for a minimum of 1 hour or left in PBS+ Sodium azide for long-term storage. Alexa Fluor® 594 Phalloidin for Actin staining was purchased from Invitrogen and used 1/40 in 2% BSA PBS-T. Polyclonal Anti-VE Cadherin antibody (ab33168) was purchased from Abcam and used 1:100 in PBS-2% BSA. After primary antibody incubation, cell were washed 3 times with PBS-T and incubated with dye-conjugated secondary antibodies (Alexa Fluor, Invitrogen) for 45 minutes at room temperature. Cells were then counterstained with DAPI (Sigma) at RT for 5 minutes and mounted with a fluorescent mounting medium (Dako). Immunofluorescence images were acquired through the Volocity software (PerkinElmer) using an Olympus IX81 inverted microscope. Images were also separately processes using the ImageJ software (http://fiji.sc/Fiji)

2.6.2 Immunofluorescence staining of HAECs.

HAECs were washed twice in PBS and then fixed in methanol for 15 minutes. After 3 washes in PBS for 5 minutes, cells were permeabilized with 0.1% Triton X-100 in PBS at RT for 15 minutes and washed three times with PBS for 5 minutes. Blocking solution (normal host serum of secondary antibody diluted 1:20 in PBS) was then applied for 1 hour at RT. Primary antibody (anti-ALK5 (Abcam) 1:100 diluted in blocking solution) was applied at RT for 1 hour or at 4°C overnight. After three washes in PBS, secondary antibodies (Alexa Fluor-488, Invitrogen) were diluted 1:1000 in blocking solution and then applied to the cells for 45 minutes at RT. Samples were then counterstained with DAPI at RT for 5 minutes, washed three times with PBS and mounted with Fluorescent mounting medium (Dako).

2.7 Morphological analysis of human endothelial cells

The quantification of cell elongation in HUVECs was performed using bright-field cell culture images (10 X magnification). A minimum of three images for each culture condition was used for analysis. Images were opened with the ImageJ software (http://fiji.sc/Fiji) and converted to 8-bit. The threshold was then automatically adjusted and in some cases manually optimized for better cell borders visualization. Thresholded images were then analysed through the ImageJ function "Analyse particle" with the following optimized parameters: size (μm^2) = 275-1200, circularity = 0-1 and "Exclude on Edges" (see Figure 22 for an illustrative example). The average values of the function "round" ($4 \times [\text{Area}] / \pi \times [\text{Major axis}]^2$) were then selected for analysis. Some figures in the Results chapter show "elongation values", which are the inverse of the round values described above.

Chapter III – Results: role of HDAC3α isoform in endothelial-mesenchymal transition (EndMT)

3.1 Introduction

As discussed in '1.5 Project Background', the HDAC3 gene generates several protein isoforms through alternative splicing. One of these isoform, HDAC3α, was found to induce a phenotype related to the endothelial-mesenchymal transition (EndMT). The EndMT is a cellular process in which ECs lose their specific markers and transform into mesenchymal cells, and is responsible for the formation of cardiac valves during embryonic development. Importantly, EndMT has been proposed to be reactivated in cardiac fibrosis and other cardiovascular diseases. Indeed, a relevant fraction of collagen-producing fibroblasts that accumulate in fibrosis is thought to emerge from the endothelium via EndMT (see Figure 8 for a summary). Therefore, the hypothesis is that the splicing of HDAC3 induce EndMT, either in cultured ECs or *in vivo*. The characterization of this cellular process may shed light on the complex mechanisms underlying tissue remodelling and could provide avenues for therapeutic intervention.

The aims of this result section are:

- To investigate the mechanisms through which HDAC3α induces the EndMT and to identify the upstream factors responsible for the splicing of HDAC3
- To determine the role of HDAC3α in EndMT *in vivo* through a mouse model of cardiac fibrosis
- To characterise the main molecular mechanisms underlying EndMT in human ECs

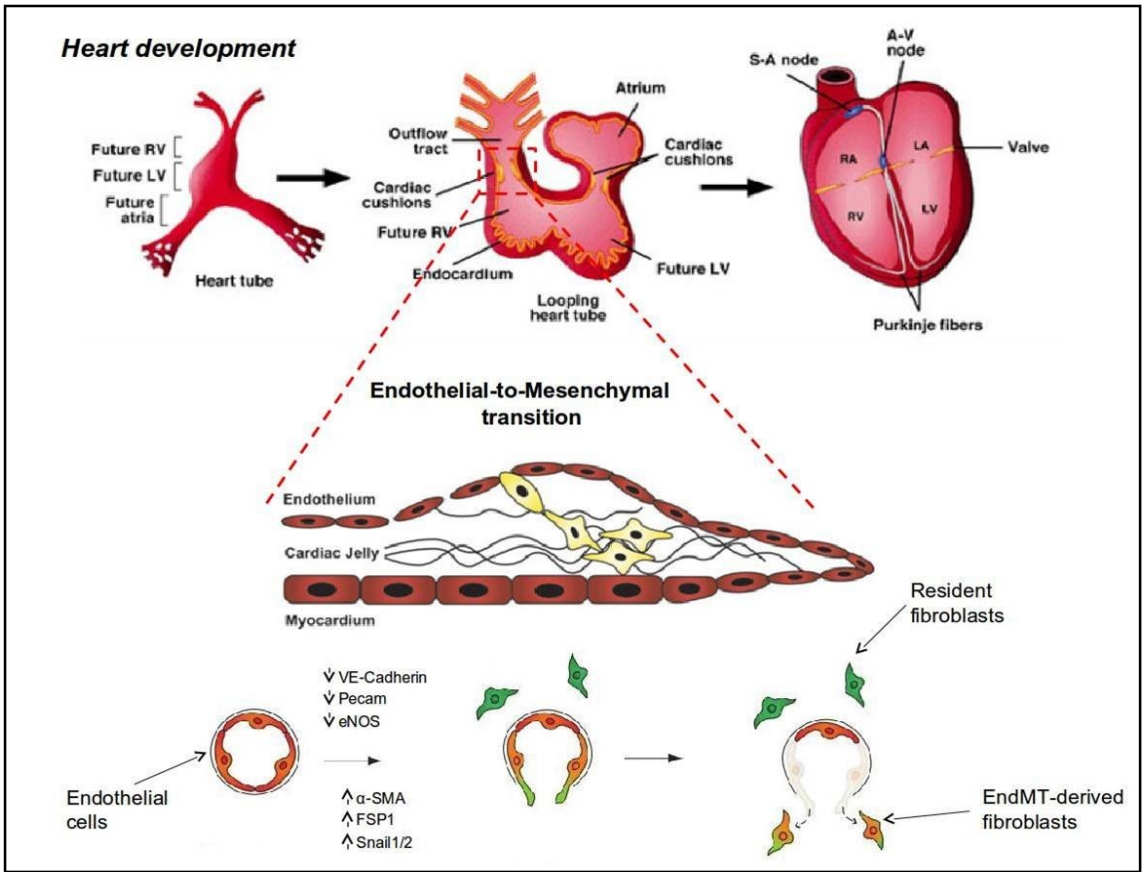

Figure 8: Developmental EndMT is reactivated in adult tissues and gives rise disease-associated fibroblasts. Schematic representation of the EndMT process responsible for the development of heart valves during cardiogenesis. This process has been proposed to occur in adult endothelial cells during disease with the downregulation of endothelial-specific markers and acquisition of mesenchymal ones, leading to their conversion into fibroblasts. The figure was adapted from Potenta et al. (133) and Armstrong et al. (75).

3.2 Results

3.2.1 HDAC3α isoform expression is induced in pressure-overload mouse hearts.

To investigate the involvement of HDAC3α in cardiac fibrosis, a pressure-overload mouse model was used. C57B1/6 mice were subjected to transverse aortic constriction (TAC) and cardiac samples were harvested at different time points after operation (see section 2.1.1). Collagen proteins were visualised by picrosirius-red staining, which reflected the extent of fibrosis. As shown in Figure 9, TAC induced fibrosis in the perivascular (top panels) and interstitial (bottom panels) cardiac areas as compared to the sham control.

To determine whether TAC-induced cardiac fibrosis was related to EndMT, the expression levels of EndMT-related genes were compared between sham and TAC groups by qPCR analysis in cardiac samples collected at 3, 7 and 14 days after surgeries. As shown in Figure 10, no significant changes were detected in both endothelial (eNOS, VE-Cadherin) and mesenchymal markers (αSMA, FSP1), possibly due to only a small subset of cardiac cells that have undergone EndMT. The only up-regulated gene in the TAC cardiac samples was collagen type I alpha I (COL1A1), consistent with the increased collagen staining observed with picrosirius-red-stained TAC heart section.

In addition, the expression levels of HDAC3 and HDAC3α were analysed by Western blot in tissue lysates from different time points (Figure 11). HDAC3α was increased in TAC samples compared to sham controls, with a stronger induction at day 14. Conversely, the main HDAC3 isoform was slightly reduced in the TAC samples. These results suggest that a shift in the splicing of HDAC3 may occur in the pathological conditions and the expression of HDAC3α may be involved in the development of cardiac fibrosis.

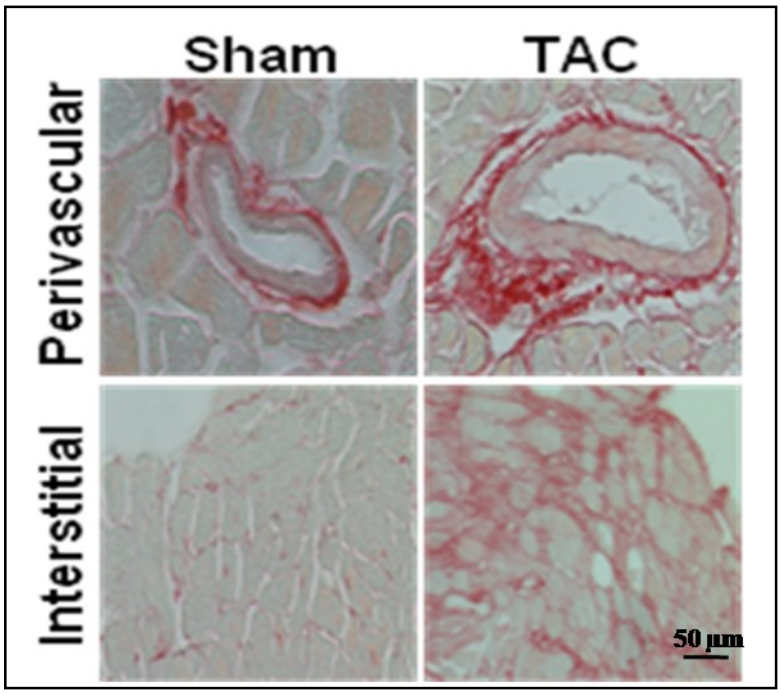

Figure 9: Aortic banding induces the development of cardiac fibrosis. Representative images of paraffin heart sections collected at 7 days after aortic banding were stained for collagen with the picrosirius-red method. Images were taken with bright-field microscope.

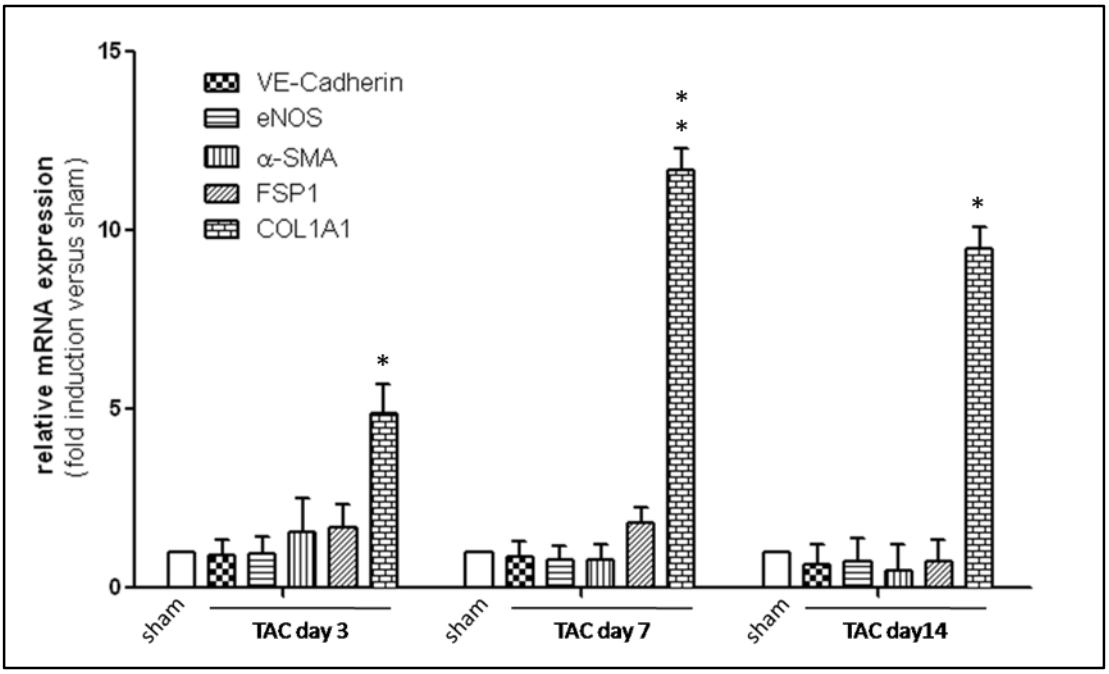

Figure 10: TAC induces collagen I expression in mouse hearts. Quantitative RT-PCR analysis was performed on total RNAs isolated from sham and TAC heart tissue samples. mRNA expression of each EndMT marker was represented as fold induction relative to the corresponding levels in sham samples. Data is presented as mean±SEM and all values were normalised with the expression of the housekeeping gene (18s). Day 3: sham n=8, TAC n=8; day 7: sham n=7, TAC n=8; day 14: sham n=4, TAC n=5. * $P < 0.05$, ** $P < 0.01$ (Student's t-test).

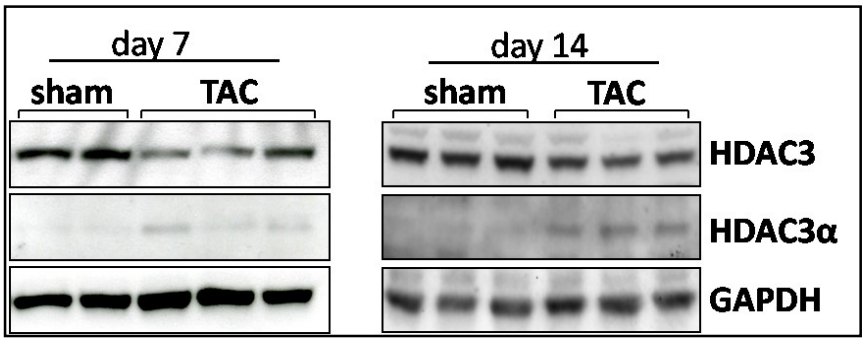

Figure 11: TAC induces HDAC3α expression in mouse hearts. Western blot analysis was performed on total protein lysates from heart tissues, which were collected at 7 and 14 days after aortic banding. The expression of GAPDH was used as a loading control. Blots are representative of at least three independent experiments.

To further confirm the induced expression of HDAC3α in TAC samples, frozen sections from sham and TAC mouse hearts (day 7 after TAC) were analysed by immunofluorescence staining. Positive green signal corresponding to the antibody against HDAC3α was detected in TAC sections but not in sham controls (Figure 12). Double staining with the endothelial marker CD31 (Pecam1) indicates that HDAC3α may be localized in proximity of vessels, although further confocal microscopy analyses would be required to confirm the cellular location of HDAC3α expression.

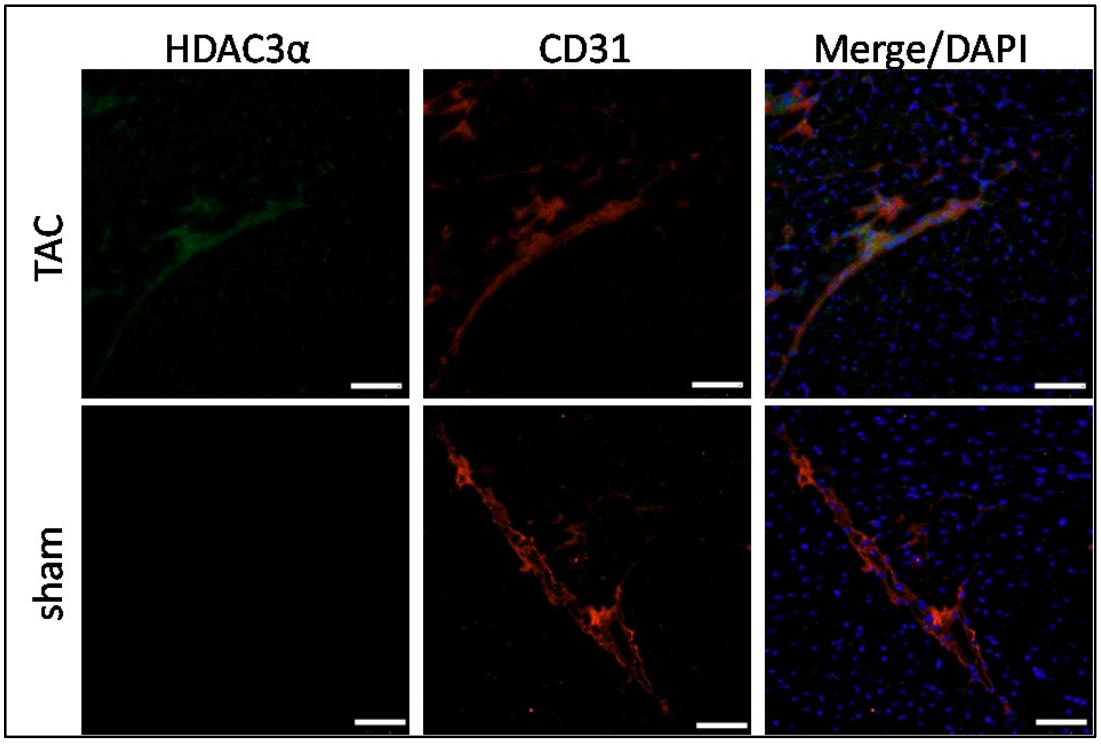

Figure 12: HDAC3α expression in mouse hearts may localise to vessels. Cryosections of mouse hearts were collected at 7 days after TAC and stained with antibodies against HDAC3α and Pecam1. Cell nuclei were counterstained in blue with DAPI (Scale bars: 70μm). Images are representative of at least three independent experiments.

3.2.2 TGFβ signalling is potentially involved in the alternative splicing of HDAC3

TGFβ1 has been found as one of the main inducers of the EndMT both *in vitro* and *in vivo* during the development of cardiac valves (134). The key questions are from where this growth factor is derived and whether it contributes to cardiac fibrosis *in vivo*.
Recently it has been found that platelets release TGFβ1 in plasma after aortic-constriction and that megakaryocyte-specific TGFβ1 knock-out mice display reduced cardiac fibrosis (135). Given these crucial roles in EndMT and TAC-induced pathological changes in heart, we then hypothesised that TGFβ signalling might constitute the upstream signal leading to the splicing of HDAC3. Consistent with our hypothesis, type I TGFβ receptor (TβRI) has been recently found to regulate RNA processing in cancer cells (136). Upon binding, TβRI translocates into the nucleus where it induces the alternative splicing of epidermal growth factor receptor (EGFR).
To test whether a similar mechanism occurred in ECs, HAECs were treated with TGFβ1 and 2 and stained with the antibody against TβRI (ALK5). Confocal images in Figure 13 show that TβRI green signal increases in the nucleus when cells were treated with TGFβ1, while in presence of TGFβ2 it localised prevalently to the cytoplasm. This result indicates that, similar to cancer cells, the activation of TGFβ signalling can lead to the translocation of type I TGFβ receptor in the nucleus of ECs, where it may mediate different nuclear functions.

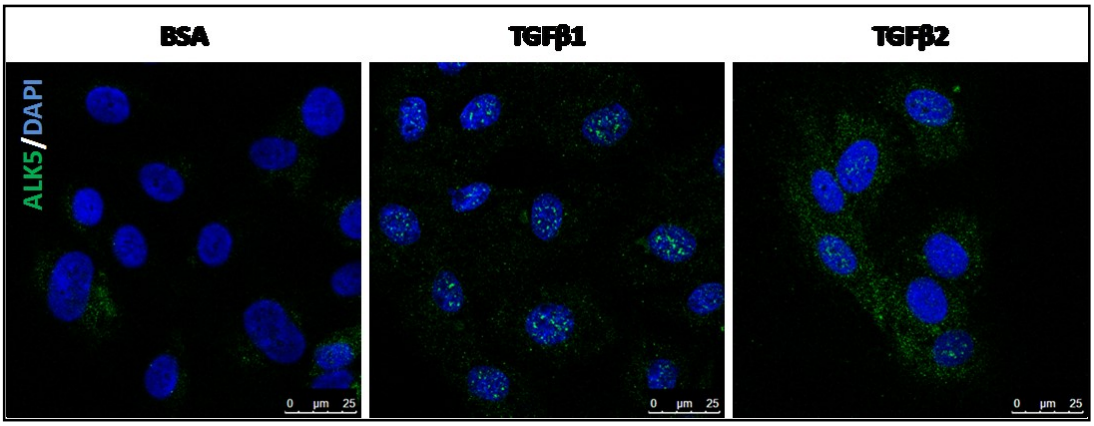

Figure 13: TGFβ1 induces ALK5 nuclear translocation in HAECs. HAECs were treated with BSA, TGFβ1 and 2 (10 ng/ml) for 24 hours and the expression of TGFβ type 1 receptor (ALK5) was analysed by immunofluorescence staining. Cell nuclei were counterstained in blue with DAPI. Images were acquired through confocal microscopy. Scale bars: 25 µm. Images are representative of at least three independent experiments.

To check whether TGFβ could induce the alternative splicing of HDAC3, mouse cells derived from aortic adventitia (see section 2.2.3) were treated with TGFβ1, 2 and 3 for 24 hours and HDAC3α protein expression was analysed by Western blot (Figure 14). All three TGFβ isoforms up-regulated the expression of αSMA and only TGFβ1 induced a slight increase of HDAC3α protein expression. However, this result can only provide some preliminary mechanistic information about the ability of TGFβ1 to induce the splicing of HDAC3α. Given the high basal expression of αSMA in BSA control, these cells are likely to be smooth muscle cells. The occurrence of TGFβ1-induced HDAC3 alternative splicing therefore needs to be demonstrated in ECs in relation to EndMT.

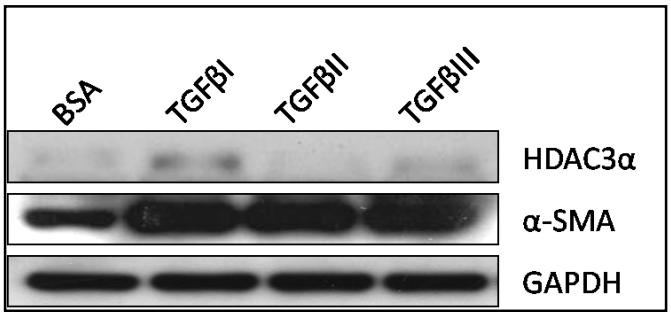

Figure 14: Western blot analysis of HDAC3α and αSMA protein expression in mouse adventitia cells treated with TGFβs. Total proteins were extracted from mouse cells derived from aortic adventitia treated with either 10 ng/ml of BSA or TGFβ1, 2, 3 and then analysed by Western blot with antibodies against HDAC3α and αSMA. GAPDH protein expression was used as a loading control. Blot is representative of at least three independent experiments.

3.2.3 TGFβ and Akt signalling pathways are involved in HDAC3α-induced EndMT

Multiple signalling pathways such as TGFβ, Map kinase, PI3K/AKT, p38, JNK and Rho have been reported to be involved in the EndMT process (see section 1.3.2). To determine which signalling pathways are involved in HDAC3α-induced EndMT phenotype, HDAC3α was overexpressed in HAECs through infection with Ad-HDAC3α virus in the presence of selective chemical inhibitors. The protein expression level of αSMA was the read-out of the experiment since it is consistently up-regulated by HDAC3α overexpression (see section 1.5.2). Both TGFβ and PI3K/AKT inhibitors (SB431542 and LY294002, respectively) abolished Ad-HDAC3α-induced αSMA expression, while other inhibitors had no effects (Figure 15).

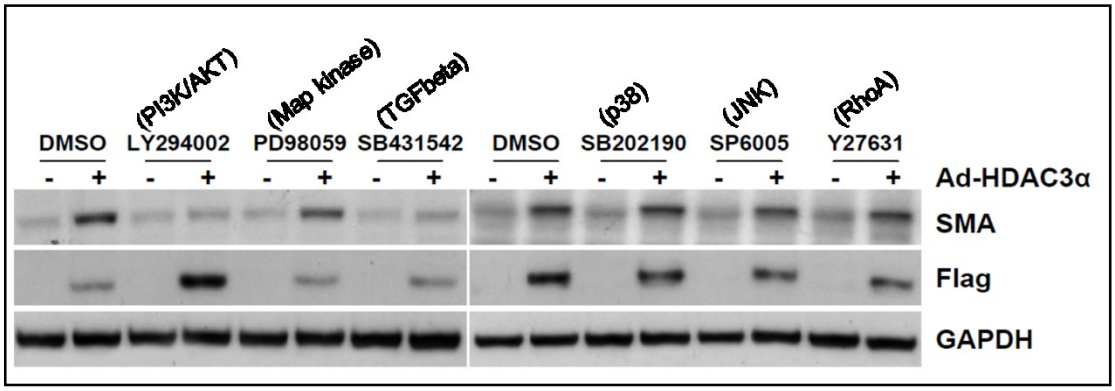

Figure 15: Western blot analysis of αSMA protein expression in HAECs infected with Ad-HDAC3α virus in the presence of signalling pathway inhibitors. HAECs were infected with Ad-HDAC3α virus (10 MOI) in the presence of 10μM of chemical inhibitors indicated. Ad-null infection was used as control. Protein level of αSMA was analysed by Western blot on total proteins extracted 72 hours after treatment with the inhibitors. The anti-Flag antibody was used to confirm the exogenous expression of HDAC3α protein expression. GAPDH expression was used as a loading control. Blots are representative of at least three independent experiments.

To confirm the effect of SB431542 and LY294002 inhibitors on HDAC3α-induced EndMT, an immunofluorescence analysis was performed in HAECs (Figure 16). In agreement with the Western blot results, the expression of αSMA (green signal) was significantly induced in HDAC3α-overexpressing HAECs treated with DMSO and markedly suppressed by both SB431542 and LY294002. HDAC3α-dependent downregulation of VE-Cadherin (red signal) was suppressed by SB431542 but not LY294002, which may suggest PI3K/AKT signalling to play a partial role in HDAC3α-induced EndMT.

Collectively, both Western blot and immunofluorescence results suggest that HDAC3α may act through TGFβ and PI3K/AKT signalling pathways to induce EndMT.

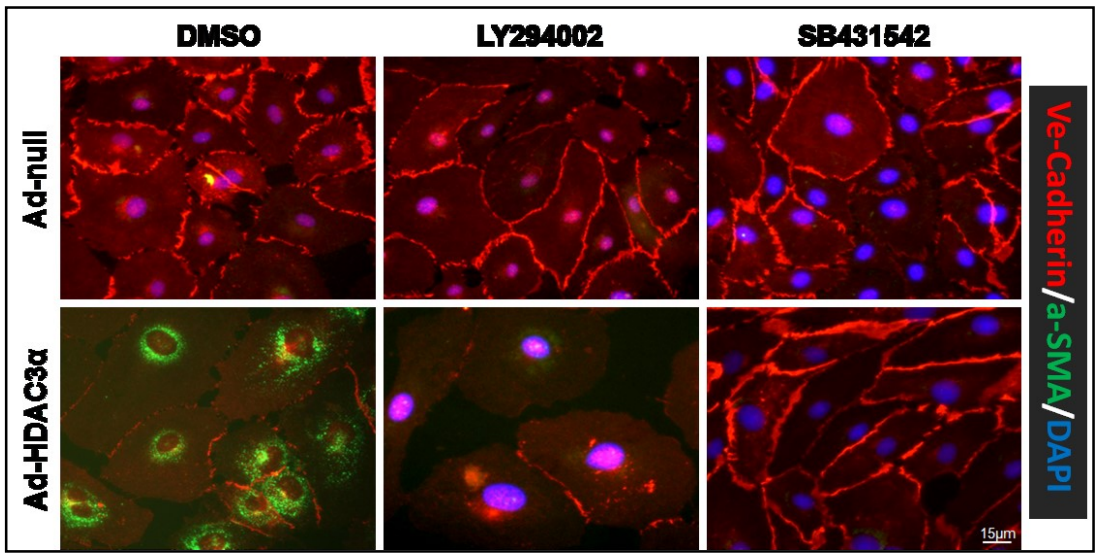

Figure 16: SB431542 and LY294002 inhibitors abolish Ad-HDAC3α-induced EndMT phenotype. HAECs were infected with Ad-HDAC3α or Ad-null virus (10 MOI) in the presence of 10μM of SB431542 and LY294002 inhibitors. DMSO was included as vehicle control. 72 hours after treatment cells were stained with antibodies against VE-Cadherin and αSMA. Cell nuclei were counterstained in blue with DAPI. (Scale bars: 15μm). Images are representative of at least three independent experiments.

3.2.4 Role of HDAC3α in the extracellular activation of TGFβ2

The ability of SB431542 inhibitor to block HDAC3α-induced EndMT may lead to the assumption that the function of HDAC3α is to induce the expression and/or secretion of TGFβ cytokines, which might in turn act in an autocrine and/or paracrine manner to induce EndMT. Since SB431542 targets specifically TGFβ type I receptors (ALK4-5-7), it is reasonable to assume that the overexpression of HDAC3α increases the expression of their ligands, which would in turn induce EndMT through the TGFβ signalling. To test this hypothesis, mRNA expression levels of TGFβ 1, 2 and 3 were measured in Ad-null and Ad-HDAC3α-infected HAECs. As shown in Figure 17, no significant changes in gene expression levels were detected. Protein expression levels of TGFβ isoforms were then analysed in cell lysates and conditioned media. Endogenous protein levels of TGFβ1 and 2 were not changed upon HDAC3α overexpression (Figure 18 A). The induction of TGFβ signalling was confirmed by the increased level of phospho-SMAD2 in DMSO-treated cells, which was suppressed by inhibitors of Akt (LY294002) and TGFβ (SB431542) signalling pathways. In conditioned media (Figure 18 B), protein levels of TGFβ1 slightly decreased in Ad-HDAC3α-infected cells compared to Ad-null control cells. In DMSO-treated Ad-null control cells, antibody against TGFβ2 detected a prevalent band of 50 kDa and a weaker band of 26 kDa. 50 kDa is the expected protein size of the TGFβ2 precursor while 26 kDa corresponds to the homodimeric active form of TGFβ2. In HAECs infected with Ad-HDAC3α virus the 50 kDa band decreased significantly, while the 26 kDa band of the active form was increased. This effect was abolished by LY294002, while the ratio between band intensities increased in favour of the 26 kDa band in the presence of SB431542, which is consistent with the extracellular accumulation of the active ligand due to the blocking of TGFβ type I receptor. These results thus suggest that HDAC3α mediates the activation of TGFβ2 in the extracellular space. To check whether this activation was required to induce the EndMT, HDAC3α-infected HAECs were treated with the neutralization antibody against TGFβ2. As shown in Figure 19, the treatment with anti-TGFβ2 antibody impaired the upregulation of αSMA protein expression, thus suggesting that the cleavage and activation of TGFβ2 may be a necessary mechanism through which HDAC3α induces the EndMT.

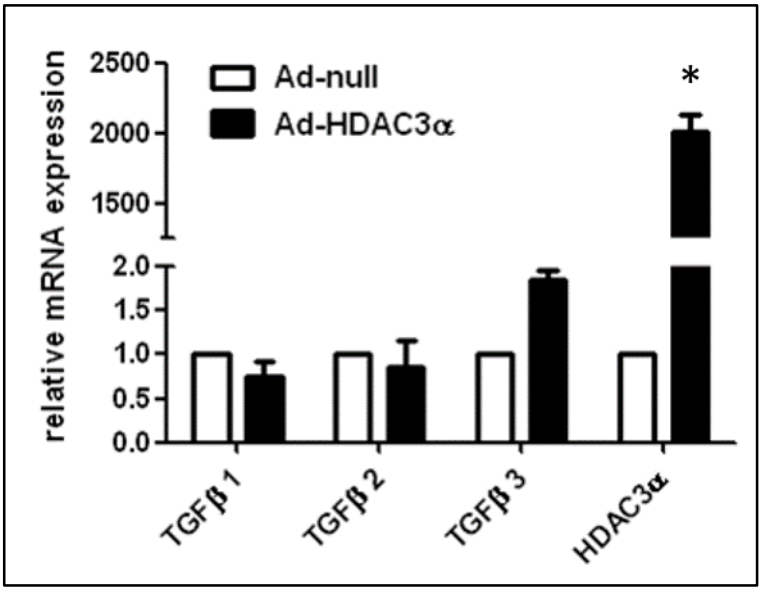

Figure 17: Ad-HDAC3α has no effect on TGFβ1-3 mRNA expression. HAECs were infected with Ad-null or Ad-HDAC3α (10 MOI) for 6 hours and then cultivated in serum-free medium for 72 hours. Quantitative RT-PCR analysis was performed on total RNA extracts to measure gene expression levels of TGFβ1, 2, 3 and exogenous HDAC3α. All values were normalized against the expression of 18s housekeeping gene. Error bars represent the mean (±SEM) of 2 independent experiments. * $P < 0.001$, all other conditions: $p > 0.05$ (Student's t-test).

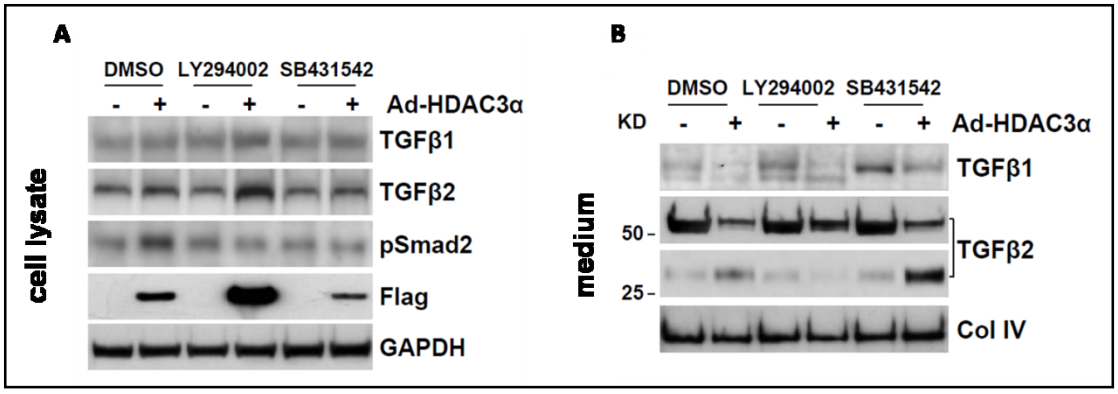

Figure 18: Overexpression of HDAC3α induces TGFβ2 cleavage in HAECs. HAECs were infected with Ad-HDAC3α or Ad-null virus (10 MOI) in the presence of 10μM of DMSO, SB431542 and LY294002. Western blot analysis was performed on total proteins extracted from cell lysate (A) or conditioned media (B) 72 hours after inhibitors treatment. Antibody against pSmad2 was used to detect TGFβ signalling activation. The anti-Flag antibody was used to measure exogenous HDAC3α protein expression. GAPDH and Collagen IV expression were used as a loading control in cell lysate and conditioned media, respectively. Blots are representative of at least three independent experiments.

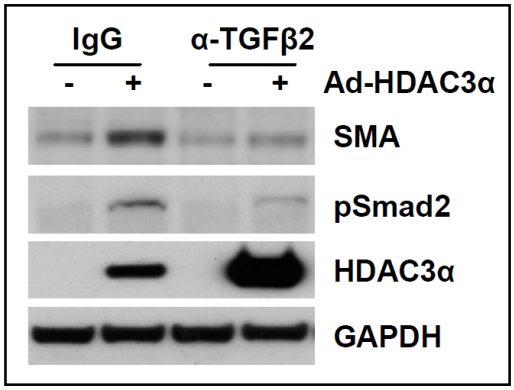

Figure 19: The anti-TGFβ2 neutralization antibody abolishes HDAC3α overexpression-induced SMA expression. HAECs were infected with Ad-HDAC3α or Ad-null virus (10 MOI) in the presence of 0.2 μg/ml of goat IgG (Immunoglobulin G) or 0.2 μg/ml of goat anti-TGFβ2 antibody. Western blot analysis was performed 72 hours after treatment. Antibody against pSmad2 was used to detect TGFβ signalling activation. The anti-Flag antibody was used to measure exogenous HDAC3α protein expression. GAPDH was used as a loading control. Blot is representative of at least three independent experiments.

3.2.5 Upregulation of ADAMTS1 by HDAC3α and its potential role in the activation of TGFβ2

The extracellular activation of TGFβs is relatively less characterised compared to the intracellular signalling triggered by these cytokines. In the extracellular matrix, a central activation mechanism is the proteolytic cleavage of the latent-TGFβ complex, which makes the active TGFβ form able to bind to its receptors. Key regulators of this process are extracellular matrix proteases such as plasmin, matrix metalloproteases (MMPs) and thrombospondin-1 (137). In a microarray analysis previously performed in my host laboratory, different genes were found to be differentially regulated in HAECs by the overexpression of HDAC3α. One of the genes that showed a significant upregulation was ADAMTS1. ADAMTS (a disintegrin and metalloproteinase with thrombospondin motifs) gene family comprises multi-domain secreted proteins involved in a variety of functions, such as angiogenesis, blood coagulation and extracellular matrix homeostasis (138). Interestingly, ADAMTS1 has been recently found to directly associate and cleave the latent-TGFβ complex, contributing to the TGFβ-induced tissue remodelling in liver fibrosis (139). This evidence made ADAMTS1 a good candidate for the cleavage of TGFβ2 latent form described above. To confirm the microarray results, ADAMTS1 gene expression was compared in Ad-null and Ad- HDAC3α-infected HAECs by qPCR. As shown in Figure 20 ADAMTS1 gene expression is increased up to 6 folds by HDAC3α.

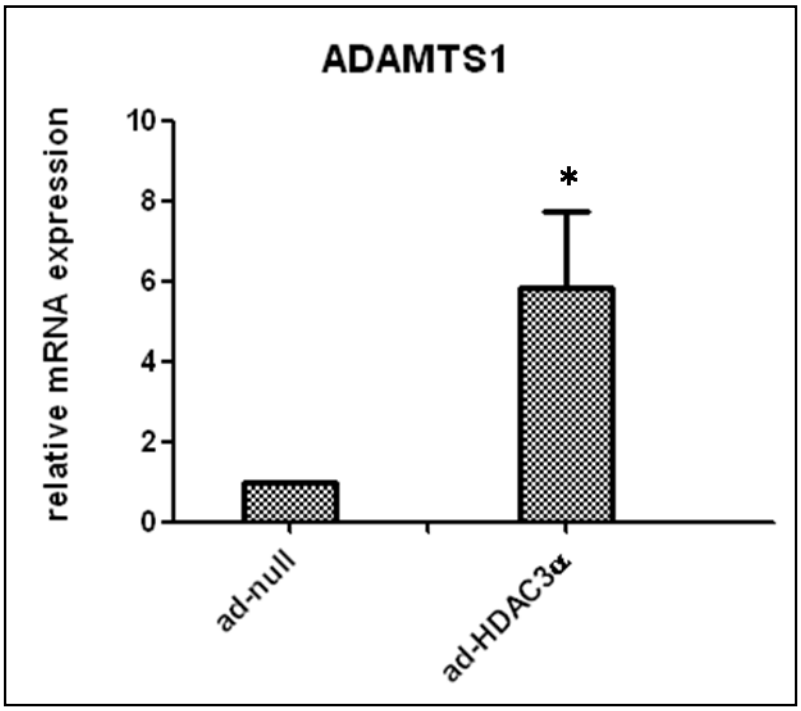

Figure 20: Overexpression of HDAC3α increases ADAMTS1 expression in HAECs. Cells were infected with Ad-null or Ad-HDAC3α virus (10 MOI) for 6 hours and then cultivated in serum-free medium for 72 hours. Quantitative RT-PCR analysis was performed on total RNA extracts to measure gene expression levels of ADAMTS1. Values represent the fold induction against Ad-null control and are normalised against the expression of 18s gene. Error bars represent the mean (±SEM) of 3 independent experiments. * $P < 0.05$ (Student's t-test).

3.3 Conclusions

In this result chapter, the ability of the splicing isoform HDAC3α to induce the EndMT was investigated. The molecular mechanisms underlying the function of HDAC3α and its relevance *in vivo* can be summarised in the following conclusions:

- TGFβ and Akt signalling pathways mediate the EndMT phenotype induced by the overexpression of HDAC3α in human ECs

- The extracellular activation of TGFβ2 and its autocrine signalling determine the HDAC3α-mediated EndMT

- Overexpression of HDAC3α upregulates gene expression of ADAMTS1, which may cleave extracellularly the latent complex of TGFβ2

- In a mouse model of cardiac fibrosis, HDAC3α protein expression is induced in fibrotic hearts compared to sham controls

3.4 Discussion

3.4.1 A splicing isoform of HDAC3 induces EndMT *in vitro*. What are the molecular events involved?

Previous work from the host laboratory revealed that during endothelial differentiation of mouse embryonic stem cells, the HDAC3 gene gave rise to different isoforms. One of these isoforms, named HDAC3α, was further reported to be involved in the endothelial mesenchymal transition (EndMT). When over-expressed in HAECs through adenoviral transfection, the phenotype obtained was in fact reminiscent of an EndMT: HAECs presented an altered morphology compared to control cells (empty adenovirus) and increased protein expression of mesenchymal markers, e.g. αSMA, N-cadherin and Snail2 (see section 1.5.2) (140).

It was initially sought to characterise the molecular events involved in HDAC3α-induced EndMT. Using different chemical inhibitors of major signalling pathways, TGFβ and AKT signalling were found to be implicated in the emergence of the EndMT phenotype (3.2.3). The TGFβ signalling was further investigated due to its established role in both EndMT and cardiac fibrosis. By analysing the secreted proteins of HDAC3α-overexpressing HAECs, it was found that HDAC3α did not change the gene expression levels of TGFβ ligands but induced instead the activation of the latent form of TGFβ2 in the extracellular space (3.2.4). Accordingly, the blockage of TGFβ2 with the neutralization antibody abolished HDAC3α-induced EndMT. These results indicate that HDAC3α could act upstream of TGFβ signalling and its function might be to release the active form of the cytokines from the extracellular matrix. This mechanism may be relevant for cardiac fibrosis as in lung and skin the fibrotic process occurs through the activation of latent TGFβ complex in the extracellular matrix rather than through transcriptional increase (141). To mediate the extracellular activation of TGFβ2, HDAC3α may increase the secretion of factors that cleave proteolytically the latent form, such as proteases. Further data supported this hypothesis: qPCR analysis showed that the overexpression of HDAC3α in HAECs increases gene transcription of ADAMTS1 (3.2.5). Interestingly, this metalloproteinase was previously reported to directly interact and to activate TGFβ1 in liver fibrosis trough a proteolysis-independent conformational mechanism, a process similar to the thrombospondin-mediated TGFβ activation (139).

These data thus suggest that in addition to the role in EndMT, the splicing of HDAC3 may be involved more broadly in the remodelling of extracellular matrix through the regulation of cytokines turnover.

Another aspect covered in the project was to definition of the regulatory mechanisms leading to the splicing of HDAC3α. Following the general principle according to which alternative splicing is influenced by external growth factors (142), the working hypothesis formulated was that TGFβ signalling could itself induce HDAC3α splicing. This hypothesis was also consistent with a recent study showing that in cancer cells the TGFβ receptor 1, upon TGFβ1 binding, translocates into the nucleus and regulates RNA processing (136, 143). Accordingly, data obtained in HAECs showed that TGFβ1 but not TGFβ2 induced the translocation of TGFβ receptor 1 into the nucleus (3.2.2. However, whether TGFβ1 has the ability to induce HDAC3 splicing in ECs hasn't been demonstrated. Results obtained in a different cell type, i.e. mouse adventitia-derived cells, provided a preliminary mechanistic indication that needs further investigation. Nonetheless, in light of the reported extracellular activation of TGFβ2, the potential induction of HDAC3 splicing by TGFβ1 would configure a feedback loop regulatory mechanism between the two isoforms. This speculation fits in the context of understanding the individual functions of TGFβ isoforms, which have already been shown to differentially regulate distinct phases of EndMT during cardiogenesis (134).

3.4.2 Is HDAC3α expressed *in vivo*?

The *in vitro* molecular studies of HDAC3α function during EndMT have been performed in parallel with *in vivo* experiments, which aimed at determining the presence of this protein in cardiac tissues and specifically, the link between HDAC3α and cardiac fibrosis (3.2.1). To this end, transverse aortic constriction (TAC) pressure-overload mouse model was used. The occurrence of fibrosis was confirmed by histological staining of collagen proteins in heart sections. However, quantitative RT-PCR analysis did not detect changes in gene expression of EndMT-associated markers. This can be explained considering that potential transcriptional changes in a small subset of cells may be masked when an entire tissue is analysed. Nevertheless, Western blot analyses showed that HDAC3α protein expression was increased in fibrotic hearts compared to sham control, while on the other

hand, the expression of HDAC3 was reduced. This balance between HDAC3 isoform during fibrosis provides an interesting clue on how HDAC enzymes may function in tissue remodelling. Furthermore, immunofluorescence staining of HDAC3α in the fibrotic and sham hearts was performed to clarify whether its expression was localized in ECs. Results confirmed an overall increase in HDAC3α expression in TAC samples compared to sham but they were unable to unequivocally demonstrate its cellular location. Therefore, in order to support a role of HDAC3α in EndMT-induced cardiac fibrosis, further investigation is needed to identify *in vivo* the cell population in which HDAC3α splicing occurs.

3.4.3 HDAC3α: critical points to address

Overall, the results obtained *in vivo* and *in vitro* offer interesting clues about the function of HDAC3α during EndMT and its potential role in cardiac fibrosis. However, it is worth to point out key questions that need to be addressed in the future in order to support the relevance of this new HDAC3 isoform. Firstly, most *in vitro* experiments relied on the overexpression of HDAC3α through adenoviral transfection, a system which may confound the analysis of specific phenotypes given the reported side effects of adenoviruses on endothelial cell physiology (144). In this regard, a functional investigation of the endogenous HDAC3α would be preferable. This option has however proven to be challenging because mouse ECs are technically difficult to grow in culture. Moreover, initial experiments in both primary and immortalized mouse ECs have not provided a clear indication of what conditions induce the splicing of HDAC3α. Determining the conditions that give rise to the endogenous HDAC3α is therefore critical to understand the real physiological role of this isoform and the underlying mechanisms. Secondly, HDAC3α is a mouse-specific isoform; an analysis of the nucleotide sequence corresponding to the intron-12 of the HDAC3 gene reveals in fact that this genomic region varies greatly across different mammalian species. Since intron-12 sequence gives rise to the c-terminal of mouse HDAC3α and is therefore functionally important (see section 1.5.1), its non-conservation would argue against a functional role generalizable to other species, thus challenging the biological and biomedical relevance of this protein. Nonetheless, it may be possible that in human, for instance, other isoforms could play similar roles of HDAC3α, regardless of the precise mechanism of splicing. The

identification of these putative human isoforms with equivalent roles in EndMT would be therefore of primary importance to make sense of the findings related to mouse HDAC3 splicing.

Chapter IV – Results: do inflammatory cytokines drive EndMT?

4.1 Introduction

TGFβ signalling has been the most prominent mechanisms described for EndMT in developmental and *in vitro* studies. However, whether TGFβ growth factor molecules are both necessary and sufficient to drive the EndMT — or whether other factors are capable of inducing it — is currently less well-known. Also, as described in '1.3.2 Literature review of EndMT', *in vitro* studies have reported conflicting results on the ability of TGFβ ligands to induce morphological changes in ECs.

In the EMT, the interplay between TGFβ-induced responses and inflammatory mechanisms are at the root of the cellular effects responsible for pathological processes (145). Similarly, the disorders in which EndMT has been shown to play a role (e.g. cardiac and renal fibrosis and neointima) are characterized by a strong inflammatory response. The molecular mechanisms linking the mesenchymal transition of ECs to inflammation have not been extensively studied; thus, it was hypothesized that inflammatory cytokines such as TNF and IL1β induce EndMT.

The aims of this result section are:

- To determine whether inflammatory cytokines induce a fibroblast-like morphology in ECs *in vitro*, comparing their effect to TGFβ.

- To analyse the expression changes of EndMT-related genes in ECs upon treatment with inflammatory cytokines

- To investigate the structural effect of inflammatory cytokines on the cytoskeleton of ECs

4.2 Results

4.2.1 Morphological changes of endothelial cells treated with different inflammatory cytokines.

In order to determine what factors induce a consistent mesenchymal phenotype in ECs, HUVECs were treated with different cytokines which have been previously reported to induce changes in endothelial cell morphology: TGFβ2, TNF and IL1β (54, 146, 147). Since synergistic effects have been reported for these factors, all possible combinations were examined.

In the control condition (see section 2.2.2), confluent HUVECs were densely packed and displayed a round phenotype, the so-called "cobblestone" morphology. Treatment with TGFβ2 did not alter this cellular architecture, whereas the same concentration of either TNF or IL1β changed cell morphology, with cells acquiring an elongated shape (Figure 21). The combination of TNF and IL1β further increased this elongation with cells being more uniformly spindle-shaped. The combinations TNF+TGFβ2 and IL1β+TGFβ2 did not increase significantly the elongation compared to TNF or IL1β alone and an increase in cell death seemed to be present. In the presence of all three cytokines together, cell elongation appeared similar to TNF+IL1β, although thin cellular protrusions were present in some cells.

Quantification of cell elongation shown in Figure 23 was consistent with the morphology observed through bright-field images (see Figure 22 and section 2.7 for method details). Control and TGFβ2-treated HUVECs returned the highest round values among the different conditions, while TNF and IL1β increased cell elongation and thus presented lower values. The combinations TNF+IL1β and TNF+IL1β+TGFβ2 gave rise to the highest cell elongation, with mean round values of 0.3±0.01 and 0.29±0.01, respectively. Taken together, these data show that the inflammatory cytokines TNF and IL1β are able to induce a consistent morphological change in HUVECs, which loose the round cobblestone phenotype and acquire an elongated spindle-shape. This effect is synergistically increased in the presence of both cytokines. On the other hand, TGFβ2 induces no discernible effects in terms of cell shape changes.

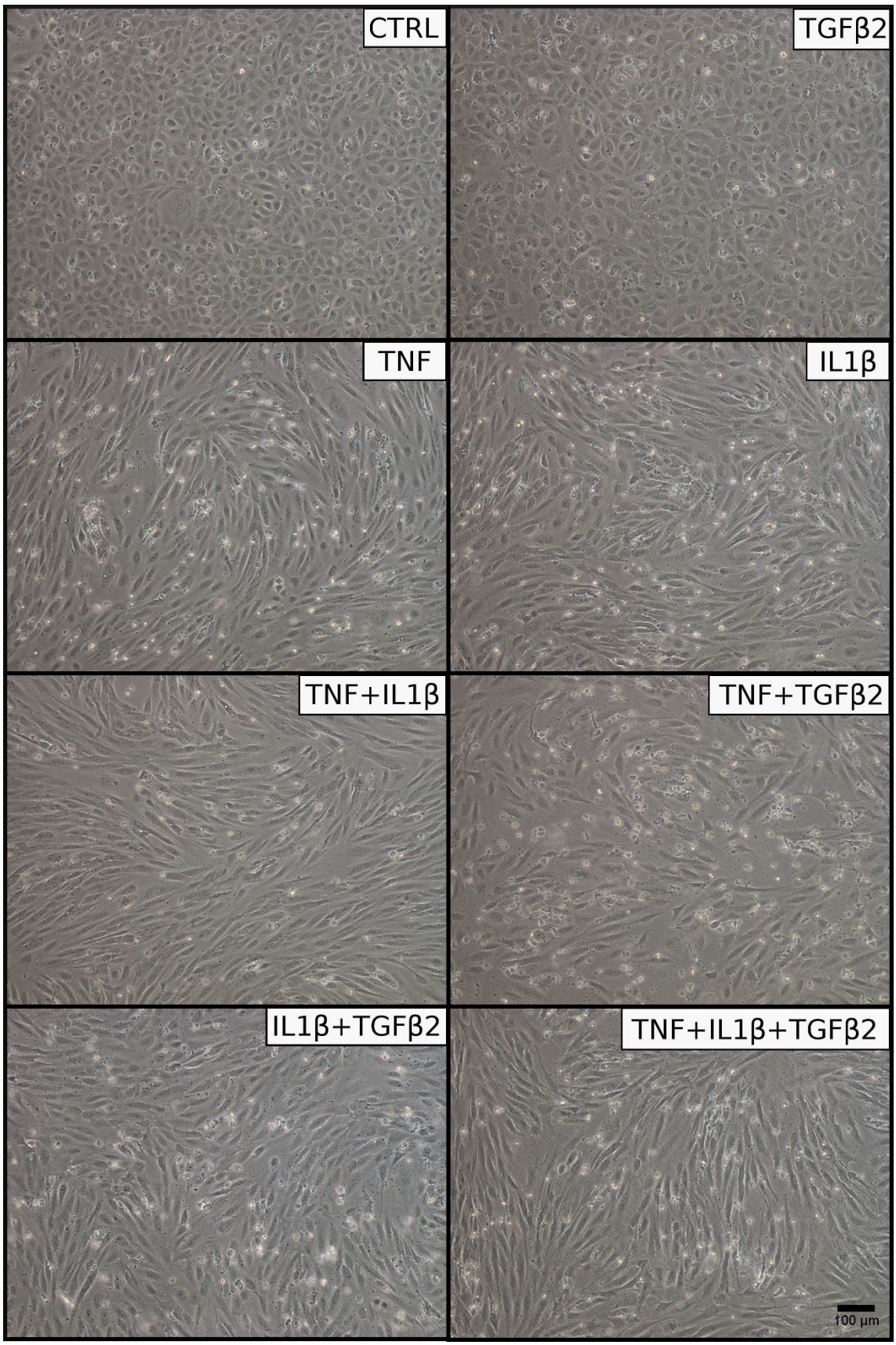

Figure 21: Effect of different combinations of cytokines on endothelial cell morphology. Representative cell culture images of HUVECs monolayers treated with different combinations of cytokines for 48 hours. Each cytokine was added at a concentration of 10 ng/ml. Images are representative of at least three independent experiments.

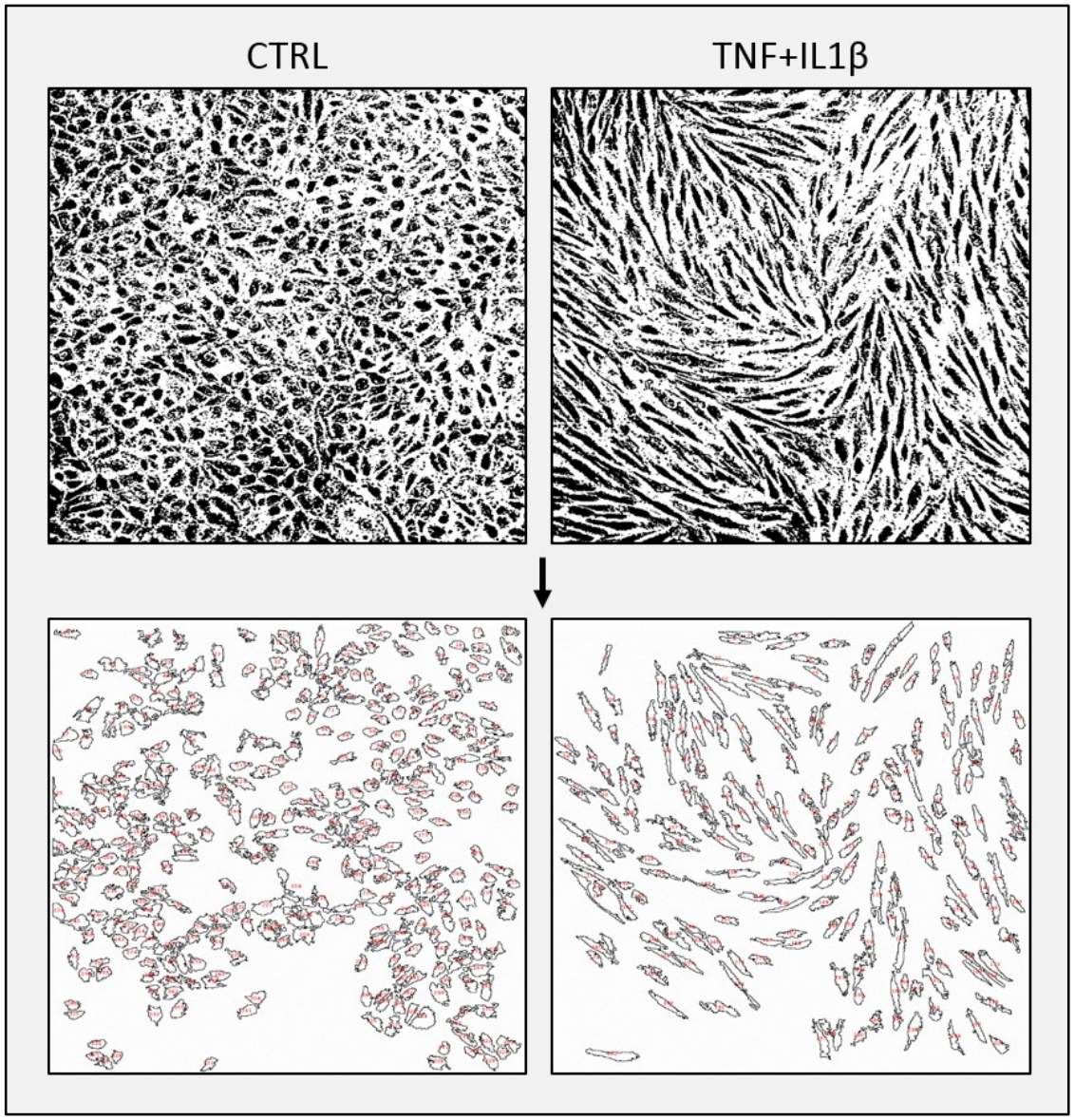

Figure 22: Morphological analysis of cytokine-treated endothelial cells. Representative example of image processing in cytokine-treated HUVECs. Bright field cell culture images were threshold-adjusted (upper panels) and the borders of individual cells were automatically detected using the ImageJ software function "analyse particles" (bottom panels). For method details see section 2.7.

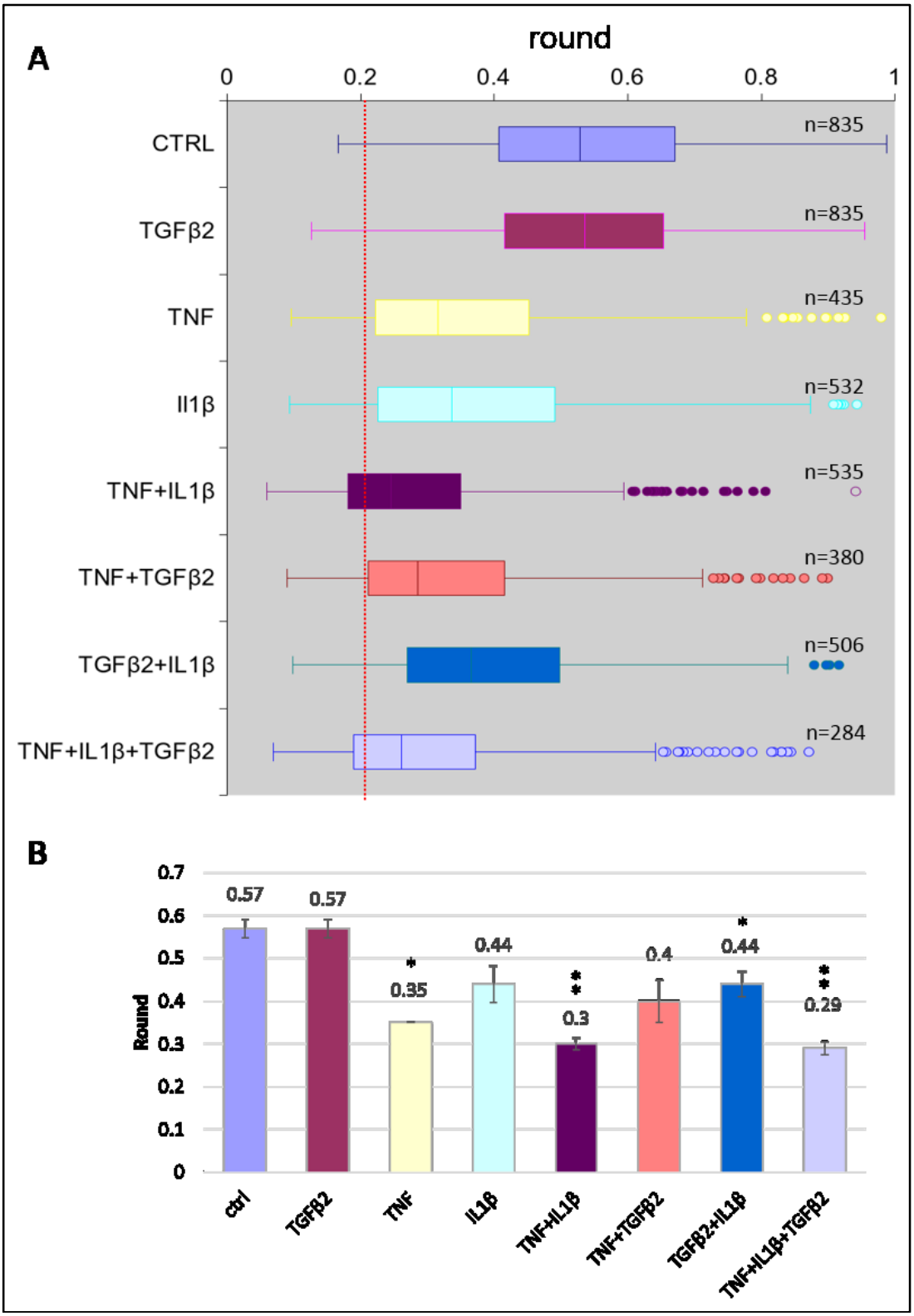

Figure 23: Quantification of cell elongation in cytokine-treated endothelial cells. Multiple cell culture images of each cytokine combination (as represented in Figure 21) were processed with ImageJ software and mean *round* values were calculated (see Figure 22 and section 2.7 for method details). *Round* measures how shapes approach a perfect circle (= 1). A) Box Plot analysis of a single representative experiment highlighting value distribution and sample size of each condition. B) Mean round values ±S.D. (Standard deviation) of two independent experiments. * P-value < 0.05, ** P <0.01, as calculated against the control using the Student's t-test.

4.2.2 Gene expression analysis of EndMT markers in cytokine-treated endothelial cells

The acquisition of mesenchymal features in ECs is thought to be driven by dramatic changes at the level of gene expression. Different genes have been reported to be either down- or upregulated. To check whether the cytokine-induced shape changes observed in ECs correlated with transcriptional regulation of EndMT markers, a quantitative RT-PCR analysis was performed in HUVECs. The graph in Figure 24 shows the expression levels of three endothelial-specific (VE-Cadherin, PECAM1, eNOS,) and three mesenchymal-specific markers (S100A4, N-cadherin, ACTA2). Relative to the control, there was no significant difference in mRNA abundance of VE-cadherin and PECAM1 in any of the conditions tested, while the expression of eNOS was downregulated less than 2-fold in HUVECs treated with IL1β or TNF+IL1β. The combined TNF+IL1β+TGFβ2 treatment induced the highest downregulation of eNOS, with almost 5-fold compared to control. The gene expression levels of mesenchymal markers showed a moderate upregulation in some of the conditions tested. Compared to untreated cells, the expression of S100A4 was induced by almost 3 folds by TNF or TNF+IL1β, while there was little difference in the remaining conditions. N-cadherin expression was upregulated in TNF- and TNF+IL1β+TGFβ2-treated cells by approximately two and three folds, respectively. The expression of ACTA2 was increased by 3 folds by TNF and to a lesser extent, by IL1β and TNF+IL1β+TGFβ2.

Taken together, these data do not reflect a loss of endothelial-specific proteins and an acquisition of mesenchymal-specific ones, a pattern that is considered a hallmark of the endothelial-mesenchymal transdifferentiation. With the exception of eNOS, the expression of the endothelial markers remains stable in all the conditions tested, whereas the mesenchymal markers show variable and modest upregulations. The latter effect may be due to either an indirect transcriptional effect induced by TNF and/or IL1β or simply by transcriptional noise.

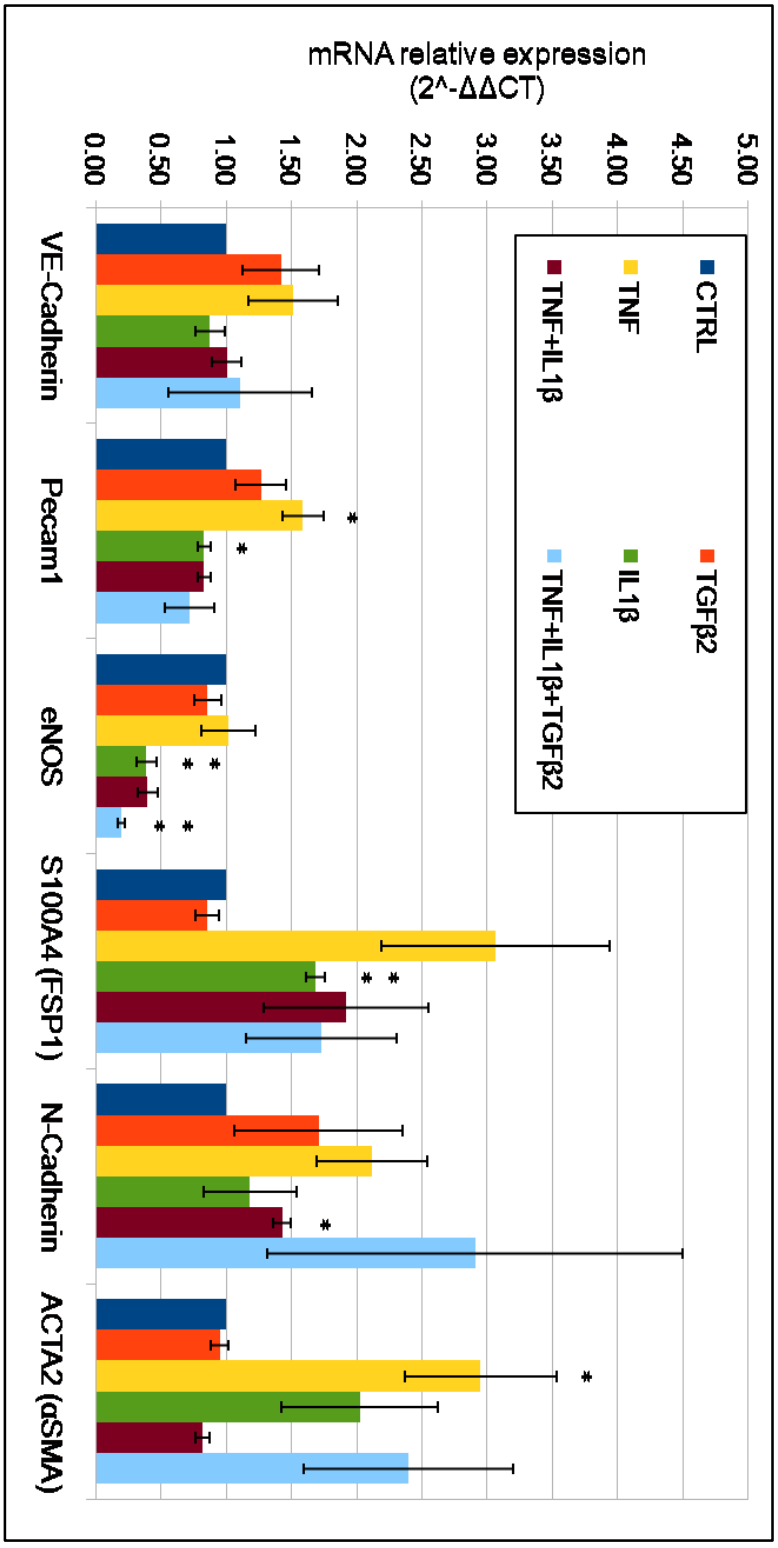

Figure 24: Gene expression analysis of EndMT markers in cytokine-treated endothelial cells. HUVECs were treated for 48 hours with different combinations of cytokines and RNA was analysed through quantitative RT-PCR. mRNA expression levels represent fold changes relative to untreated cells (CTRL). All values were normalized against the expression of the RPL13A housekeeping gene and represent the mean ±S.D (n=3). ** $P < 0.01$, * $P < 0.05$; for all other conditions $P > 0.05$ (Student's t-test).

To check whether the lack of gene expression differences of endothelial markers is reflected in protein levels, HUVECs were treated with cytokines for 48 hours and protein extracts were analysed by Western blot (Figure 25). Consistent with qPCR data, there was no significant difference in VE-Cadherin protein expression in all conditions tested. Furthermore, the expression of eNOS was decreased in all conditions except TGFβ2, partly reflecting the gene expression results.

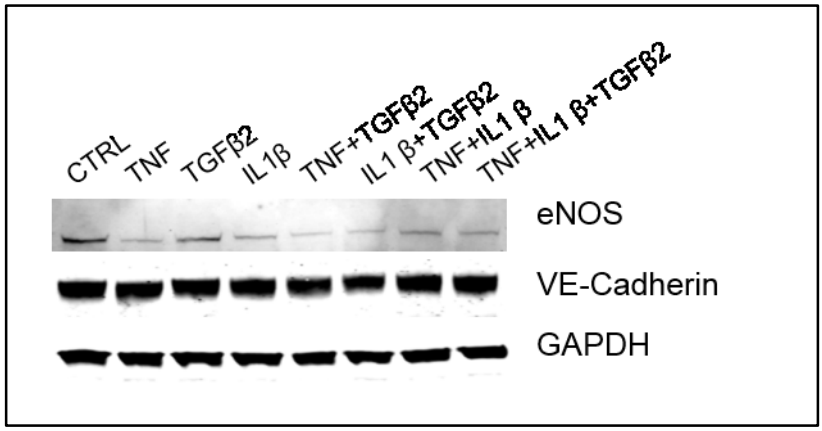

Figure 25: Protein expression analysis of endothelial markers in cytokines-treated endothelial cells. HUVECs were treated for 48 hours with different combinations of cytokines. Protein lysates were then analysed through Western blot. GAPDH was used as the loading control. Blot is representative of three independent experiments.

4.2.3 Role of TGFβ2 in cytokine-induce elongation of ECs

The inability of TGFβ2 to induce EndMT features, such as cell morphology and gene/protein expression changes, despite its prominent role in EndMT described in literature, prompted to investigate whether its signalling pathway is active in the current cellular model. To this end, TGFβ2-treated HUVECs were analysed by Western blot to detect the phosphorylation of Smad2, an essential transducer for TGFβ signalling (148). The results shown in Figure 26 indicate that TGFβ2 robustly induces Smad2 phosphorylation 1 hour after treatment and this effect persists after 24 hours. The expression of total Smad2 wasn't changed significantly, suggesting that the phosphorylation is directly induced by TGFβ2 and not due to an increase in the amount of total protein. On the other hand, in the presence of TNF and IL1β, Smad2 was not phosphorylated, thus ruling out the possibility that these inflammatory cytokines could activate indirectly the TGFβ signalling. Furthermore, the baseline Smad2 phosphorylation appeared to be inhibited at 1 hour by TNF+IL1β, in agreement with studies in other cell types showing an antagonist effect inflammatory cytokines on TGFβ signalling (149, 150). In the presence of all three cytokines (TNF+IL1β+TGFβ2) there was no further increase in the phosphorylation of Smad2 compared to TGFβ2 alone. The activation of Smad2 by TGFβ2, furthermore, was confirmed to be mediated by the ALK5, since the phosphorylation was totally inhibited at both time points in the presence of the SB431542, a chemical inhibitor specific for the type-1 receptor.

Taken together, these results show that, under the current experimental settings, TGFβ2 is biochemically active and the inflammatory cytokines do not transactivate the TGFβ-Smad2 signalling.

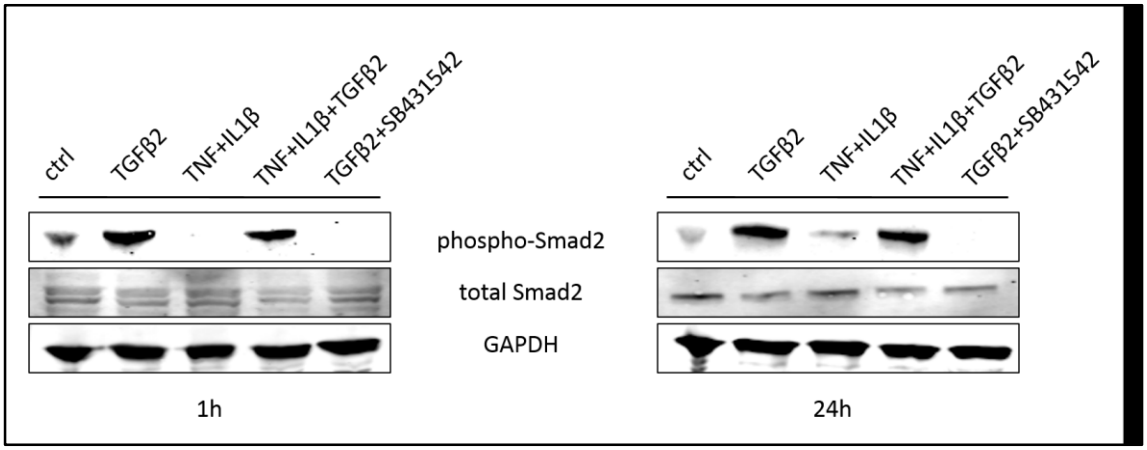

Figure 26: TNF and IL1β do not activate TGFβ signalling. HUVECs were treated with different cytokine for 1 and 24 hours and protein expression was analysed by Western blot. GAPDH expression was used as a protein loading control. SB431542 inhibitor was added at a concentration of 10 μM concomitantly with cytokines. Blots are representative of three independent experiments.

To get further insights about the role of TGFβ signalling in cytokine-induced shape changes of ECs, SB431542 was added in combination with TNF and IL1β and cell elongation was quantified. Compared to control (DMSO), SB431542 treatment alone induced a slight increase in cell elongation (Figure 27). The presence of brighter light around the cell body suggest that this effect may be due to an alteration of cell junctions. Nonetheless, the elongation induced by SB431542 appeared phenotypically different from the one induced in TNF+IL1β-treated cells, which were instead characterised by an overall extension of the cell body. Interestingly, when ECs were treated with both SB431542 and TNF-IL1β, cell elongation reached its highest value and cells became extremely spindle-shaped, a morphology reminiscent of fibroblast cells.

Overall, these results confirm the lack of effect of TGFβ signalling in inducing a mesenchymal-like phenotype. Conversely, the inhibition of TGFβ signalling enhanced cell elongation induced by TNF and IL1β, thus suggesting that TGFβ may act on ECs to preserve junctional integrity.

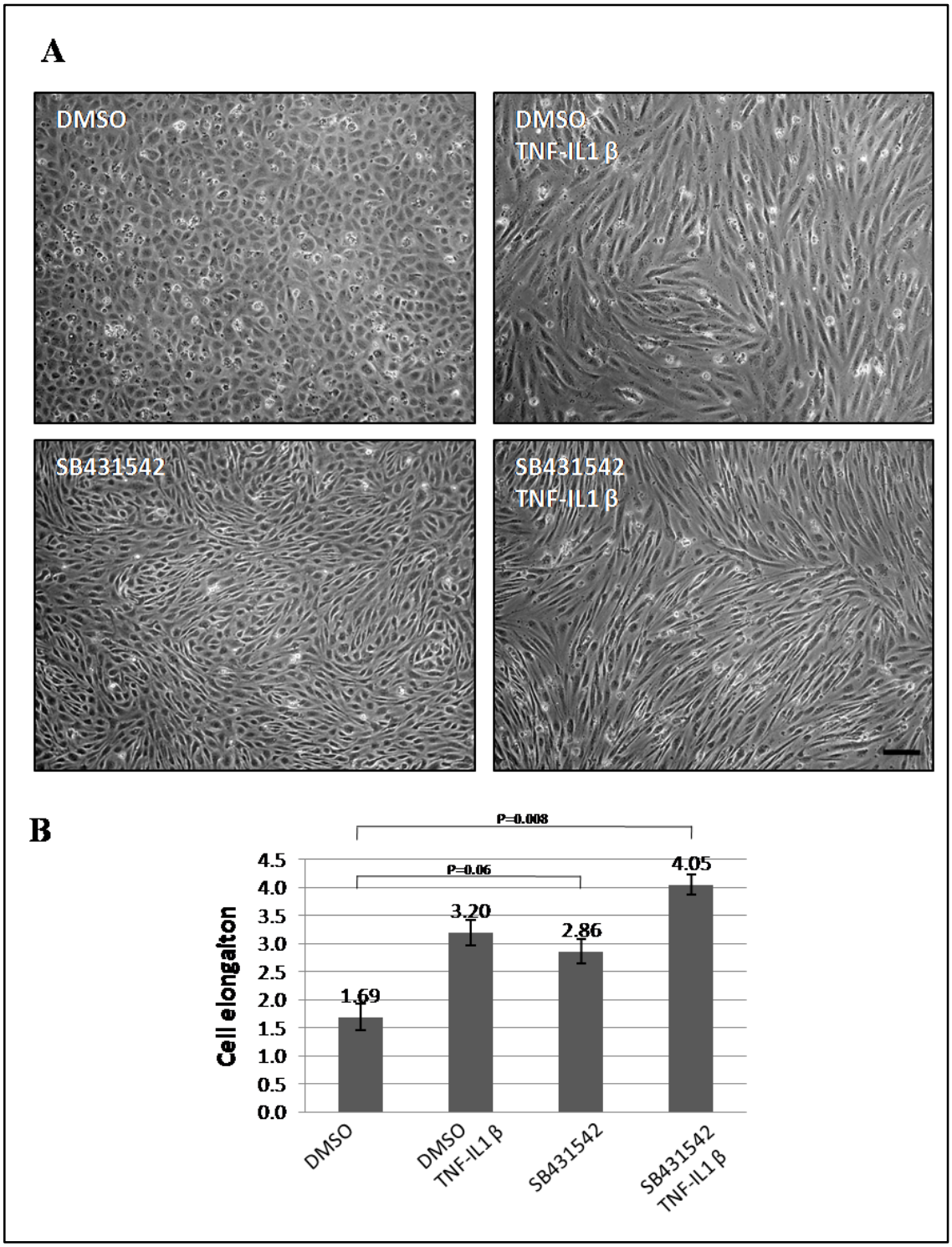

Figure 27: Inactivation of TGFβ signalling increases cytokine-induced cell elongation. A) Representative images of HUVECs grown to confluence and treated for 24 hours with 10 ng/ml of TNF and IL1β in the presence of SB431542 inhibitor or DMSO. Scale bar: 100µm. **B)** Quantification of cell elongation was performed on multiple images of each condition using ImageJ software (see section 2.7 for method details). Error bars represent S.D. (n=3). * $P < 0.05$ (Student's t-test).

The TGFβ signalling-dependent activation of transcription has been reported to play a significant role in the EndMT, with several mesenchymal genes dramatically induced and thus considered markers for the process (71, 72). The expression of two of those genes, SM22 (TAGLN) and PDFGβ, was then analysed in HUVECs treated with TNF and IL1β in the presence of SB431542 to check whether there was any correlation between increased transcription and morphological change. The expression of SM22 was moderately induced by almost 2.5 folds in TGFβ2-treated cells compared to control, while it was not increased by either TNF-IL1β or SB431542 (Figure 28). When HUVECs were treated with both SB431542 and TNF+IL1β, the expression of SM22 was downregulated by almost 5 folds compared to untreated cells. Thus, these results indicate that SM22 expression does not correlate with cell elongation and that its transcription is not activated by inflammatory cytokines in ECs. On the other hand, the expression of PDFGβ was up-regulated by TNF+IL1β by 4 folds compared to control, while there were no consistent changes in TGFβ2 or SB431542-treated cells. Interestingly, in the presence of SB431542 inhibitor the effect of TNF-IL1β was abrogated.

Taken together, these data show that PDFGβ expression is induced by pro-inflammatory cytokines and that this effect is dependent on TGFβ signalling. Yet, the increased expression does not seem to reflect the dramatic difference expected for newly acquired mesenchymal markers.

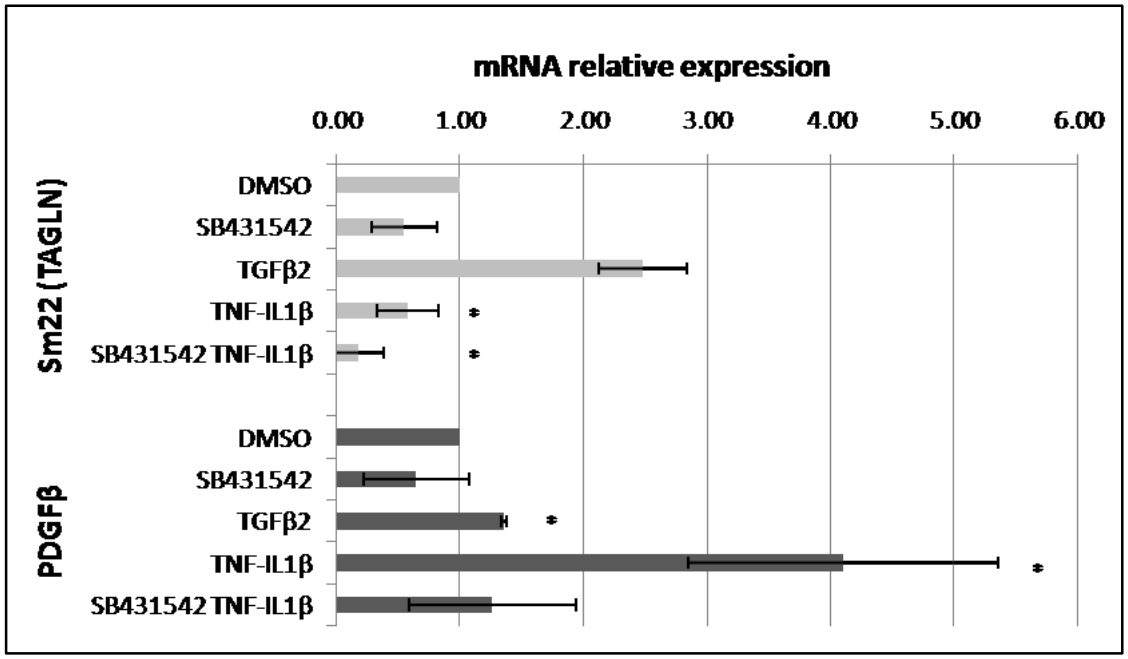

Figure 28: Gene expression analysis of mesenchymal markers in cytokine-treated endothelial cells. HUVECs were treated with the indicated cytokines for 24 hours in the presence of the SB431542 inhibitor. Extracted RNA was analysed through quantitative RT-PCR. The mRNA expression levels were represented as fold change relative to control (DMSO). All values were normalized with the expression of RPL13A housekeeping gene and represent the mean ±S.D. (n=3). * $P < 0.05$, all other values $P > 0.05$ (Student's t-test).

4.2.4 Immunofluorescence staining of ECs treated with inflammatory cytokines

To gain more insights into the morphological changes induced by pro-inflammatory cytokines in ECs, HUVECs were stained for F-actin and VE-Cadherin, two main constituents of the cytoskeleton and cell junctions, respectively. In the immunofluorescence pictures shown in Figure 29, the compact arrangement of untreated cells was dramatically altered by TNF+IL1β: cells became enlarged with disrupted cell junctions, although the expression of VE-Cadherin did not seem to be reduced significantly. Moreover, F-actin staining of control cells highlighted the distribution of actin around the cytoplasm, while in the presence of TNF+IL1β actin filaments became predominantly parallel to the long cell body axis. Overall, these data suggest that pro-inflammatory cytokines induce extensive structural reorganisations in the actin cytoskeleton and junctions of ECs.

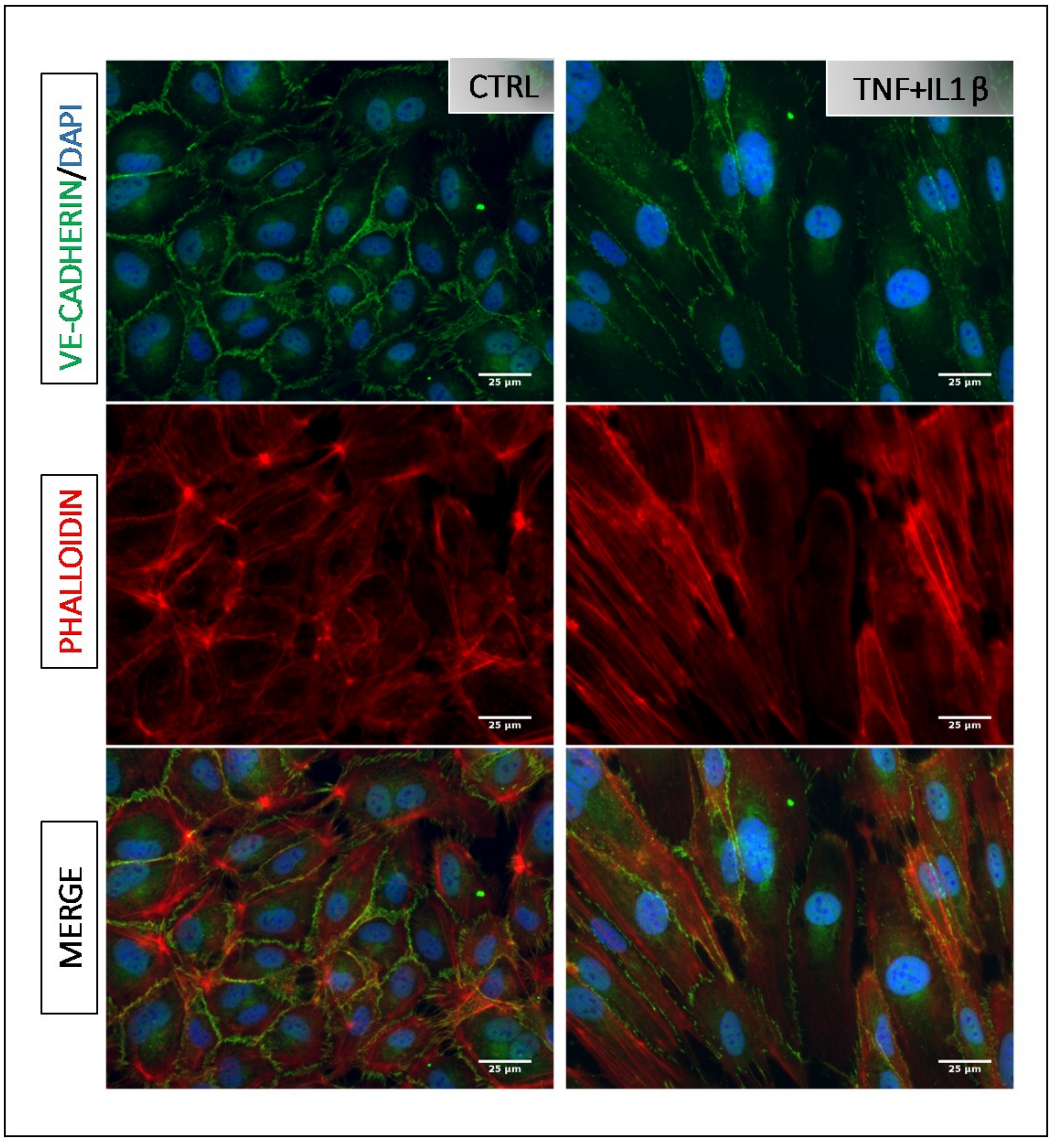

Figure 29: Immunofluorescent staining of HUVECs treated with inflammatory cytokines. Confluent HUVECs were either left untreated or stimulated with 10 ng/ml TNF+IL1β for 24 hours. Cells were stained for F-Actin (red) and VE-Cadherin (green). Cell nuclei were stained with DAPI (blue). Scale bars = 25µm. Images are representative of at least three independent experiments.

4.3 Conclusions

In this result chapter, the effect of inflammatory cytokine treatment on EC morphology was examined *in vitro*. The results are summarized in the following points:

- Both TNF and IL1β induce a consistent morphological change in ECs, determining the acquisition of a spindle-shape. Cell elongation is increased in presence of both cytokines. In contrast, TGFβ2 has no effect on EC morphology

- TGFβ signalling is active in ECs and its blockage increases cytokine-induced cell elongation; it may thus preserve vessel integrity in inflammatory conditions

- Gene expression analysis of endothelial and mesenchymal markers in presence of inflammatory cytokines does not suggest the transition of ECs into a mesenchymal cell type

- TNF and IL1β induce the rearrangement of the actin cytoskeleton of ECs and the formation of gaps at cell junctions

4.4 Discussion

4.4.1 What factors induce EndMT *in vitro*?

ECs cultured *in vitro* have been shown to recapitulate the EndMT occurring *in vivo* during fibrosis, thereby offering the opportunity to decipher the underlying molecular mechanism and to find potential therapeutic targets. The key factor that has been shown to induce EndMT *in vitro* is TGFβ2 (67, 87). Contrary to these studies, results presented in this thesis do not support a role of TGFβ2 in inducing EndMT in human ECs (4.2.1). In the presence of this growth factor, HUVECs retain a rounded, cobblestone morphology and the expression of a panel of EndMT markers, as measured by quantitative RT-PCR, is not significantly changed. Moreover, the unaffected expression of the endothelial specific marker VE-Cadherin was also confirmed at protein level. The discrepancy between these data and those reported in previous publications (54, 67, 87) may have different explanations. First of all, the experimental setting used in this study is different from those in the aforementioned publications as HUVECs have been cultured with complete medium, thus in the presence of different growth factors that could interfere with the analysis. To induce EndMT, Medici et al. cultured HUVECs for 72 hours in serum-free medium (67, 87). Initial experiments aiming at reproducing this protocol failed as in the serum-free condition most HUVECs died within 24 hours. The use of complete medium was then adopted to overcome this limitation. Nonetheless, further analyses showed that TGFβ signalling was biochemically active in HUVECs; upon cytokine/growth factor treatment, Smad2 phosphorylation was increased and downstream target genes were transcriptionally increased. Taken together, these data suggest that TGFβ2 is not able to induce the EndMT in human ECs.

Although in conflict with recent influential publications and related reviews putting the TGFβ-EndMT axiom forward, the results obtained here are consistent with other reports in the literature that examined the effect of TGFβ in ECs. For instance, several studies failed to induce morphological change and/or expression of αSMA in different types of human ECs, including HUVECs, HAECs and HMECs (60, 63, 64, 151). The inability of TGFβ alone to induce EndMT was also reported in earlier studies of endocardial cushions formation that highlighted instead how multiple factors and related signalling pathways are necessary for the different steps of endothelial transdifferentiation (152, 153). Furthermore, experiments with TGFβ inhibitors in combination with inflammatory

cytokines suggested that constitutive TGFβ signalling may actually serve to maintain the integrity of endothelial junctions, in agreement with other reports showing its role in vascular integrity (see next section) (154, 155).

4.4.2 Inflammatory cytokines induce a morphological change in human endothelial cells: is this an EndMT?

A recent study reported that inflammatory cytokines such as TNF and IL1β could induce the EndMT in intestinal ECs, describing this process "inflammation-induced EndMT" (156). The results obtained here reveal that both TNF and IL1β significantly increased cell elongation of HUVECs, as assessed quantitatively through a morphological analysis on bright-field cell culture images (4.2.1). Furthermore, cell elongation was further increased when both TNF and IL1β were added together. This indicates a synergistic effect among cytokines, consistent with previous studies (156, 157). To check whether this observed phenotype could be interpreted as an EndMT, the expression of several EndMT-related markers were measured in HUVECs treated with different combinations of inflammatory cytokines. Upon 48 hours treatment, no significant changes were observed in the expression of the endothelial markers VE-Cadherin and Pecam1 in any of the conditions tested, whereas eNOS was downregulated when all cytokines where administered together. The expression of classical mesenchymal markers, e.g. αSMA, FSP1 and N-cadherin, was also unaltered in the presence of cytokines (4.2.2). The unchanged expression of VE-Cadherin was also confirmed by Western blot analyses and immunofluorescence staining. Thus, these results suggest that the fibroblast-like elongation phenotype induced by inflammatory cytokines is not consistent with the EndMT. Interestingly, when HUVECs were stimulated with TNF+IL1β in the presence of the TGFβ inhibitor SB431542, cell elongation was further increased compared to TNF+IL1β treatment alone (4.2.3). Also, the administration of SB431542 resulted in altered cell junctions visible in bright field images as brighter light around cell borders. These results confirm on one hand the independence of the observed shape changes from TGFβ signalling and on the other hand, highlight the importance of the crosstalk between TGFβ and inflammatory signals in the maintenance of vascular integrity, as previously reported (154, 155).

Furthermore, F-actin/VE-Cadherin immunofluorescence co-staining of TNF+IL1β-

treated HUVECs revealed cytoskeletal rearrangements and formation of junctional gaps (4.2.4). Actin fibres, which were present around the cell cortex in untreated cells, formed long bundles parallel to the cell axis in the presence of inflammatory cytokines. These structural features are consistent with earlier studies showing a similar response of cytokine-treated human ECs (146, 158).

Overall, in light of earlier literature the results obtained here suggest that the phenotype resulting from TNF+IL1β treatment can be interpreted as a structural cell remodelling rather than a differentiation towards different cell lineages such as fibroblast or smooth muscle cells. As described in the introduction (1.1.3.4) during inflammation the endothelium becomes "activated", resulting in several biochemical and structural changes. Among these responses, the modulation of endothelial cell-cell junctions plays a prominent role as it facilitates the transmigration of immune cells from the bloodstream to the site of injury/infection (29).

Chapter V – Results: regulation cytokine-induced morphology changes of endothelial cells

5.1 Introduction

Shape is an important indicator for cell physiology and is tightly controlled in development during tissue morphogenesis. The dramatic morphological changes of individual cells occurring in EMT during gastrulation are essential to drive the formation of germ layers. In ECs, shape changes correlate with the physiological status of blood vessels and are controlled by both cellular and environmental factors. For instance, hemodynamic forces generated by blood flow have been shown to induce dramatic morphological changes in ECs (159, 160). Both cytoskeletal rearrangements and external forces concur in cellular mechanotransduction, which is an emerging component of disease pathogenesis.

EndMT have been often described with a consistent change of cellular shape. Conversion of the rounded (and static) phenotype — the cobblestone morphology — into a fibroblast-like spindle shape, has been considered a hallmark of the mesenchymal transition (see section 1.3). EC undergoing EndMT acquire invasive and secretory properties that eventually contribute to fibrosis and other disorders.

As shown in Chapter IV, inflammatory cytokines are also able to induce a morphological change in ECs, which is seemingly consistent with the EndMT reported previously; therefore, it was sought to identify the regulators of this phenotype, in order to shed light on the physiological and pathological relevance of this process.

The aims of this result section are:

- To identify cytokine-induced genes that might play a role in the morphological change of ECs *in vitro*

- To dissect the inflammation-induced signalling pathways involved in the acquisition of an elongated phenotype in ECs

5.2 Results

5.2.1 Role of the cytoskeletal regulator RND1 in endothelial cell elongation

To find new potential mediators of the morphological changes of ECs, published microarray data of gene expression of inflammation-stimulated ECs were searched. One study presented an informative list of novel genes activated by TNF in human ECs (161). Among those genes, a GTP-binding protein was reported to be significantly induced by TNF, with a fold induction relative to control >5. This gene corresponds to the Rho-GTPase RND1, a protein which was previously shown to be involved in the regulation of actin cytoskeleton (162). To confirm the transcriptional activation of RND1, HUVECs were stimulated with inflammatory cytokines and RND1 expression was analysed by qPCR at two different time points, 6 and 48 hours. As shown in Figure 30, RND1 expression was dramatically increased 6 hours after treatment, with >20 folds induction in both TNF- and IL1β-treated cells. Interestingly, when cells were treated with both cytokines together the expression of RND1 raised to almost 80 folds compared to control, suggesting a synergistic effect of TNF and IL1β on its activation. However, due to high variability of expression levels, the differences between the conditions did not reach statistical significance. At 48 hours the expression of RND1 was still increased relative to control but all values were lower compared to the 6 hours time point. In TNF- and IL1β-treated cells RND1 expression reached a 5-fold change compared to control, while in cells treated with TNF+IL1β, similarly to the 6 hours time point, RND1 expression was further increased compared to cells treated with either cytokines alone (27-fold). These results thus indicate that RND1 is rapidly activated by an inflammatory stimulus in human ECs and notably, its expression seems to be synergistically increased by TNF and IL1β. This effect correlates well with the increased cell elongation induced by TNF+IL1β and make this gene a potential regulator of the morphological changes observed in ECs.

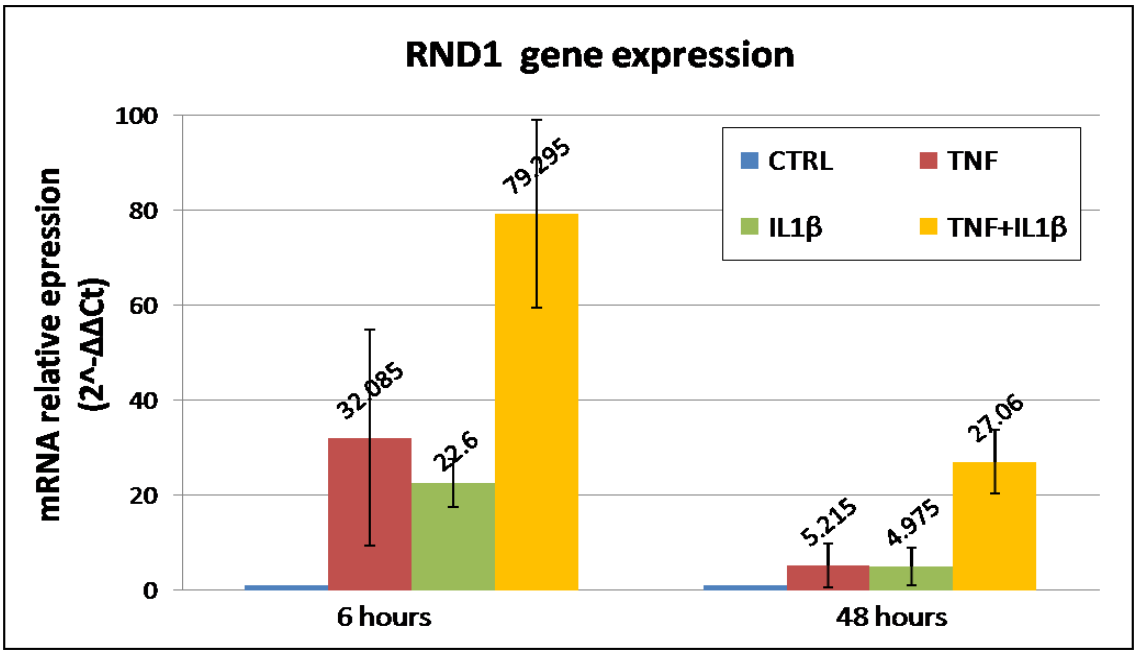

Figure 30: RND1 is upregulated in cytokine-treated human endothelial cells. HUVECs were treated with TNF, IL1β or TNF+IL1β for 6 or 48 hours. Extracted RNA was analysed through quantitative RT-PCR. mRNA expression levels were represented as fold change relative to untreated cells (CTRL). All values were normalized with the expression of RPL13A housekeeping gene and represent the mean ±S.D. (n=2). $P > 0.05$ for all conditions (Student's t-test).

To test the hypothesis that RND1 regulates the cytoskeletal rearrangements of ECs induced by inflammatory cytokines, a siRNA gene silencing approach was used. The activation of RND1 expression by TNF and IL1β was blocked through a siRNA pool that targets RND1 mRNAs. This inhibition was achieved with high efficiency, as in HUVECs treated with RND1 siRNA the expression of RND1 was reduced >90% compared to the baseline level of untreated cells (Figure 31). In unstimulated cells, the addition of RND1 siRNA had no detectable effect on cell morphology (Figure 32 A). As expected, the addition of TNF and IL1β induced an increase in cell elongation. However, in the presence of RND1 siRNA, cell elongation was still higher than that in untreated cells and it was even slightly increased compared to inflammation-induced RND1-unsilenced cells (Figure 32 B). Therefore, these results refute the hypothesis that Rho-GTPase RND1 regulates inflammation-induced cytoskeletal rearrangements of ECs. Nonetheless, the magnitude of cytokines-induced transcriptional activation of RND1 suggests potential unknown functions of this protein in ECs during inflammation.

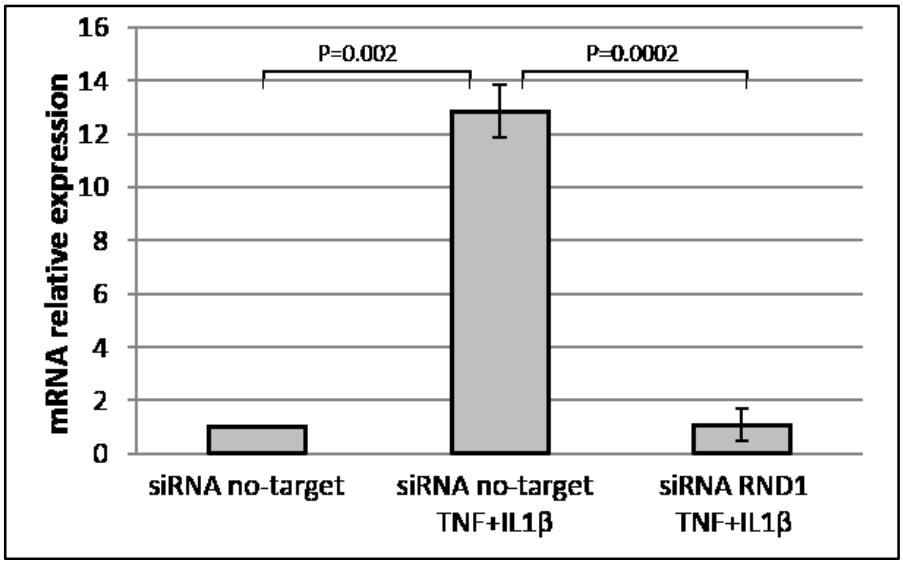

Figure 31: Efficiency of RND1 gene silencing in endothelial cells. HUVECs were treated with a combination of TNF and IL1β together with either RND1-targeting siRNAs or non-targeting siRNAs as a control. RNA from each condition was extracted 24 hours after treatment and analysed through quantitative RT-PCR. The mRNA expression levels were represented as fold change relative to siRNA no-target. All values were normalized with expression levels of the RPL13A housekeeping gene and represent the mean ±S.D. (n=3). P-values were calculated using the Student's t-test.

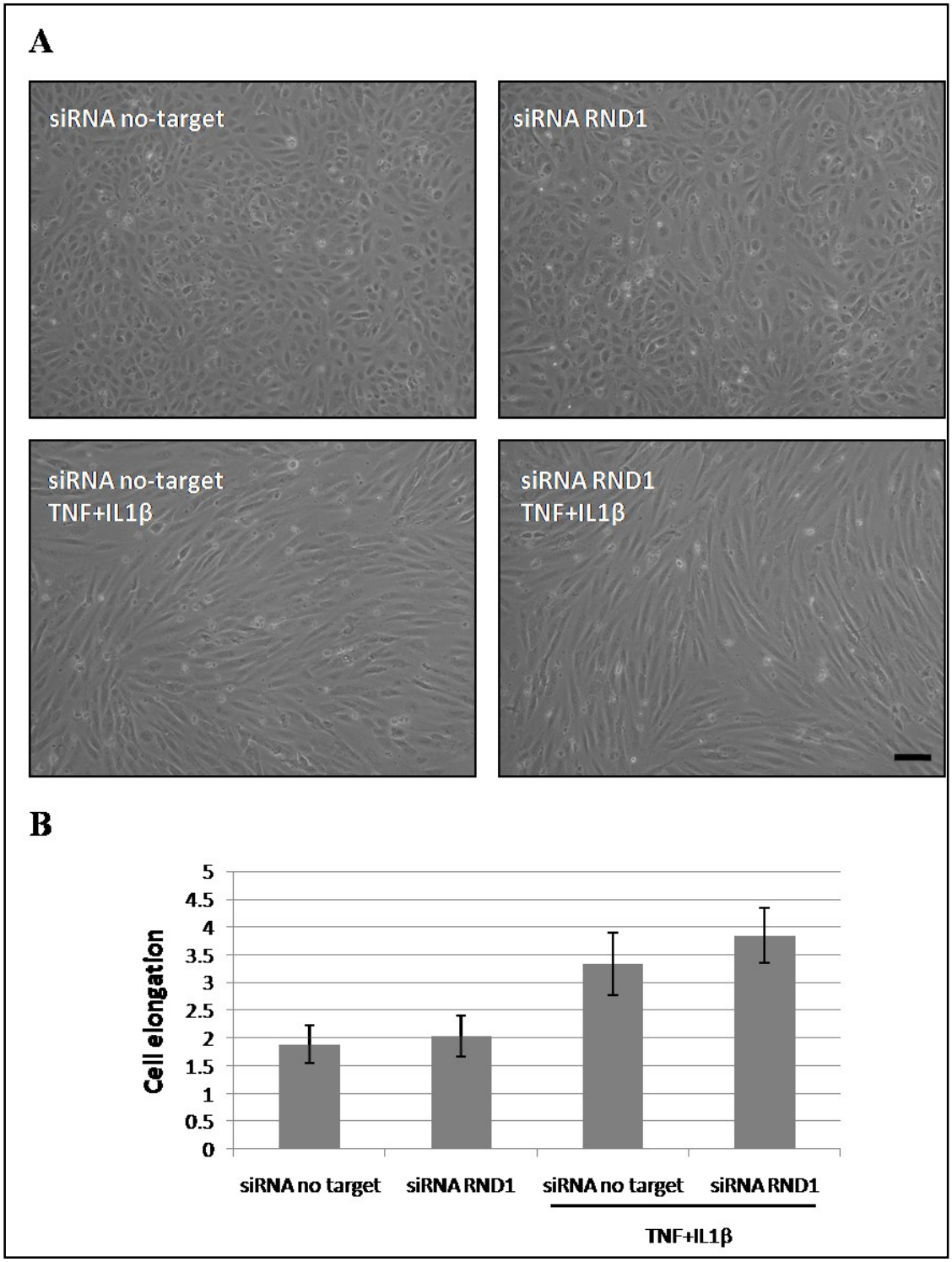

Figure 32: RND1 gene silencing has no effect on cytokine-induced endothelial cell elongation. A) HUVECs were treated for with either RND1 siRNAs or non-targeting siRNAs as a control, together with a combination of the inflammatory cytokines TNF and IL1β. Cell culture images were acquired 24 hours after treatment. Scale bar: 100 μm. B) Quantification of cell elongation was performed on multiple images of each condition using ImageJ software (see section 2.7 for method details). Error bars represent S.D. (n=4). * $P < 0.05$ (Student's t-test).

5.2.2 Signalling pathways involved in endothelial cell elongation

Several signalling pathways have been associated with the remodelling and dynamics of cell cytoskeleton (163). In order to define which signalling is involved in inflammation-induced morphological changes of ECs, different chemical inhibitors were used to target specific proteins. A highly characterised regulator of the actin cytoskeleton is protein kinase ROCK (Rho-associated protein kinase), which is an effector in the Rho-signalling pathway and involved in different cellular functions, including cell shape, motility and migration(164). To check whether ROCK plays a role in the cell elongation observed in HUVECs, cells were stimulated with TNF and IL1β in the presence of the potent inhibitor Y27632 (165). Inhibition of ROCK had the visible effect of reducing cytokine-induced morphological rearrangement, which was confirmed by quantification of cell elongation (Figure 33). These results are consistent with earlier study showing a ROCK-mediated effect of TNF on the morphology of ECs (146, 158). Nonetheless, ROCK inhibition altered the cytoskeleton of HUVECs by inducing the formation of thin cellular protrusions, which seemed to increase in number upon TNF+IL1β stimulation (Figure 34). In agreement with this, ROCK has been previously reported to limit membrane protrusion induced by integrins in leukocytes (166).

To investigate additional components of the Rho-signalling pathway involved in the cytoskeletal rearrangements of HUVECs, cells were treated with inhibitors that target Rho GTPase family (RhoA, B, C) and Myosin Light Chain Kinase, which act upstream and downstream of ROCK kinase, respectively. As shown in Figure 35, both inhibitors (C3 transferase and ML7) failed to prevent the cell elongation induced by TNF+IL1β. Inhibition of Rho gave rise to a significant cell shrinking and rarefaction of the cytoskeleton, while the inhibition of MLCK did not produce a discernible phenotype. These data indicate that although ROCK kinase has a consistent effect in TNF+IL1β-induced endothelial cell elongation, the mediators that transmit the signalling to the cytoskeleton may not include the Rho GTPase-MLCK axis.

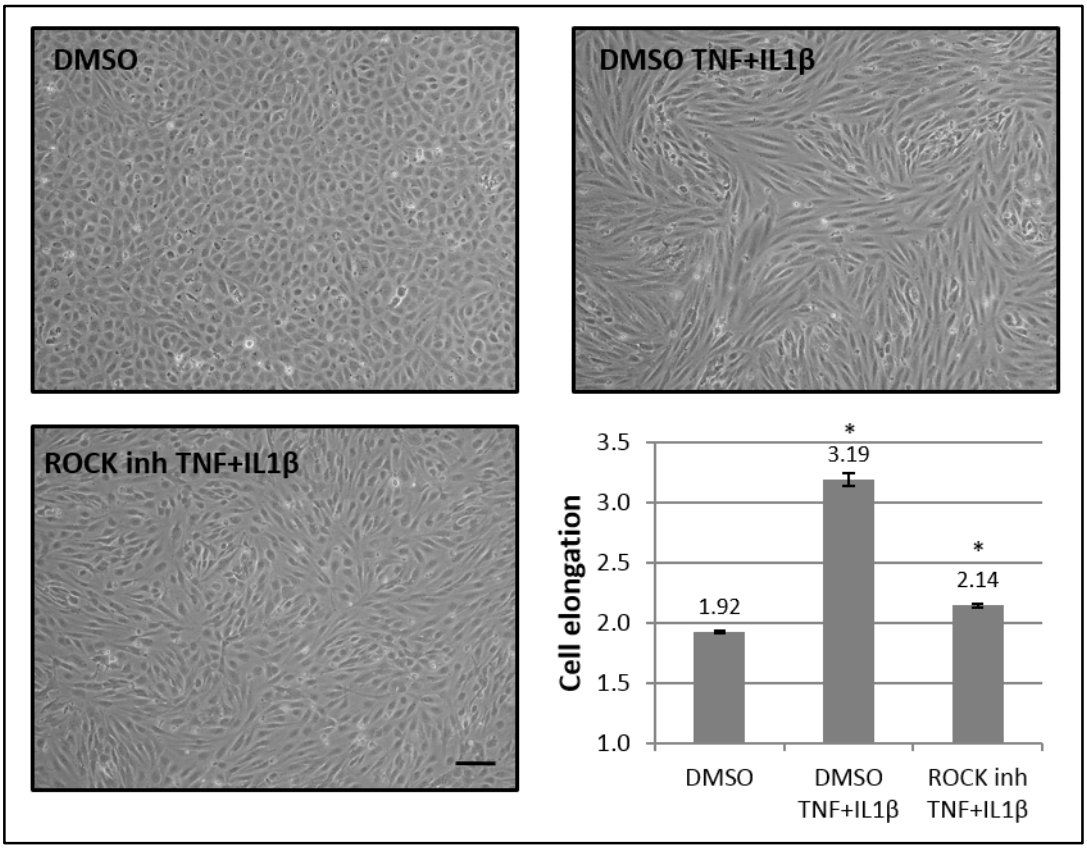

Figure 33: ROCK inhibition abolishes TNF+IL1β-induced endothelial cell elongation. HUVECs were treated with a combination of TNF and IL1β in the presence of 5μM of ROCK1 inhibitor Y27632. Control cells were treated with DMSO. Bright field images were acquired after 24 hours. Scale bar: 100 μm. Quantification of cell elongation was performed on multiple images of each condition using ImageJ software (see section 2.7 for method details). * $P < 0.05$ (Student's t-test).

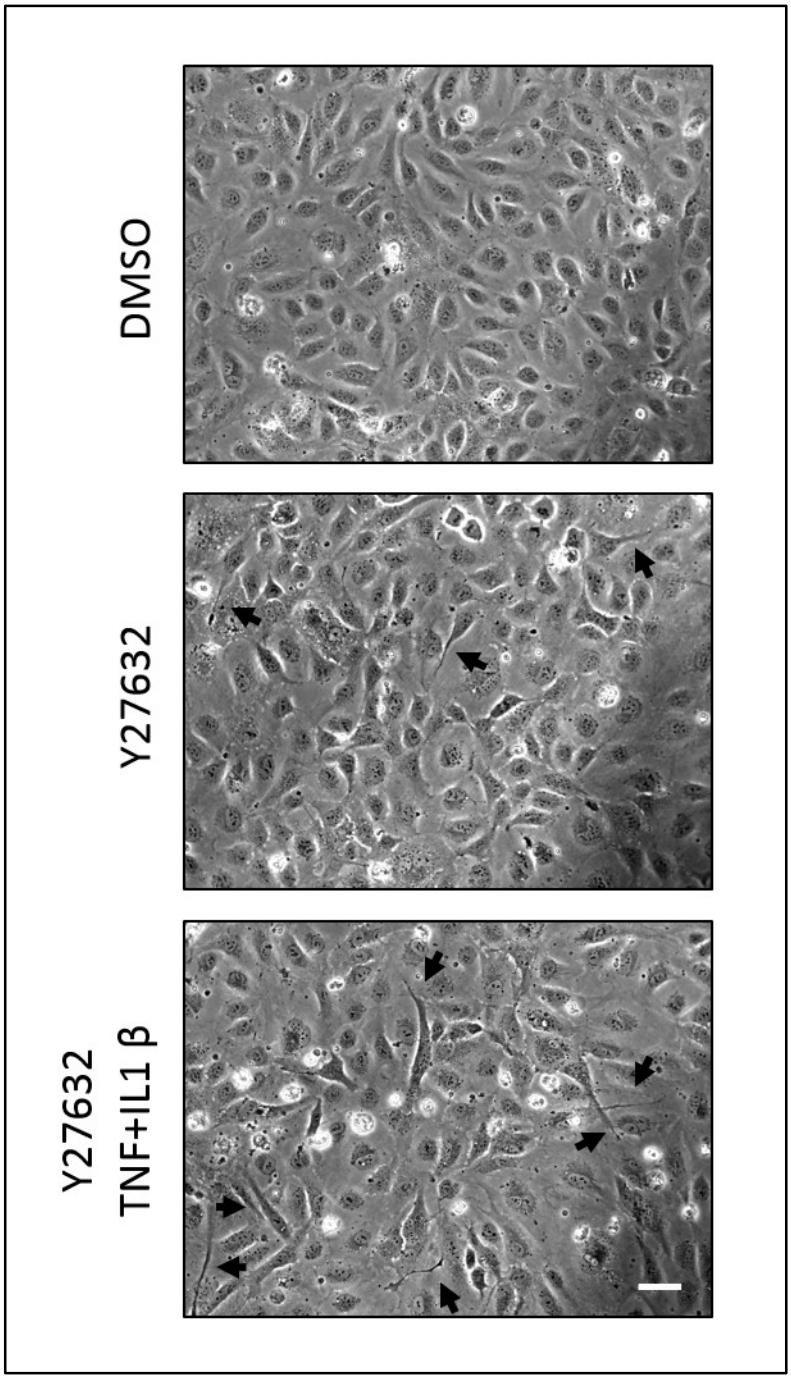

Figure 34: ROCK inhibition induces cell protrusions in endothelial cells. 20X magnification bright-field images of HUVECs treated with the ROCK inhibitor Y27632 (5μM) in the presence of TNF and IL1β (10ng/ml). Images were acquired at 24 hours post treatment. Black arrows indicate cell protrusions. Scale bar: 50μm. Images are representative of two independent experiments.

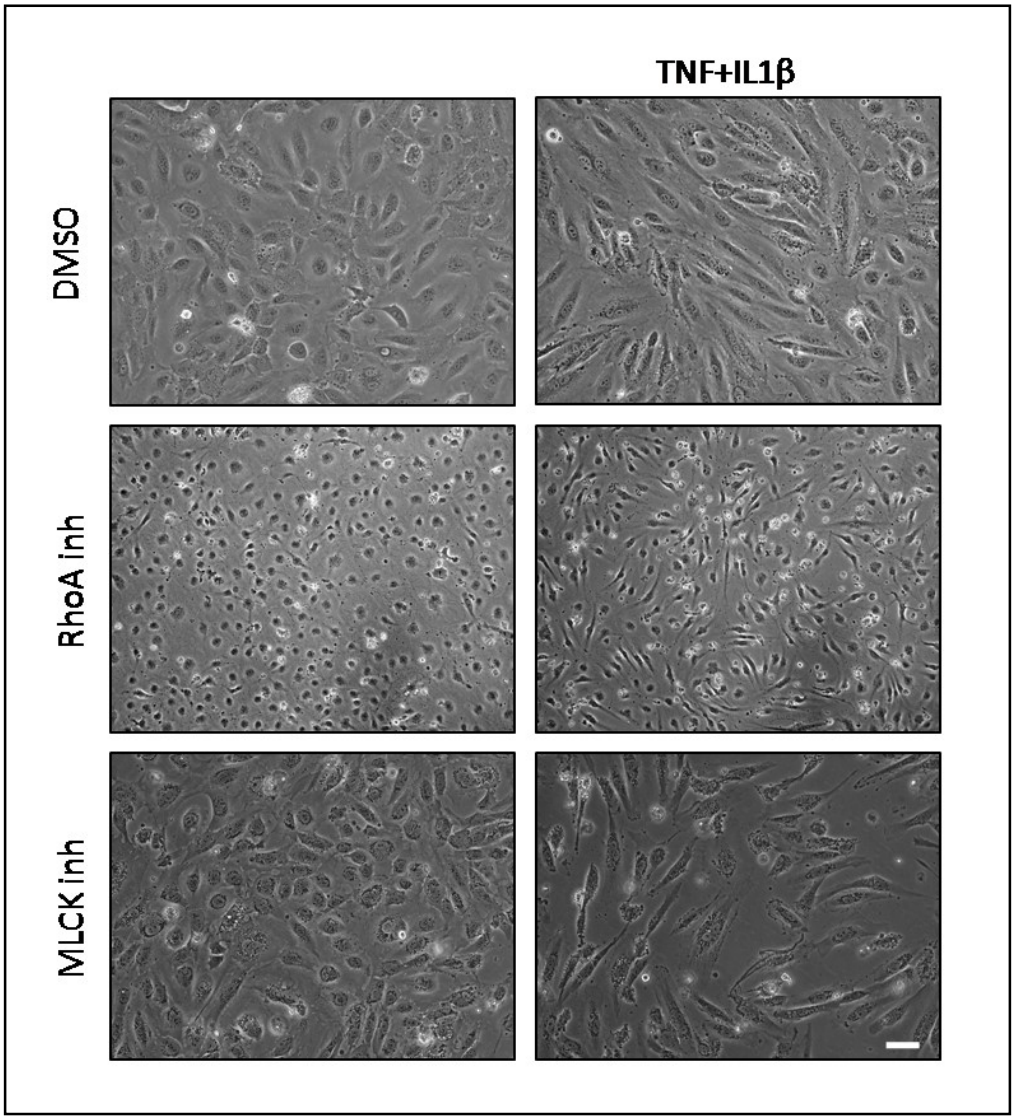

Figure 35: Chemical inhibition of Rho signalling mediators has no effect on cytokine-induced endothelial cell elongation. HUVECs were treated with a combination of TNF and IL1β in the presence of the RhoA, B, C inhibitor C3 transferase (1μg/ml) or the Myosin Light Chain Kinase (MLCK) inhibitor ML7 (10μM). Images were acquired at 24 hours post treatment. Scale bar: 100 μm. Images are representative of three independent experiments.

5.2.3 Role of NF-κB signalling in cytokine-induced cell shape changes in endothelial cells

The canonical signal transduction pathway triggered by the pro-inflammatory cytokines TNF and IL1β results in the activation of the transcription factor NF-κB, which in turn induces or represses the transcription of genes necessary for innate immunity and cell survival (167). In normal conditions, NF-κB is retained in the cytoplasm bound to the inhibitors IκB. In response to inflammatory stimuli, the enzymatic kinase complex IKK phosphorylates IκB, leading to its degradation and the consequent release of NF-κB.

As shown in the time-course analysis in Figure 36, IκBα was rapidly degraded in HUVECs after 15 minutes of TNF+IL1β treatment. The protein level remained relatively low at 30 minutes, while after 1 hour, it returned of comparable levels to that of untreated cells. From 2 hours onwards, IκBα was robustly expressed at a higher level than that observed in control. These data suggest that the transcriptional activity of NF-κB is concentrated in a short time window and that after the initial stimulus, ECs may quickly become resistant to further signals by expressing the IκBα inhibitor.

In order to investigate whether the modulation of NF-κB affects the morphological change of ECs, HUVECs were treated with the chemical inhibitor *Wedelolactone*, a natural molecule derived from the herbal medicine *Eclipta alba* that acts as a cell irreversible inhibitor of IKKα and β kinase activity (168). Cell culture images of HUVECs in Figure 37 show that the cytoskeletal rearrangements induced by TNF+IL1β were significantly reduced in the presence of the IKK inhibitor. Cell shape quantification further confirmed that the elongation scores of cytokine-stimulated HUVECs were similar to that of DMSO-treated cells.

Taken together, these results indicate that NF-κB signalling is directly involved in cell shape changes of ECs through the activity of IKK kinases. It remains to be determined whether this function involves the NF-κB-dependent transcription or just the direct modulation of cytoskeletal regulators.

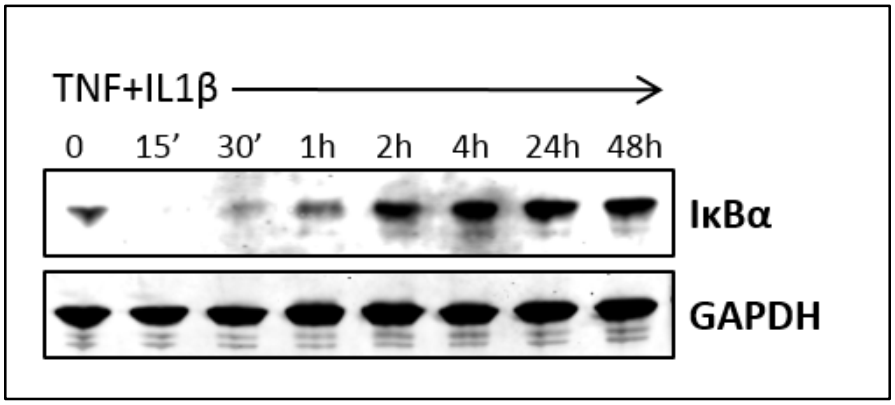

Figure 36: TNF and IL1β induce a transient degradation of IκBα in endothelial cells. HUVECs were treated with a combination of TNF and IL1β for 15 minutes up to 48 hours. Protein lysates were collected at the indicated time points and subjected to Western blot analysis with the IκBα antibody. GAPDH was used as a loading control. Blot is representative of at least three independent experiments.

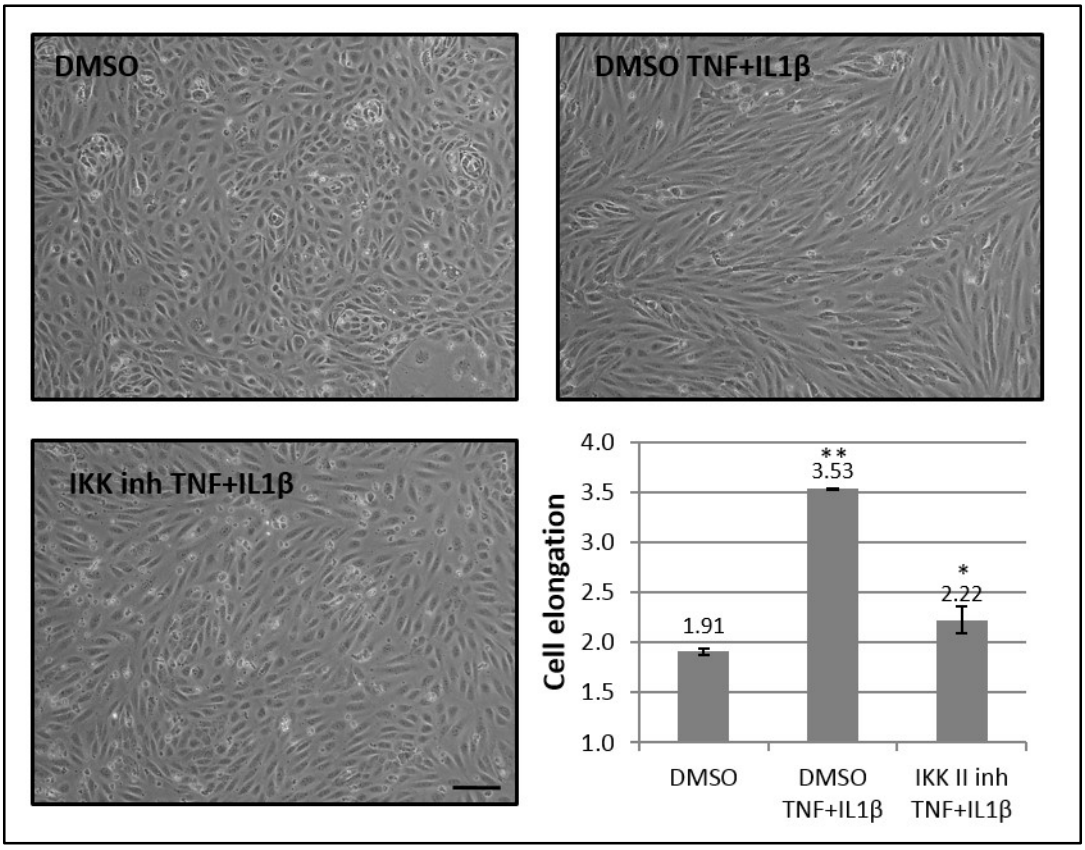

Figure 37: IKK inhibition abolishes TNF+IL1β-induced endothelial cell elongation. HUVECs were treated with a combination of TNF and IL1β in the presence of 10μM of IκB kinase (IKK) inhibitor. Control cells were treated with DMSO. Scale bar: 100 μm. Quantification of cell elongation was automatically calculated with ImageJ software from multiple image of each condition.

In order to determine which regulators are involved downstream of NF-κB and ROCK signalling pathways in the rearrangement of endothelial cell shape, Western blot analyses was performed in HUVECs treated with the pro-inflammatory cytokines. It was initially speculated that the protein cofilin, an established factor that regulates the dynamic of F-actin (169), could participate in the inflammation-induced cell elongation of HUVECs. The time-course analysis of cofilin phosphorylation shown in Figure 38 confirms this hypothesis. Cofilin became increasingly phosphorylated throughout TNF+IL1β stimulation, reaching its peak at 48 hours. Phosphorylation of cofilin is thought to inhibit its actin-depolymerizing activity (170), although this mode of regulation has been shown to be more complex that previously appreciated (171). Nevertheless, the phosphorylation of cofilin induced by the pro-inflammatory cytokines is consistent with the hypothesis that the activation of this cytoskeletal regulator may be responsible for the F-actin rearrangement observed in HUVECs.

To further investigate the role of cofilin phosphorylation in endothelial cell elongation, cytokine-stimulated HUVECs were treated with ROCK and IKK inhibitors and analysed by Western blot. As shown in Figure 39, the increased phosphorylation of cofilin induced by TNF+IL1β was abolished in the presence of both inhibitors, suggesting a possible role of cofilin phosphorylation in the cytokine-induced elongation of HUVECs. However, the IKK inhibitor alone increased cofilin phosphorylation compared to that in control cells, even though it did not induce cell elongation. This data would then suggest that the phosphorylation of cofilin is correlated to cytoskeletal elongation but it may not have a causal role in the process. Further experiments would be required to assess the nature of this causality (i.e., blocking directly cofilin phosphorylation).

The phosphorylation of VE-Cadherin was also examined, as it has been shown to play a role in the reorganisation of endothelial junctions and the increase in vascular permeability during inflammation (172). In HUVECs treated with TNF+IL1β the phosphorylation of VE-Cadherin at residue Y731 was increased, confirming the previous findings. In the presence of the elongation-blocking inhibitors Y27632 and IKK II however, the increased phosphorylation was not inhibited. These results suggest that VE-Cadherin phosphorylation may not be necessary for the rearrangement of the actin cytoskeleton but independently required for adherens junction maintenance during inflammation.

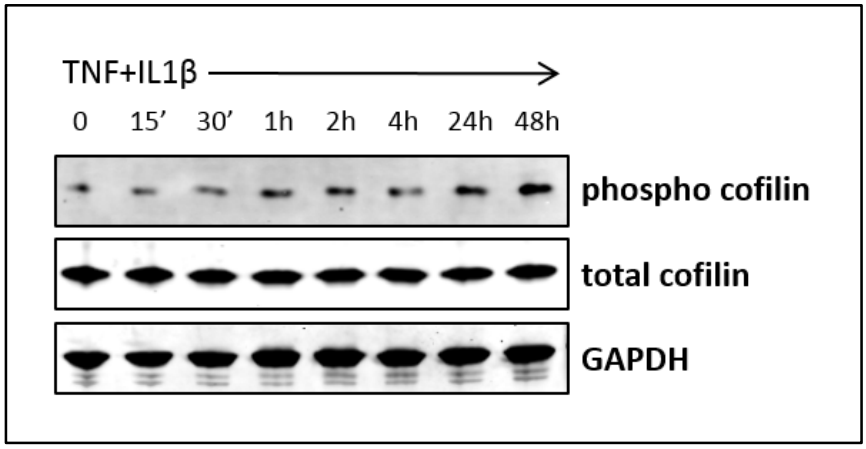

Figure 38: TNF and IL1β induce cofilin phosphorylation in a time-dependent manner. HUVECs were treated with a combination of TNF and IL1β for 48 hours. Protein lysates were collected at the indicated time points and subjected to Western blot analysis with different antibodies. GAPDH was used as a loading control. Blot is representative of three independent experiments. Blot is representative of at least three independent experiments.

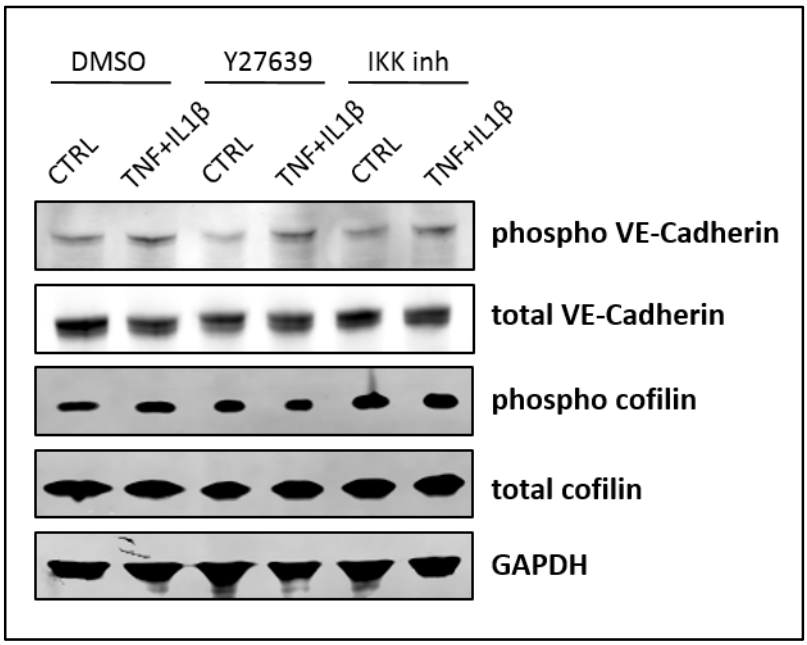

Figure 39: Protein phosphorylation in cytokine-treated endothelial cells in the presence of chemical inhibitors. HUVECs were treated for 24 hours with a combination of TNF and IL1β in the presence of the Rho inhibitor Y27632 and the IKK inhibitor. Control cells were treated with DMSO. GAPDH was used as a loading control. Blot is representative of three independent experiments.

5.2.4 Notch signalling role in inflammation-induced endothelial cell elongation.

The cellular effects induced by the pro-inflammatory cytokines TNF and IL1β on ECs have been recently interpreted in the literature as a "mesenchymal transition", mainly because of the elongated shape reminiscent of fibroblast-like cells (71, 156). However, this morphological change is also consistent with ECs acquiring a tip cell phenotype (see section 1.1.2 and Figure 2). During angiogenesis, endothelial tip cells are the leading cells that are located at the tips of vascular sprouts and are characterised by several functional and molecular changes (173). The angiogenic tip cell phenotype plays a crucial role during vascular development but can also be induced by inflammation in adult vasculature (174, 175). To determine whether the molecular changes in inflammation-induced ECs reflect an angiogenic response, the expression of members of the Notch signalling was examined, as this pathway has a central role in the process (176). The qPCR analysis shown in Figure 40 indicated that when HUVECs were stimulated with pro-inflammatory cytokines the transcriptional activity of Notch-related genes was affected. HEY1, a transcriptional repressor which acts downstream of Notch, was significantly induced by TNF+IL1β, with a fold induction of mRNA level >20 compared to that in untreated cells. Furthermore, the gene expression of two Notch ligands, Jagged1 (JAG1) and Delta-Like 4 (DLL4) were differentially regulated; JAG1 expression was increased around 5-folds by TNF+IL1β, while the mRNA expression level of DLL4 was downregulated by 4 folds. This regulation pattern was consistent with a recent report showing that the ratio of JAG1/DDL4 expression was an important mechanism for tip cell selection during angiogenesis (177). The increased expression of the JAG1 ligand by pro-inflammatory cytokines in HUVECs was further confirmed at protein level by Western blot (Figure 41). Taken together, these results show that TNF and IL1β activate Notch signalling in ECs and induce a differential regulation of two Notch ligands. This corroborates the hypothesis that the morphological and molecular changes observed in HUVECs are indicative of an angiogenic response.

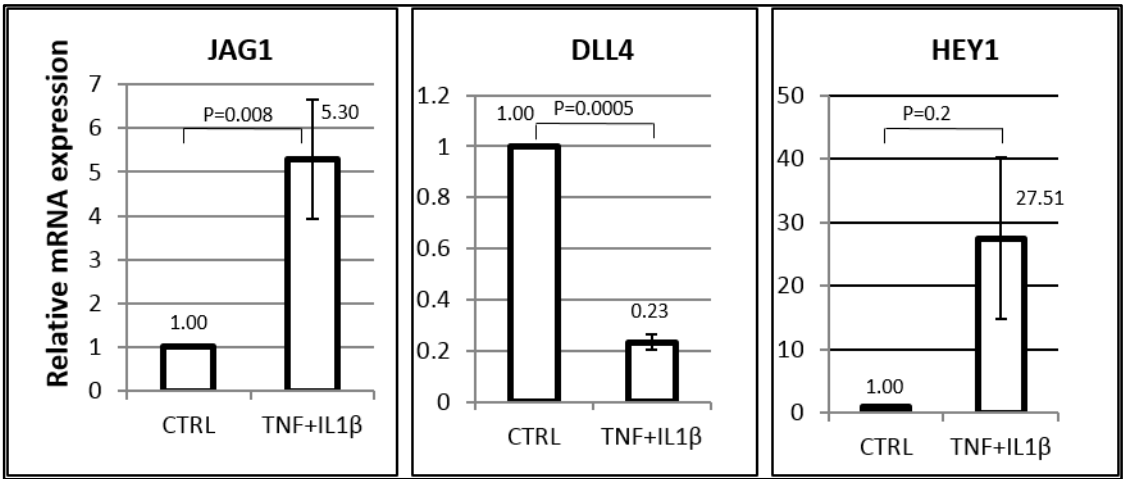

Figure 40: Gene expression analysis of Notch signalling members in cytokine-treated endothelial cells. HUVECs were treated with either a combination of TNF and IL1β or left untreated. RNA from each condition was extracted 24 hours after treatment and analysed through quantitative RT-PCR. mRNA expression levels are represented as fold change relative to that in control (untreated) cells. All values were normalized with the expression levels of the housekeeping gene RPL13A and represent the mean ±S.D. (n=3). P-values were calculated using the Student's t-test.

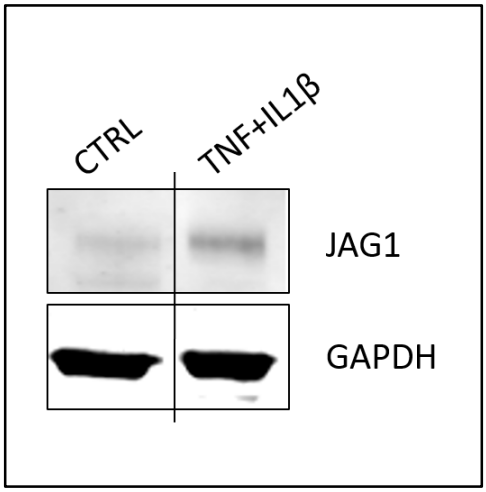

Figure 41: TNF+IL1β induced JAG1 expression in endothelial cells. HUVECs were treated with a combination of TNF and IL1β for 24 hours and protein lysates were analysed by Western blot with the antibody against JAG1. GAPDH expression was used as a loading control. Blot is representative of at least three independent experiments.

To investigate whether the upregulation of JAG1 in ECs could contribute to the activation/maintenance of the TNF+IL1β-induced cell elongation via a paracrine signalling, JAG1 mRNA expression was blocked through siRNA and the morphology of HUVECs was examined. As shown in Figure 42, JAG1 siRNA totally abolished cytokine-induced JAG1 upregulation. However, cell culture images and the respective shape analysis shown in Figure 43 revealed that the cell elongation induced by TNF and IL1β was not affected by JAG1 siRNA. Therefore, these results indicate that the upregulation of JAG1 was not related to the cytoskeletal rearrangements of ECs triggered by pro-inflammatory cytokines.

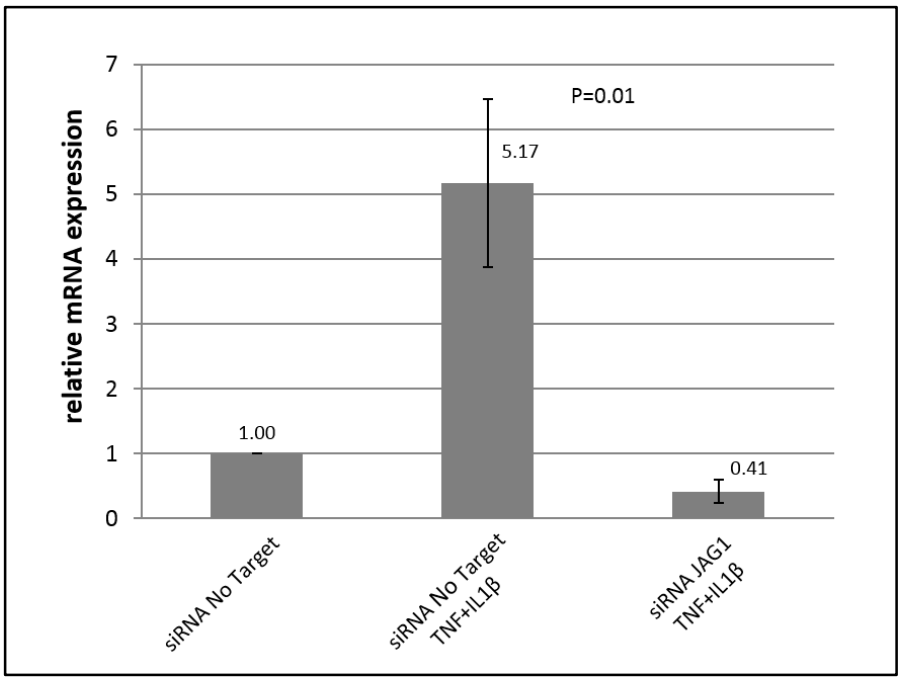

Figure 42: Efficiency of JAG1 gene silencing in endothelial cells. HUVECs were treated with a combination of TNF and IL1β together with either JAG1-targeting siRNAs or non-targeting siRNAs as a control. RNA from each condition was extracted 24 hours after treatment and analysed through quantitative RT-PCR. The mRNA expression levels were represented as fold change relative to siRNA no-target. All values were normalized with expression levels of the RPL13A housekeeping gene and represent the mean ±S.D. (n=3). P-value was calculated using the Student's t-test.

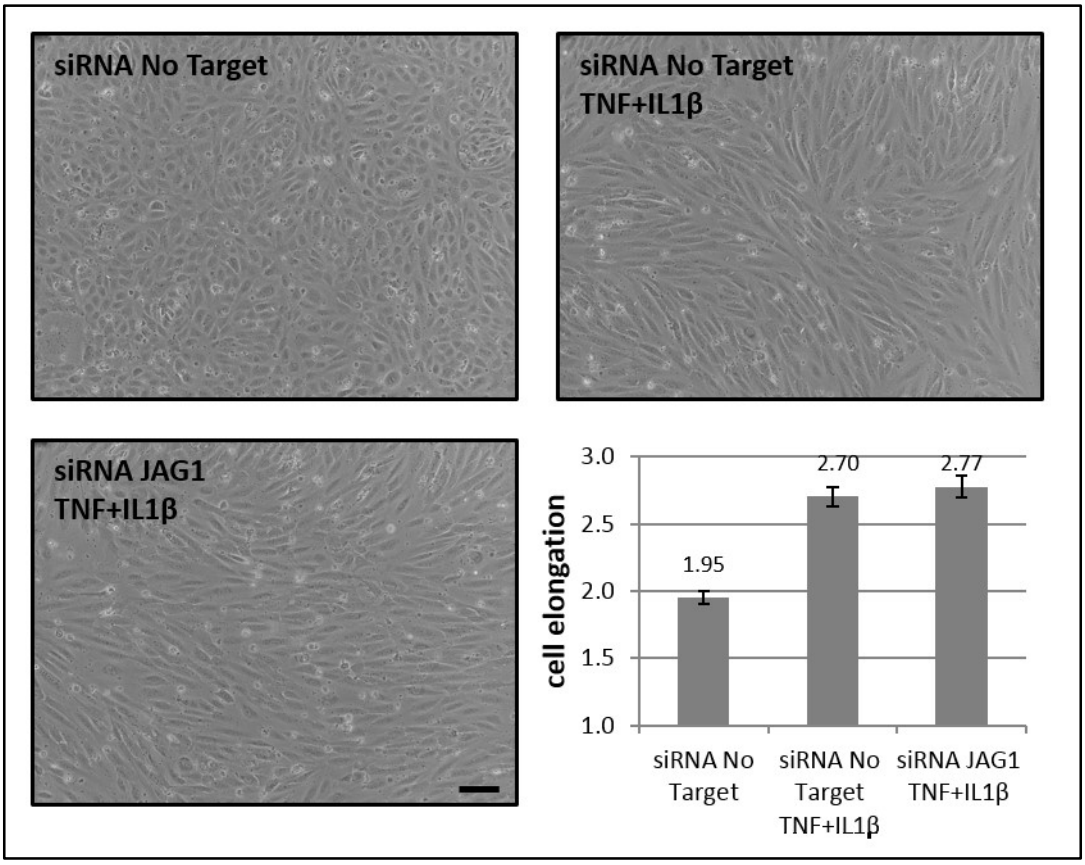

Figure 43: JAG1 gene silencing has no effect on cytokine-induced endothelial cell elongation. HUVECs were treated with either JAG1 siRNAs or non-targeting siRNAs as a control, together with a combination of the inflammatory cytokines TNF and IL1β (10µg/ml). Cell culture images were acquired 48 hours after treatment. Scale bar = 100µm. Quantification of cell elongation was performed on multiple images of each condition using ImageJ software (see section 2.7 for method details). Error bars represent S.D. (n=3).

5.2.5 Effect of global inhibition of transcription and translation on HUVECs stimulated with pro-inflammatory cytokines

One of the main functions of pro-inflammatory cytokines in the endothelium is the recruitment of leukocytes to the site of inflammation. This process is characterised by complex sequence of structural and molecular changes of ECs which are in turn regulated by several signalling pathways and gene expression programs (28, 161).

In order to investigate whether the cytoskeletal rearrangements induced by proinflammatory cytokines were mainly due to gene transcription, or rather due to the post-translational modification of cytoplasmic proteins, HUVECs were stimulated with TNF and IL1β in the presence of Actinomycin-D and Cycloheximide, inhibitors of transcription and translation, respectively. Actinomycin-D is an antibiotic derived from bacteria that intercalate into DNA thus preventing the progression of RNA polymerases (178), while Cycloheximide is an inhibitor of protein synthesis that blocks the translational elongation in eukaryotic organisms. As shown in Figure 44, 24 hours Actinomycin-D treatment decreased the number HUVECs in the monolayer. When Actinomycin-D was added in the presence of TNF and IL1β there was a significant increase in cell death. This indicates that the transcriptional activation induced by proinflammatory cytokines could be necessary for the expression of essential anti-apoptotic genes. Similar results were obtained when HUVECs were treated with Cycloheximide (Figure 45). Thus, investigating the individual contribution of the two processes (de novo transcription/translation versus post-translational modification of pre-existing proteins) to the rearrangement of the cytoskeleton appears to be unfeasible using this strategy. More specific approaches, i.e. targeting specific transcription factors, would then be required in order to achieve this.

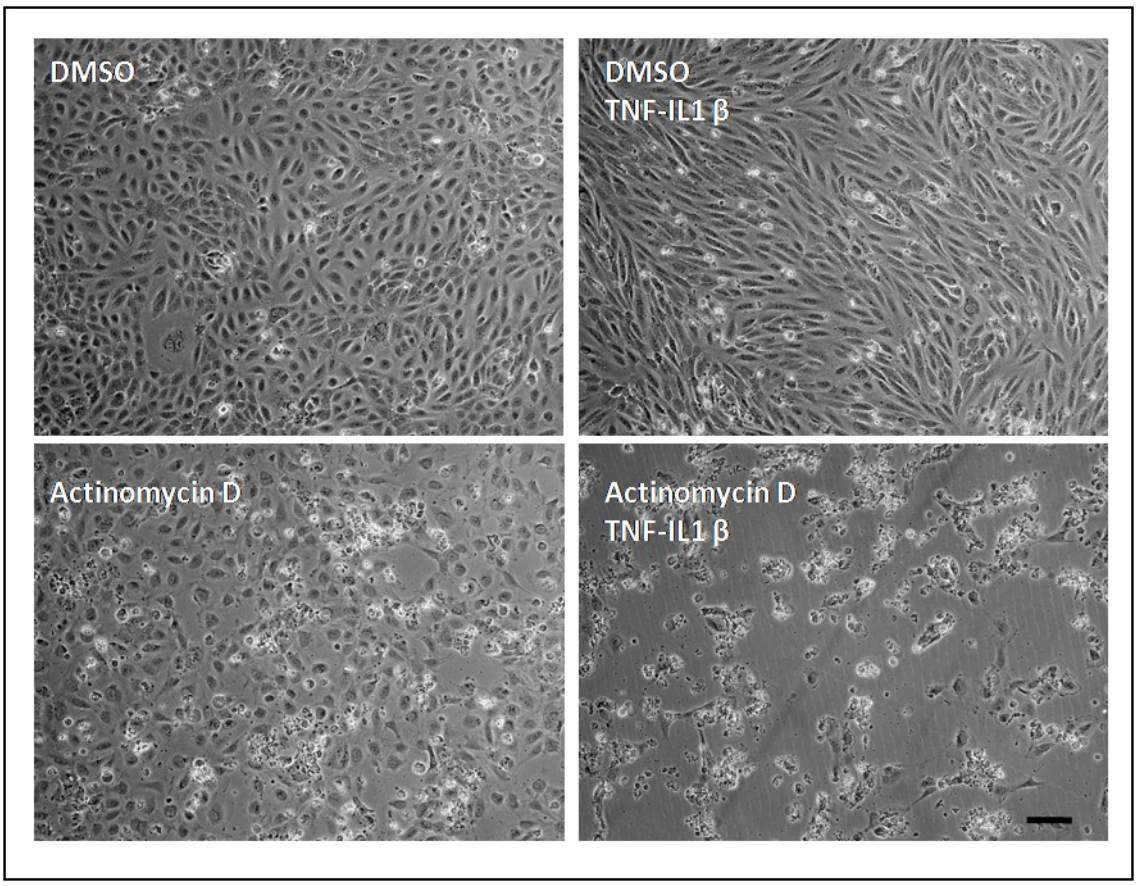

Figure 44: Global inhibition of gene transcription in endothelial cells treated with proinflammatory cytokines. HUVECs approaching confluence were either stimulated with TNF and IL1β or left untreated, in the presence of the chemical inhibitor Actinomycin-D (1µg/ml). Cell culture images were acquired 24 hours after treatment. Scale bar: 100µm. Images are representative of three independent experiments.

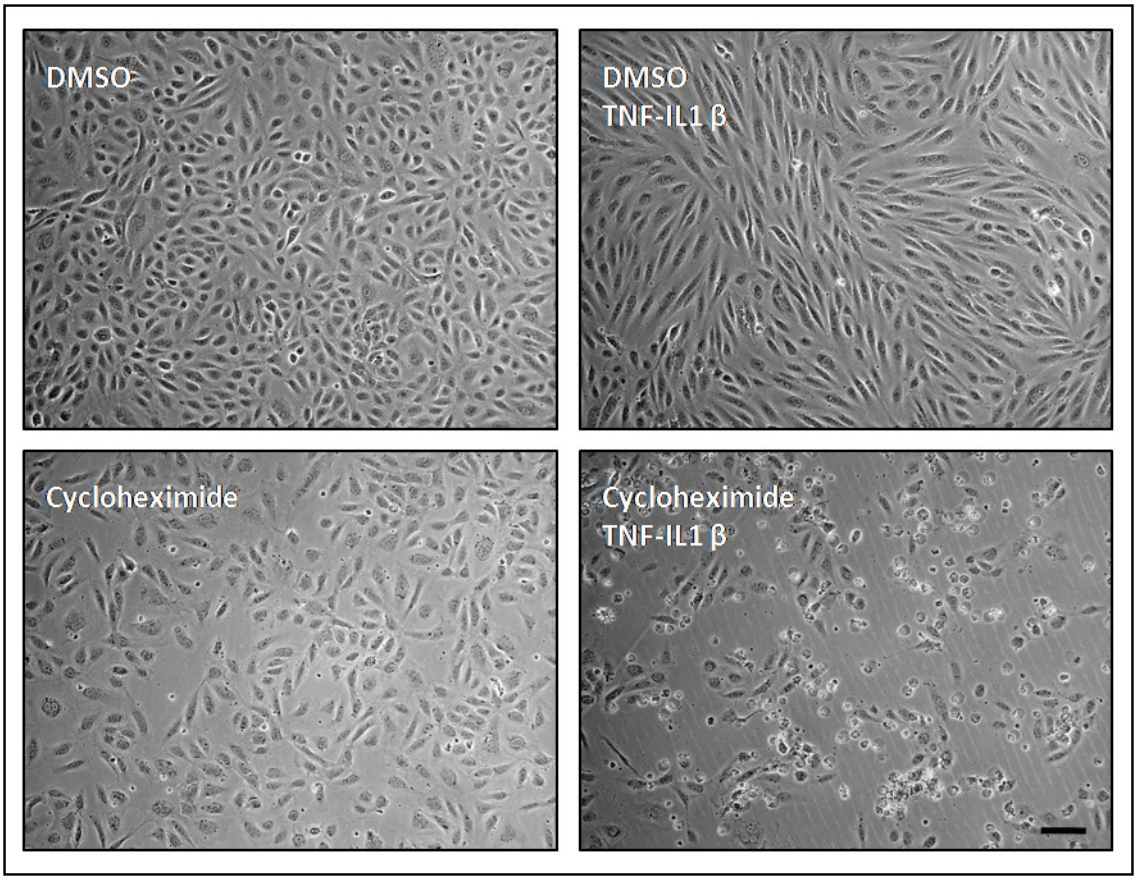

Figure 45: Global inhibition of protein translation in endothelial cells treated with proinflammatory cytokines. HUVECs approaching confluence were either stimulated with TNF and IL1β or left untreated, in the presence of the chemical inhibitor Cycloheximide (10µg/ml). Cell culture images were acquired 24 hours after treatment. Scale bar: 100µm. Images are representative of three independent experiments.

5.2.6 Gene expression analysis of secreted proteins in inflammation-induced endothelial cells

Besides the regulation of vascular permeability and the recruitment of immune cells from blood, ECs also have an active role in the remodelling of extracellular matrix (ECM) of the surrounding tissue, whose function is to provide the optimal environment for the progression and resolution of inflammation (174). At the molecular level, ECs secrete several ECM components when activated by pro-inflammatory cytokines, such as protease and collagens (179). Understanding the variety of these proteins and dynamics of their expression by ECs may give important insights into pathological conditions associated with the composition and turnover of ECM.

To determine whether pro-inflammatory stimuli on HUVECs have significant regulatory effects on ECM proteins, the gene expression of ECM genes that were previously associated with fibrotic disorders was analysed by qPCR. Treatment with cytokines consistently downregulated the mRNA levels of ELASTIN and COL1A2 compared to that in the untreated cells, with negligible differences when TNF and IL1β were used alone or in combination (Figure 46). COL16A1 expression was upregulated by both cytokines, although its level in IL1β-treated cells was an order of magnitude higher than that in TNF-treated cells. TNF+IL1β treatment induced the highest upregulation of COL16A1 expression, indicating a synergistic effect of the two cytokines. Tenascin-C expression changes revealed a switch-on effect for this gene. The mRNA was undetectable in untreated cells and its cycle threshold (Ct) was given an arbitrary value. This transcriptional activation was preferentially induced by IL1β, as mRNA level was two orders of magnitude higher than that by TNF. No significant difference in Tenascin-C expression was detected in the presence of both cytokines. Finally, the gene expression levels of MMP1 and LOX were not changed among the different conditions, while the mRNA expression of COL1A1, COL4A3 and COL22A1 was not detected.

Taken together, these data indicate that pro-inflammatory cytokines differentially regulate the expression of ECM genes in ECs, which in turn may have important effects on how blood vessels regulate the surrounding tissues under inflammatory conditions.

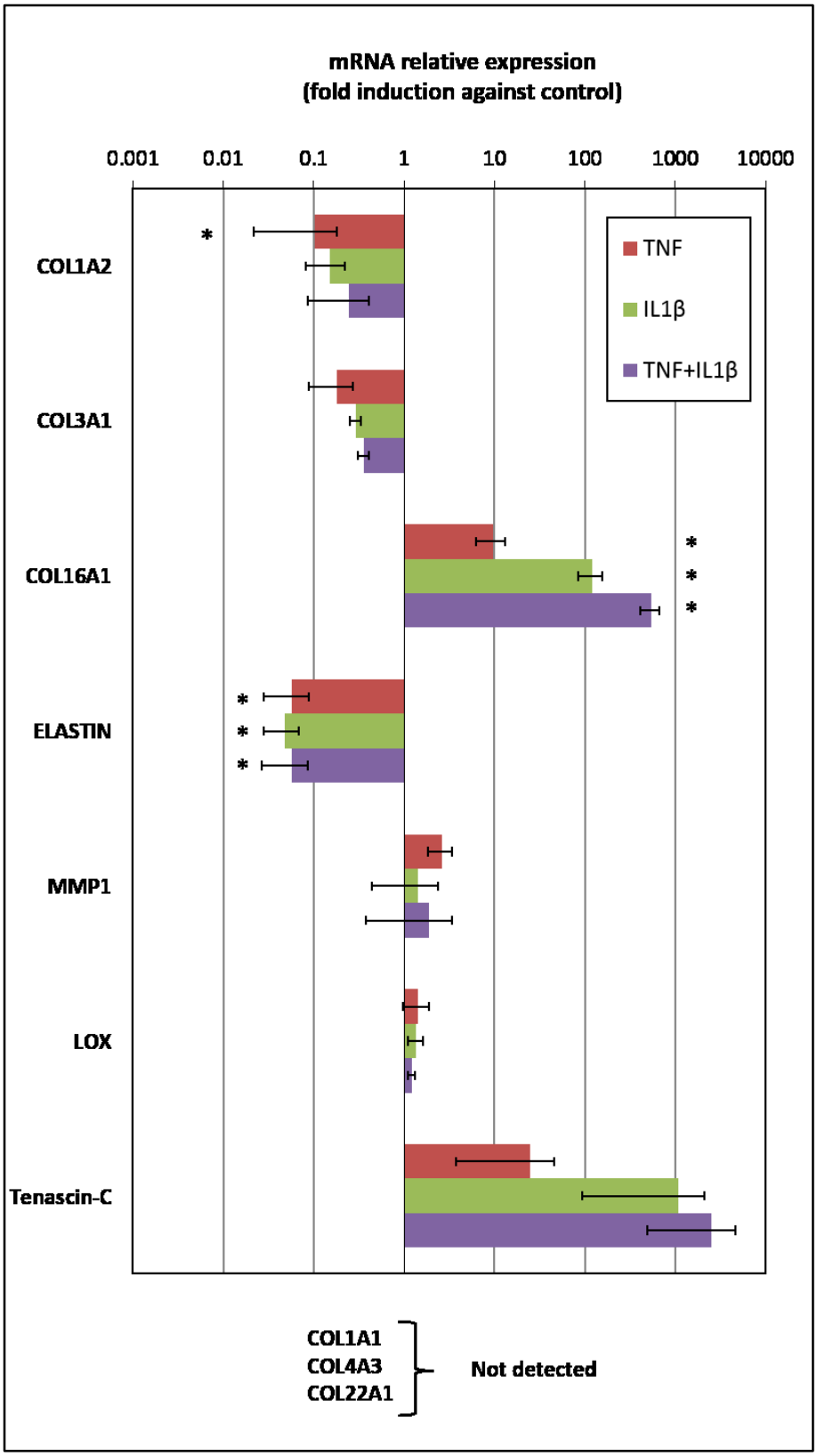

Figure 46: Gene expression analysis of ECM genes in cytokine-treated endothelial cells. HUVECs were treated with TNF, IL1β or a combination of the two cytokines for 24 hours and RNA samples were analysed by quantitative RT-PCR. The mRNA expression levels were represented as fold change relative to untreated cells. All values were normalised against the RPL13A housekeeping gene and represent the mean ±S.D. (n=3). ** $P < 0.01$, * $P < 0.05$; for all other conditions $P > 0.05$ (Student's t-test).

5.3 Conclusions

In this result section, the regulators of cytokine-induced EC shape elongation have been investigated. The main results are summarized in the following points:

- TNF and IL1β synergistically induce gene transcription of the cytoskeletal regulator RND1. Blocking its expression does not impair EC elongation, indicating the RND1 is not involved in the phenotypic change

- ROCK kinase mediates cytokine-induced EC elongation; however, shape change is not determined by the Rho GTPase-MLCK axis

- NF-κB signalling controls EC elongation through IKK kinases

- Notch ligand Jagged1 is induced transcriptionally by TNF and IL1β, but it is not involved in morphological change of ECs

- TNF and IL1β synergistically induce dramatic transcriptional upregulation of fibrosis-related secreted proteins, which might be involved in tissue remodelling during inflammation

5.4 Discussion

5.4.1 Molecular mechanisms underlying shape elongation of ECs

Inflammatory cytokines induce the transcription of a multitude of genes that are necessary to perform a variety of molecular events. Likely, several of those genes are necessary to modulate the cellular architecture of ECs. It was then sought to identify new inflammation-induced cytoskeletal regulators and the attention was focused on the Rho-GTPase RND1, since it was previously shown to be upregulated by TNF in a published gene microarray study (161). Interestingly, this gene was also known to regulate actin reorganization and cell adhesion (162), but its role in ECs is currently not established. The transcriptional upregulation of RND1 was confirmed in HUVECs treated with TNF and IL1β (5.2.1). Furthermore, the expression was found to be further increased in the presence of both cytokines, which correlates with the synergistic effect of TNF and IL1β on cell elongation. However, siRNA-mediated blockage of RND1 upregulation did not affect TNF+IL1β-induced morphological changes. Thus, these results indicate that RND1 is not involved in the inflammation-induced cell elongation of ECs. The magnitude of the gene expression induction is nonetheless indicative of potential functional role of RND1 during inflammation. Emerging evidence suggests for instance that RND proteins are involved in the migration of neurons (180). Similarly, RND proteins may play a role in endothelial migration during angiogenesis.

The signalling pathways related to the Rho-subfamily of GTPase were then examined since these small proteins, which include the founding trio Rho, Rac1 and Cdc42, are critical in the regulation of cell motility and cytoskeletal dynamics (181). Indeed, inhibition of ROCK, a serine-threonine kinase and downstream effector of RhoA, prevented the cell elongation of HUVECs induced by TNF+IL1β, consistently with a previous study (5.2.2) (146). The blockage of ROCK activity also resulted in the formation of thin cellular protrusion, probably due to the altered balance of actin regulators and/or off-target effects of the inhibitors. Furthermore, inhibitors targeting Rho members (C3 transferase) or the downstream ROCK effector MLCK (ML7), failed to prevent the TNF+IL1β–induced cytoskeletal rearrangements. These results thus suggest that the ROCK kinase is involved in cell elongation of HUVECs, but it may participate in a signalling axis different from the canonical Rho-MLC pathway.

NF-κB is the common transcription factor activated by different inflammatory cytokines

and its role has been linked to many diseases, including cancer and EMT (145, 167). Time course analysis on TNF+IL1β-treated HUVECS showed that the NF-κB inhibitor IκBα was rapidly degraded upon stimulation and returned to normal levels within 2 hours, indicating that the transcriptional program induced by TNF and IL1β is activated in an early and short time window (5.2.3). Furthermore, the blockage of the NF-κB upstream kinases IKK resulted in reduced cell elongation of HUVECs, consistently with recent studies reporting the involvement of NF-κB in morphological rearrangements of ECs (157, 182, 183). These results leave open the possibility that the transcriptional activity of NF-κB and/or the cytoplasmic function of the upstream IKK complex are responsible for actin reorganization of inflammation-induced ECs. The latter appears more plausible given that the morphological changes are induced rapidly and thus may not involve de novo transcription. Moreover, recent research has shown a role of IKK kinases in the NF-κB-independent signalling pathways (184). For instance, IKKβ has been shown to be involved in Tumour angiogenesis through the mTOR pathway (185).

The ability of ROCK and IKK inhibitors to prevent cell elongation in HUVECs was subsequently exploited to identify molecular effectors involved in the cytoskeletal rearrangements (5.2.2). Phosphorylation of cofilin, an actin-regulating protein (169), was increased upon TNF+IL1β treatment but the phosphorylation status was not altered in the presence of ROCK and IKK inhibitors, thus excluding its involvement in the observed morphological changes. Similar results were also observed with the junctional protein VE-Cadherin, whose phosphorylation correlated with but not determined the TNF+IL1β-induced elongation of ECs.

Taken together, these results suggest that both Rho-GTPase and NF-κB signalling pathways are involved in cytokine-induced cytoskeletal rearrangements of human ECs. The crosstalk between Rho and NF-κB in the shape changes of ECs would be an interesting possibility to test, since their interaction has been shown to be involved in cellular processes such as motility and matrix remodelling during chronic inflammatory diseases (186).

5.4.2 Angiocrine functions of endothelial cells in disease

Within the cardiovascular system, the EndMT has been described *in vivo* as a cellular source of dysfunctional cells: collagen-producing fibroblasts in cardiac fibrosis and contractile smooth-muscle cells in atherosclerosis and vein graft remodelling (54, 71).

Although the *in vivo* evidence for this pathogenic role has been recently challenged, as it will be discussed in the next paragraph, it may be worth considering other possible mechanisms through which the endothelium may contribute to the emergence of chronic cardiovascular diseases. An emerging research subject is the so-called *vascular niche*, namely the microenvironmental set of signals used by ECs to communicate with other cell types. These signals, which have also been termed "angiocrine factors", include different molecules such as cytokines, growth factors, proteases and miRNAs. Angiocrine factors have been shown to contribute to a broad range of physiological and pathological processes such as fibrosis, cancer and stem cell maintenance (187-189).

In light of the importance of the above-mentioned mechanisms, the gene expression of several extracellular-matrix proteins was measured in HUVECs treated with TNF and IL1β (5.2.6). Results showed that mRNA levels were changed for several proteins, thus suggesting that ECs may qualitatively influence the remodelling of the surrounding extracellular matrix. For instance, COL1A2 and elastin were downregulated, whereas COL16A1 and Tenascin-C were upregulated. Interestingly, Tenascin-C gene expression was literally switched on, as in most experiments its expression was not detected in untreated cells. The activation seemed to be preferentially induced by IL1β since its expression was significantly higher compared to TNF-treated cells. As far as one can tell from the literature, the molecular signalling leading to Tenascin-C gene expression has not been previously identified in ECs.

Tenascin-C is large extracellular glycoprotein which has been found to play disparate roles in both embryonic development and disease (190). It is absent in normal tissues but it is rapidly reactivated during tissue injury. Furthermore, Tenascin-C has been suggested to play critical roles in cardiac and arterial remodelling (191). Interestingly, Tenascin-C was originally described to be involved in EndMT during the development of the heart valves. This protein was in fact found to be deposited in the extracellular space of the endocardium prior to endothelial cell activation. It may therefore be tempting to speculate that this protein, during inflammation, could be secreted in the extracellular space at the onset of tissue injury to provide a supporting guide for the migration of pro-angiogenic ECs. Alternatively, endothelial-secreted Tenascin-C may constitute a paracrine signal for the activation of fibroblasts during fibrotic remodelling.

5.4.3 A sober pro-angiogenic alternative to the drunk EndMT?

Genes belonging to the Notch signalling pathway were found to be differentially regulated by inflammatory cytokines in HUVECs (5.2.4). Jagged 1 (JAG1), the ligand of the receptor Notch-1 which has been linked to Alagille syndrome and the development of the cardiovascular system (192), was indeed found to be induced by TNF+IL1β treatment at both mRNA and protein level. This result is consistent with a previous study showing that TNF induces JAG1 in an NF-κB-dependent manner (193). Furthermore, the gene expression level of DLL4, another Notch ligand, was significantly reduced while HEY1, a Notch-related transcription factor, was upregulated by the inflammatory cytokines. It may be worth considering these results in light of new reported functions of Notch signalling in ECs. Indeed, the balance between JAG1 and DLL4 expression has been recently shown to control sprouting angiogenesis in the context of tip and stalk cell selection (177). DLL4 expression in tip cells is known to induce Notch signalling and suppress a tip cell phenotype in adjacent stalk cells, while JAG1 was instead shown to antagonize DLL4-Notch signalling and therefore to act as a pro-angiogenic ligand. The inflammatory stimulus is therefore thought to be able to dynamically modulate the angiogenic response of ECs through the regulation of the balance of these two opposing ligands. In agreement with this, another study showed that TNF-induced JAG1 upregulation in ECs induced a tip-cell, migratory phenotype, with the duration of the inflammatory stimulus representing a critical factor for a successful angiogenic response (175). In summary, these findings indicate that the inflammation-induced Notch-mediated genetic response activated in processes such as wound healing, enables ECs to expand toward an angiogenic stimulus and to regenerate the vasculature.

It is also interesting to note how the angiogenic remodelling of blood vessels during inflammation and tissue repair shares many similarities with the EndMT; the endothelial tip cells that guide the front of an angiogenic sprouting are in fact highly polarized, are rich in filopodia and present a behaviour characterised by increased migratory and proteolytic activity, since tip cells need to explore and invade the surrounding matrix (194). Although these features are mesenchymal in nature, it seems incorrect to frame the behaviour of endothelial tip cells as an EndMT, as it has been suggested (133): firstly, the angiogenic migration of endothelial tip cells is *collective;* it is in fact coordinated among several cells of the blood vessel. Secondly, endothelial tip cells do not normally become individualized mesenchymal cells, namely they do not lose contact with other ECs. Thirdly, the downregulation of VE-Cadherin by transcriptional repressors such as Snail1 and 2, which would represent the genetic pillar of a true EndMT, has not been

unequivocally demonstrated *in vivo* (see section 1.3.2.4). In agreement with these observations, a recent work looking at the role of SNAI2 in the sprouting of HUVECs described the angiogenic phenotype as a *partial* EndMT, as SNAI2 was not found to regulate the transcription of VE-Cadherin (195, 196).

In conclusion, these observations suggest that the EndMT does not describe correctly the cellular behaviour of ECs during angiogenesis. Nonetheless, the tip-stalk concept underlying inflammation-induced angiogenesis may be a valid alternative to the EndMT in explaining the cellular response of the endothelium during chronic cardiovascular conditions.

Chapter VI – Conclusion: final considerations

6.2 Project Background

Fibrosis is a scarring process characterised by the excessive production of ECM, which changes the architecture of organs and impairs their function. Fibrosis underlies the development of several chronic diseases in many organs, such as heart, lung, kidney, liver, skin, intestine and bone marrow (197). The heart is an efficient pump formed of different cell types. Cardiomyocytes, the cells responsible for muscle contraction, account for almost one third of all cells. The other two thirds are non-myocyte cells that comprise ECs, vascular smooth muscle cells and fibroblasts. All these cell types are surrounded and held together by the ECM, which is like concrete in a wall of bricks. The balance of each cellular constituent is fundamental to maintain the correct function of the heart. The accumulation of fibrillar collagen in the ECM renders the heart tissue stiffer and less able to cope dynamically with mechanical forces, resulting in adverse cardiac events such as cardiac failure (198). Myocardial fibrosis is among the main causes of diastolic dysfunction and accompanies the development of most heart diseases (199). There are currently no specific anti-fibrotic therapies and more research is needed to define the molecular and cellular features of this pathological process.

From a physiological point of view, myocardial fibrosis progresses as a maladaptive regenerative reaction aimed at replacing dying muscle cells in the tissue following myocardial ischemia (198). However, fibrosis also occurs in response to the overgrowth of cardiomyocytes in hypertrophic cardiomyopathy (HCM) caused by genetic mutations in sarcomere proteins (200). Nevertheless, irrespective of the diverse pathophysiologic causes of myocardial fibrosis, research now is focused on the common cellular effectors of this complex disease: the fibroblasts.

It is known since the work of the German pathologist Rudolph Virchow in 19th century that fibroblasts are the predominant source of the ECM in fibrosis (197). Collagen is secreted by fibroblasts that acquire increased proliferative and biosynthetic activities. They are thus defined “activated fibroblasts” or myofibroblasts, since they express the contractile protein αSMA (201). What is still unknown is the source of myofibroblasts in cardiac fibrosis. The highly heterogeneous nature of this cell type, which displays

different subpopulations even in the same organ, and the lack of univocal markers, has so far hampered the clear identification of their origin (202). Several studies have so far identified multiple sources of fibroblasts in the cardiac tissue; the traditional view holds that they accumulate through proliferation of the resident fibroblasts (203), but recent evidence has suggested additional sources (204): bone marrow cells and endothelial cells (54) (see Figure 47 for an illustrative summary).

Fibroblasts are thought to originate from ECs through the EndMT process, which is defined as the transdifferentiation of ECs into mesenchymal cells. ECs form the internal lining of blood vessels. They display an apical-basal polarity and express specific junction proteins (VE-Cadherin, Pecam-1) that allow them to closely bind together (205). During the EndMT ECs loose these characteristics and acquire a mesenchymal phenotype, which includes a front-rear polarity, a spindle-shaped morphology and increased migratory and contractile properties (206). These changes are underlined by the downregulation of endothelial specific proteins and the concomitant expression of mesenchymal markers, such as N-Cadherin, Fibroblast Specific Protein-1 (FSP1) and αSMA (207). The set of molecular processes occurring in EndMT are closely related to the epithelial-mesenchymal transition (EMT), and the EndMT has been indeed categorised as a specialized form of EMT. EMT is a fundamental biological process involved in the formation of tissues and organs during embryogenesis and its reactivation in adulthood leads to a wide range of diseases, including fibrosis and cancer (35).

EndMT was originally described in the formation of heart valves during early cardiogenesis. In the primitive heart tube, the ECs of the atrioventricular canal region delaminate and transdifferentiate into mesenchymal cells, which invade the cardiac jelly between the myocardium and endocardium to form the endocardial cushions, the structures that develop into heart valves (53). This developmental EndMT is thought to be recapitulated at the onset and progression of cardiac fibrosis in the adult heart tissue.

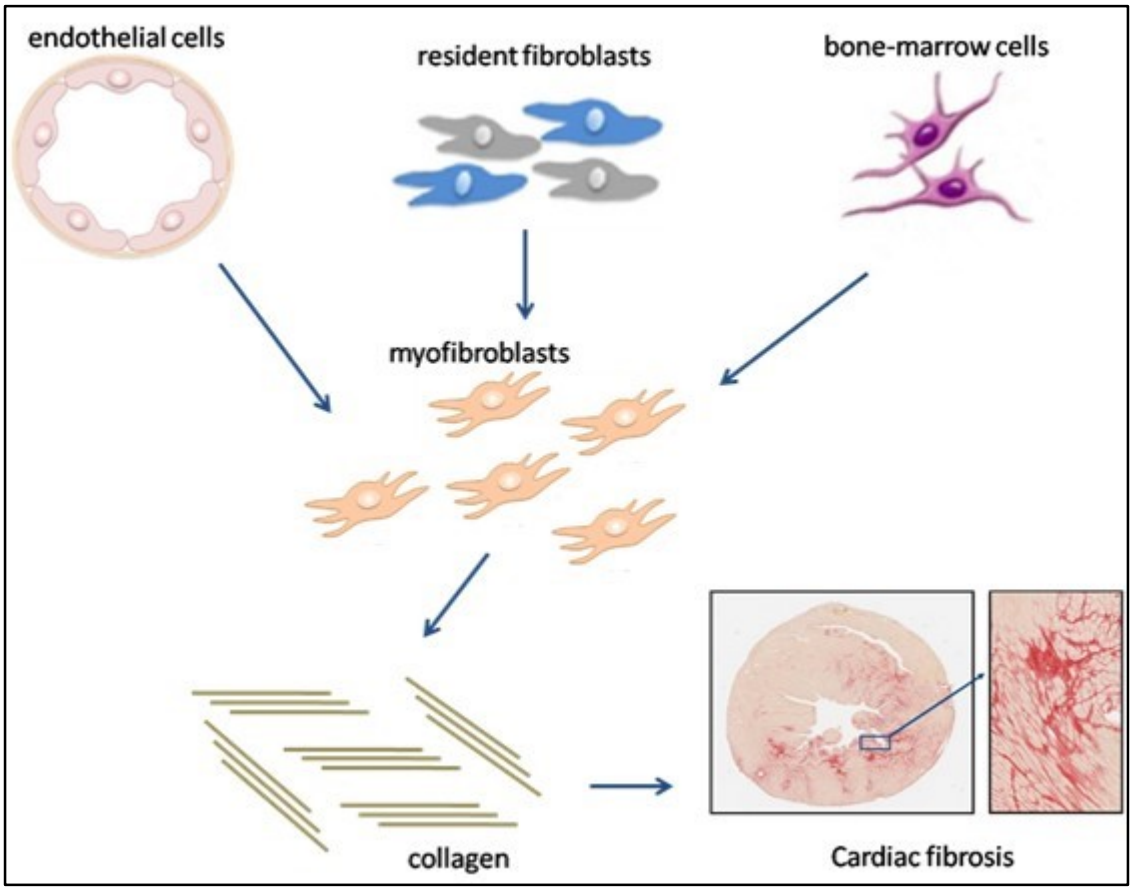

Figure 47: Schematic illustration of the potential cellular sources of collagen-producing myofibroblasts during cardiac fibrosis. Activated fibroblasts (myofibroblasts) contribute to cardiac fibrosis through the secretion of collagen. The traditional view that myofibroblasts derives uniquely from proliferation of resident fibroblasts has been recently challenged by studies showing that bone-marrow cells and endothelial cells (via EndMT) significantly contribute to their emergence. Figure adapted from Piera-Velazquez et al. (208).

6.2 EndMT in adult tissues: a theory stabbed in the heart?

Recent studies have linked the EndMT to different pathologies. For instance, Maddaluno et al. reported the involvement of EndMT in Cerebral Cavernous Malformation (CCM), a form of vascular dysplasia in which blood vessels in the brain present an irregular structure (209). This condition causes vascular leakage and fatal brain haemorrhage. Maddaluno et al. showed that ECs in these vascular lesions expressed a set of mesenchymal (Slug, N-Cadherin, αSMA, Id1) and stem cell markers (Sca1, CD44). Furthermore, ECs extracted from mouse brains indicated that this altered gene expression was dependent on TGFβ and BMP signalling. The authors interpreted their findings as an ongoing EndMT process. Similarly, Cooley et al. implicated the EndMT in the neointimal hyperplasia that occurs during vein graft remodelling (72). To demonstrate this, the authors used the Tie2-Cre mouse model, the lineage tracing system used to demonstrate EndMT in previous publications (see section 1.3.2.3). The authors concluded that half of the cells composing the neointimal lesions were derived from ECs and that this process was mechanistically driven by the TGFβ-Smad2/3 pathway. Additionally, two recent papers reported the EndMT in pulmonary hypertension; Ranchoux et al. showed in both human and animal samples the cellular co-localization of VE-Cadherin and αSMA, while Good et al. observed that 5% of cells lung cells in pulmonary hypertension patients were positive for both vWF and αSMA (210, 211)

The *in vivo* experimental technique that can conclusively demonstrate the ontogeny of cells in an organism is the lineage-tracing model. Such evidence was firstly provided in 2007 by the seminal paper by Zeisberg et al., who used the Tie1-Cre model (133). How accurate is their model? The fundamental assumption made was that Tie1 is specifically expressed by ECs. A recent study challenged this very assumption and refuted in toto the idea that accumulating fibroblasts in cardiac fibrosis derive from ECs (212). First, Moore-Morris et al. noted that FSP1 was not a fibroblast-specific marker, for it is also found to be expressed in immune cells, ECs and vascular smooth muscle cells (213, 214). Second, the authors observed that the Tie1 gene also lacks specificity as it was reported to be expressed in immune cells (215). To overcome these limitations, Moore-Morris et al. used an updated lineage tracing strategy in which fibroblasts were marked through a collagen1a1-GFP enhancer. They thus showed that pressure overload-induced cardiac fibrosis activated the proliferation of two resident fibroblast lineages. Furthermore, they

ruled out the occurrence of EndMT through VE-Cadherin-Cre mouse lines. In agreement with the findings of Moore-Morris et al., Ali et al. identified two distinct lineages of fibroblasts in the heart through an in-depth FACS-based analysis (216). The authors found that both fibroblast lineages contributed equally to pressure-overload fibrosis, thus ruling out the occurrence of an alternative EndMT process.

Together, the findings of Moore-Morris et al. and Ali et al. findings seriously question the existence of an EndMT process in cardiac fibrosis. Similarly, the occurrence of EMT in kidney and liver fibrosis has also been vehemently questioned (217-219). At the heart of the controversy are the specificity of FSP1 and αSMA as markers of myofibroblasts and the lack of anatomical and ultrastructural evidence directly demonstrating the ongoing EMT process. Most *in vivo* studies have in fact provided static and indirect evidence that provides little information about the dynamic nature of the EMT. In this regard, it may worth pointing out that the involvement of both EndMT and EMT in fibrotic diseases was demonstrated *in vivo* using the same experimental strategies developed in laboratory of Eric Neilson in the early 2000's (1.2.4) (50, 51). Those findings have not been thoroughly reproduced by independent labs with different methodologies.

Adding to the inherent inconsistencies of the EndMT concept, the *in vitro* evidence supporting EndMT also appear to be weak, as most studies used ECs to indirectly corroborate major *in vivo* findings. No studies have in fact thoroughly analysed the EndMT process from a pure molecular cell biology perspective. As reviewed in the introduction (see section 1.3.2.2 and Table 1), initial studies provided in fact circumstantial evidence, such as the upregulation/downregulation of selected markers or the appearance of a spindle-shape morphology. The apparent readiness of human ECs to become mesenchymal-like cell, as it was spectacularly demonstrated by Medici et al. (67), has so far received little if any confirmation.

In the cancer field, the EMT still represents the prevailing view of how cancer cells become able to metastasize. However, EMT in cancer is not immune from criticism as well (220-222). Critical issues regard the fact that the complexity of the EMT process is often reduced to too simple linear mechanism (TGFβ→epithelial marker down→mesenchymal marker up→cancer). This carries the risk of oversimplifying the concept leading to an "EMT-centric" view, where every single cellular event involving for instance suppression of adhesion, shape change and motility, could be interpreted as an EMT, even though they belong to completely different cellular processes (223). The EndMT, as a subtype of EMT, may have suffered similar issues but, in addition, it is based

on much less molecular and cellular evidence.

In conclusion, in light of the new updated lineage-tracing *in vivo* models, the inconsistent literature regarding endothelial transdifferentiation *in vitro*, and the results obtained in HUVECs in the present project, it may seem reasonable to consider the EndMT a wrong hypothesis. Nonetheless, the plasticity of the endothelium and its largely unexplored interaction with the immune system and other tissues during inflammatory condition are research subjects of great importance for the understanding of many complex diseases.

Bibliography

1. Burggren WW & Reiber CL (2007) *Evolution of Cardiovascular Systems and Their Endothelial Linings*

Endothelial Biomedicine (Cambridge University Press).

2. Ruppert EE & Carle KJ (1983) Morphology of Metazoan Circulatory Systems. *Zoomorphology* 103(3):193-208.
3. Munoz-Chapuli R, Carmona R, Guadix JA, Macias D, & Perez-Pomares JM (2005) The origin of the endothelial cells: an evo-devo approach for the invertebrate/vertebrate transition of the circulatory system. *Evolution & development* 7(4):351-358.
4. Monahan-Earley R, Dvorak AM, & Aird WC (2013) Evolutionary origins of the blood vascular system and endothelium. *Journal of thrombosis and haemostasis : JTH* 11 Suppl 1:46-66.
5. Huber TL, Kouskoff V, Fehling HJ, Palis J, & Keller G (2004) Haemangioblast commitment is initiated in the primitive streak of the mouse embryo. *Nature* 432(7017):625-630.
6. Suburo AM & D'Amore PA (2006) Development of the Endothelium. *The Vascular Endothelium I,* Handbook of Experimental Pharmacology, eds Moncada S & Higgs A (Springer Berlin Heidelberg), Vol 176/I, pp 71-105.
7. Jin SW, Beis D, Mitchell T, Chen JN, & Stainier DY (2005) Cellular and molecular analyses of vascular tube and lumen formation in zebrafish. *Development* 132(23):5199-5209.
8. Herbert SP & Stainier DY (2011) Molecular control of endothelial cell behaviour during blood vessel morphogenesis. *Nature reviews. Molecular cell biology* 12(9):551-564.
9. Geudens I & Gerhardt H (2011) Coordinating cell behaviour during blood vessel formation. *Development* 138(21):4569-4583.
10. Jakobsson L*, et al.* (2010) Endothelial cells dynamically compete for the tip cell position during angiogenic sprouting. *Nature cell biology* 12(10):943-953.
11. Jain RK (2003) Molecular regulation of vessel maturation. *Nature medicine* 9(6):685-693.
12. Thomas M & Augustin HG (2009) The role of the Angiopoietins in vascular

morphogenesis. *Angiogenesis* 12(2):125-137.

13. Roca C & Adams RH (2007) Regulation of vascular morphogenesis by Notch signaling. *Genes & development* 21(20):2511-2524.
14. Lohela M, Bry M, Tammela T, & Alitalo K (2009) VEGFs and receptors involved in angiogenesis versus lymphangiogenesis. *Current opinion in cell biology* 21(2):154-165.
15. Ladomery MR, Harper SJ, & Bates DO (2007) Alternative splicing in angiogenesis: the vascular endothelial growth factor paradigm. *Cancer letters* 249(2):133-142.
16. Pugh CW & Ratcliffe PJ (2003) Regulation of angiogenesis by hypoxia: role of the HIF system. *Nature medicine* 9(6):677-684.
17. Aird WC (2007) Phenotypic heterogeneity of the endothelium: I. Structure, function, and mechanisms. *Circulation research* 100(2):158-173.
18. Tse D & Stan RV (2010) Morphological heterogeneity of endothelium. *Seminars in thrombosis and hemostasis* 36(3):236-245.
19. Komarova Y & Malik AB (2010) Regulation of endothelial permeability via paracellular and transcellular transport pathways. *Annual review of physiology* 72:463-493.
20. Dejana E, Tournier-Lasserve E, & Weinstein BM (2009) The control of vascular integrity by endothelial cell junctions: molecular basis and pathological implications. *Developmental cell* 16(2):209-221.
21. Dejana E, Orsenigo F, Molendini C, Baluk P, & McDonald DM (2009) Organization and signaling of endothelial cell-to-cell junctions in various regions of the blood and lymphatic vascular trees. *Cell and tissue research* 335(1):17-25.
22. Mehta D & Malik AB (2006) Signaling mechanisms regulating endothelial permeability. *Physiological reviews* 86(1):279-367.
23. Frank PG, Woodman SE, Park DS, & Lisanti MP (2003) Caveolin, caveolae, and endothelial cell function. *Arteriosclerosis, thrombosis, and vascular biology* 23(7):1161-1168.
24. Wendehenne D, Pugin A, Klessig DF, & Durner J (2001) Nitric oxide: comparative synthesis and signaling in animal and plant cells. *Trends in plant science* 6(4):177-183.
25. Arnout J, Hoylaerts MF, & Lijnen HR (2006) Haemostasis. *Handbook of experimental pharmacology* (176 Pt 2):1-41.

26. Springer TA (2014) von Willebrand factor, Jedi knight of the bloodstream. *Blood* 124(9):1412-1425.
27. Chapin JC & Hajjar KA (2015) Fibrinolysis and the control of blood coagulation. *Blood reviews* 29(1):17-24.
28. Pober JS & Sessa WC (2007) Evolving functions of endothelial cells in inflammation. *Nature reviews. Immunology* 7(10):803-815.
29. Ley K, Laudanna C, Cybulsky MI, & Nourshargh S (2007) Getting to the site of inflammation: the leukocyte adhesion cascade updated. *Nature reviews. Immunology* 7(9):678-689.
30. Vestweber D (2007) Molecular mechanisms that control leukocyte extravasation through endothelial cell contacts. *Ernst Schering Foundation symposium proceedings* (3):151-167.
31. Morali O, Savagner P, & Larue L (2005) Epithelium-Mesenchyme Transitions Are Crucial Morphogenetic Events Occurring during Early Development. *Rise and Fall of Epithelial Phenotype,* Molecular Biology Intelligence Unit, (Springer US), pp 12-28.
32. Baum B, Settleman J, & Quinlan MP (2008) Transitions between epithelial and mesenchymal states in development and disease. *Seminars in cell & developmental biology* 19(3):294-308.
33. Cereijido M, Contreras RG, & Shoshani L (2004) Cell adhesion, polarity, and epithelia in the dawn of metazoans. *Physiological reviews* 84(4):1229-1262.
34. Hay ED (2005) The mesenchymal cell, its role in the embryo, and the remarkable signaling mechanisms that create it. *Developmental dynamics : an official publication of the American Association of Anatomists* 233(3):706-720.
35. Thiery JP, Acloque H, Huang RY, & Nieto MA (2009) Epithelial-mesenchymal transitions in development and disease. *Cell* 139(5):871-890.
36. Hay ED (1995) An overview of epithelio-mesenchymal transformation. *Acta anatomica* 154(1):8-20.
37. Lim J & Thiery JP (2012) Epithelial-mesenchymal transitions: insights from development. *Development* 139(19):3471-3486.
38. Magie CR & Martindale MQ (2008) Cell-cell adhesion in the cnidaria: insights into the evolution of tissue morphogenesis. *The Biological bulletin* 214(3):218-232.
39. Takeichi M (1988) The cadherins: cell-cell adhesion molecules controlling animal

morphogenesis. *Development* 102(4):639-655.

40. Takeichi M (2014) Dynamic contacts: rearranging adherens junctions to drive epithelial remodelling. *Nature reviews. Molecular cell biology* 15(6):397-410.
41. Greenburg G & Hay ED (1982) Epithelia suspended in collagen gels can lose polarity and express characteristics of migrating mesenchymal cells. *The Journal of cell biology* 95(1):333-339.
42. Boyer B, Tucker GC, Valles AM, Gavrilovic J, & Thiery JP (1989) Reversible transition towards a fibroblastic phenotype in a rat carcinoma cell line. *International journal of cancer. Supplement = Journal international du cancer. Supplement* 4:69-75.
43. Naldini L*, et al.* (1991) Scatter factor and hepatocyte growth factor are indistinguishable ligands for the MET receptor. *The EMBO journal* 10(10):2867-2878.
44. Stoker M, Gherardi E, Perryman M, & Gray J (1987) Scatter factor is a fibroblast-derived modulator of epithelial cell mobility. *Nature* 327(6119):239-242.
45. Thiery JP (2002) Epithelial-mesenchymal transitions in tumour progression. *Nature reviews. Cancer* 2(6):442-454.
46. Batlle E*, et al.* (2000) The transcription factor snail is a repressor of E-cadherin gene expression in epithelial tumour cells. *Nature cell biology* 2(2):84-89.
47. Cano A*, et al.* (2000) The transcription factor snail controls epithelial-mesenchymal transitions by repressing E-cadherin expression. *Nature cell biology* 2(2):76-83.
48. Yang J*, et al.* (2004) Twist, a master regulator of morphogenesis, plays an essential role in tumor metastasis. *Cell* 117(7):927-939.
49. Leptin M (1991) twist and snail as positive and negative regulators during Drosophila mesoderm development. *Genes & development* 5(9):1568-1576.
50. Strutz F*, et al.* (1995) Identification and characterization of a fibroblast marker: FSP1. *The Journal of cell biology* 130(2):393-405.
51. Iwano M*, et al.* (2002) Evidence that fibroblasts derive from epithelium during tissue fibrosis. *The Journal of clinical investigation* 110(3):341-350.
52. Nieto MA (2011) The ins and outs of the epithelial to mesenchymal transition in health and disease. *Annual review of cell and developmental biology* 27:347-376.
53. Markwald RR, Fitzharris TP, & Manasek FJ (1977) Structural development of endocardial cushions. *The American journal of anatomy* 148(1):85-119.

54. Zeisberg EM*, et al.* (2007) Endothelial-to-mesenchymal transition contributes to cardiac fibrosis. *Nature medicine* 13(8):952-961.
55. Zeisberg EM, Potenta S, Xie L, Zeisberg M, & Kalluri R (2007) Discovery of endothelial to mesenchymal transition as a source for carcinoma-associated fibroblasts. *Cancer Res* 67(21):10123-10128.
56. Zeisberg EM, Potenta SE, Sugimoto H, Zeisberg M, & Kalluri R (2008) Fibroblasts in Kidney Fibrosis Emerge via Endothelial-to-Mesenchymal Transition. *J Am Soc Nephrol* 19(12):2282-2287.
57. Owens GK, Loeb A, Gordon D, & Thompson MM (1986) Expression of smooth muscle-specific alpha-isoactin in cultured vascular smooth muscle cells: relationship between growth and cytodifferentiation. *The Journal of cell biology* 102(2):343-352.
58. Arciniegas E, Sutton AB, Allen TD, & Schor AM (1992) Transforming growth factor beta 1 promotes the differentiation of endothelial cells into smooth muscle-like cells in vitro. *Journal of cell science* 103 (Pt 2):521-529.
59. DeRuiter MC*, et al.* (1997) Embryonic endothelial cells transdifferentiate into mesenchymal cells expressing smooth muscle actins in vivo and in vitro. *Circulation research* 80(4):444-451.
60. Paranya G*, et al.* (2001) Aortic valve endothelial cells undergo transforming growth factor-beta-mediated and non-transforming growth factor-beta-mediated transdifferentiation in vitro. *The American journal of pathology* 159(4):1335-1343.
61. Condorelli G*, et al.* (2001) Cardiomyocytes induce endothelial cells to trans-differentiate into cardiac muscle: implications for myocardium regeneration. *Proceedings of the National Academy of Sciences of the United States of America* 98(19):10733-10738.
62. Frid MG, Kale VA, & Stenmark KR (2002) Mature vascular endothelium can give rise to smooth muscle cells via endothelial-mesenchymal transdifferentiation: in vitro analysis. *Circulation research* 90(11):1189-1196.
63. Ishisaki A, Hayashi H, Li AJ, & Imamura T (2003) Human umbilical vein endothelium-derived cells retain potential to differentiate into smooth muscle-like cells. *The Journal of biological chemistry* 278(2):1303-1309.
64. Noseda M*, et al.* (2004) Notch activation induces endothelial cell cycle arrest and participates in contact inhibition: role of p21Cip1 repression. *Molecular and*

cellular biology 24(20):8813-8822.

65. Liebner S*, et al.* (2004) Beta-catenin is required for endothelial-mesenchymal transformation during heart cushion development in the mouse. *The Journal of cell biology* 166(3):359-367.
66. Watanabe M, Oike M, Ohta Y, Nawata H, & Ito Y (2006) Sustained contraction and loss of NO production in TGFbeta1-treated endothelial cells. *British journal of pharmacology* 149(4):355-364.
67. Medici D*, et al.* (2010) Conversion of vascular endothelial cells into multipotent stem-like cells. *Nature medicine* 16(12):1400-1406.
68. Kretzschmar K & Watt FM (2012) Lineage tracing. *Cell* 148(1-2):33-45.
69. Horwitz EM (2010) Building bone from blood vessels. *Nature medicine* 16(12):1373-1374.
70. Hashimoto N*, et al.* (2010) Endothelial-mesenchymal transition in bleomycin-induced pulmonary fibrosis. *American journal of respiratory cell and molecular biology* 43(2):161-172.
71. Chen PY*, et al.* (2012) FGF regulates TGF-beta signaling and endothelial-to-mesenchymal transition via control of let-7 miRNA expression. *Cell reports* 2(6):1684-1696.
72. Cooley BC*, et al.* (2014) TGF-beta signaling mediates endothelial-to-mesenchymal transition (EndMT) during vein graft remodeling. *Science translational medicine* 6(227):227ra234.
73. Bernanke DH & Markwald RR (1982) Migratory behavior of cardiac cushion tissue cells in a collagen-lattice culture system. *Developmental biology* 91(2):235-245.
74. Eisenberg LM & Markwald RR (1995) Molecular regulation of atrioventricular valvuloseptal morphogenesis. *Circulation research* 77(1):1-6.
75. Armstrong EJ & Bischoff J (2004) Heart valve development: endothelial cell signaling and differentiation. *Circulation research* 95(5):459-470.
76. Goumans MJ, van Zonneveld AJ, & ten Dijke P (2008) Transforming growth factor beta-induced endothelial-to-mesenchymal transition: a switch to cardiac fibrosis? *Trends in cardiovascular medicine* 18(8):293-298.
77. Kruithof BP, Duim SN, Moerkamp AT, & Goumans MJ (2012) TGFbeta and BMP signaling in cardiac cushion formation: lessons from mice and chicken. *Differentiation; research in biological diversity* 84(1):89-102.

78. Massague J (1998) TGF-beta signal transduction. *Annual review of biochemistry* 67:753-791.
79. Massague J (2000) How cells read TGF-beta signals. *Nature reviews. Molecular cell biology* 1(3):169-178.
80. Azhar M*, et al.* (2009) Ligand-specific function of transforming growth factor beta in epithelial-mesenchymal transition in heart development. *Developmental dynamics : an official publication of the American Association of Anatomists* 238(2):431-442.
81. Camenisch TD*, et al.* (2002) Temporal and distinct TGFbeta ligand requirements during mouse and avian endocardial cushion morphogenesis. *Developmental biology* 248(1):170-181.
82. Mercado-Pimentel ME, Hubbard AD, & Runyan RB (2007) Endoglin and Alk5 regulate epithelial-mesenchymal transformation during cardiac valve formation. *Developmental biology* 304(1):420-432.
83. Moskowitz IP*, et al.* (2011) Transcription factor genes Smad4 and Gata4 cooperatively regulate cardiac valve development. [corrected]. *Proceedings of the National Academy of Sciences of the United States of America* 108(10):4006-4011.
84. Timmerman LA*, et al.* (2004) Notch promotes epithelial-mesenchymal transition during cardiac development and oncogenic transformation. *Genes & development* 18(1):99-115.
85. Niessen K*, et al.* (2008) Slug is a direct Notch target required for initiation of cardiac cushion cellularization. *The Journal of cell biology* 182(2):315-325.
86. Kokudo T*, et al.* (2008) Snail is required for TGFbeta-induced endothelial-mesenchymal transition of embryonic stem cell-derived endothelial cells. *Journal of cell science* 121(Pt 20):3317-3324.
87. Medici D, Potenta S, & Kalluri R (2011) Transforming growth factor-beta2 promotes Snail-mediated endothelial-mesenchymal transition through convergence of Smad-dependent and Smad-independent signalling. *The Biochemical journal* 437(3):515-520.
88. Feng XH & Derynck R (2005) Specificity and versatility in tgf-beta signaling through Smads. *Annual review of cell and developmental biology* 21:659-693.
89. Derynck R & Zhang YE (2003) Smad-dependent and Smad-independent pathways in TGF-beta family signalling. *Nature* 425(6958):577-584.

90. Wu CY, Tsai YP, Wu MZ, Teng SC, & Wu KJ (2012) Epigenetic reprogramming and post-transcriptional regulation during the epithelial-mesenchymal transition. *Trends in genetics : TIG* 28(9):454-463.
91. Kouzarides T (2007) Chromatin modifications and their function. *Cell* 128(4):693-705.
92. Narlikar GJ, Fan HY, & Kingston RE (2002) Cooperation between complexes that regulate chromatin structure and transcription. *Cell* 108(4):475-487.
93. Thiagalingam S*, et al.* (2003) Histone deacetylases: unique players in shaping the epigenetic histone code. *Annals of the New York Academy of Sciences* 983:84-100.
94. Longworth MS & Laimins LA (2006) Histone deacetylase 3 localizes to the plasma membrane and is a substrate of Src. *Oncogene* 25(32):4495-4500.
95. Waltregny D*, et al.* (2004) Expression of histone deacetylase 8, a class I histone deacetylase, is restricted to cells showing smooth muscle differentiation in normal human tissues. *American Journal of Pathology* 165(2):553-564.
96. Yang XJ & Seto E (2008) The Rpd3/Hda1 family of lysine deacetylases: from bacteria and yeast to mice and men. *Nature reviews. Molecular cell biology* 9(3):206-218.
97. Haberland M, Montgomery RL, & Olson EN (2009) The many roles of histone deacetylases in development and physiology: implications for disease and therapy. *Nature reviews. Genetics* 10(1):32-42.
98. Yang XJ & Gregoire S (2005) Class II histone deacetylases: from sequence to function, regulation, and clinical implication. *Molecular and cellular biology* 25(8):2873-2884.
99. Longo VD & Kennedy BK (2006) Sirtuins in aging and age-related disease. *Cell* 126(2):257-268.
100. Gao L, Cueto MA, Asselbergs F, & Atadja P (2002) Cloning and functional characterization of HDAC11, a novel member of the human histone deacetylase family. *The Journal of biological chemistry* 277(28):25748-25755.
101. Tovar-Castillo LE*, et al.* (2007) Under-expression of VHL and over-expression of HDAC-1, HIF-1alpha, LL-37, and IAP-2 in affected skin biopsies of patients with psoriasis. *International journal of dermatology* 46(3):239-246.
102. Lee DY*, et al.* (2012) Role of histone deacetylases in transcription factor regulation and cell cycle modulation in endothelial cells in response to disturbed flow. *Proceedings of the National Academy of Sciences of the United States of*

America 109(6):1967-1972.

103. Chang S*, et al.* (2006) Histone deacetylase 7 maintains vascular integrity by repressing matrix metalloproteinase 10. *Cell* 126(2):321-334.
104. Wang S*, et al.* (2008) Control of endothelial cell proliferation and migration by VEGF signaling to histone deacetylase 7. *Proceedings of the National Academy of Sciences of the United States of America* 105(22):7738-7743.
105. Margariti A*, et al.* (2010) Histone Deacetylase 7 Controls Endothelial Cell Growth Through Modulation of beta-Catenin. *Circulation research* 106(7):1202-U1275.
106. Mottet D*, et al.* (2007) Histone deacetylase 7 silencing alters endothelial cell migration, a key step in angiogenesis. *Circulation research* 101(12):1237-1246.
107. Urbich C*, et al.* (2009) HDAC5 is a repressor of angiogenesis and determines the angiogenic gene expression pattern of endothelial cells. *Blood* 113(22):5669-5679.
108. Ha CH*, et al.* (2008) Protein kinase D-dependent phosphorylation and nuclear export of histone deacetylase 5 mediates vascular endothelial growth factor-induced gene expression and angiogenesis. *The Journal of biological chemistry* 283(21):14590-14599.
109. Valenzuela-Fernandez A, Cabrero JR, Serrador JM, & Sanchez-Madrid F (2008) HDAC6: a key regulator of cytoskeleton, cell migration and cell-cell interactions. *Trends in cell biology* 18(6):291-297.
110. Li D*, et al.* (2011) Microtubule-associated deacetylase HDAC6 promotes angiogenesis by regulating cell migration in an EB1-dependent manner. *Protein & cell* 2(2):150-160.
111. Kaluza D*, et al.* (2011) Class IIb HDAC6 regulates endothelial cell migration and angiogenesis by deacetylation of cortactin. *The EMBO journal* 30(20):4142-4156.
112. Kaluza D*, et al.* (2013) Histone Deacetylase 9 Promotes Angiogenesis by Targeting the Antiangiogenic MicroRNA 17-92 Cluster in Endothelial Cells. *Arteriosclerosis, thrombosis, and vascular biology*.
113. Chavakis E & Dimmeler S (2002) Regulation of endothelial cell survival and apoptosis during angiogenesis. *Arteriosclerosis, thrombosis, and vascular biology* 22(6):887-893.
114. Zeng L, Zhang Y, Chien S, Liu X, & Shyy JY (2003) The role of p53 deacetylation in p21Waf1 regulation by laminar flow. *The Journal of biological chemistry* 278(27):24594-24599.

115. Aurora AB, *et al.* (2010) NF-kappaB balances vascular regression and angiogenesis via chromatin remodeling and NFAT displacement. *Blood* 116(3):475-484.
116. Zampetaki A, *et al.* (2010) Histone Deacetylase 3 Is Critical in Endothelial Survival and Atherosclerosis Development in Response to Disturbed Flow. *Circulation* 121(1):132-142.
117. Asahara T, *et al.* (1997) Isolation of putative progenitor endothelial cells for angiogenesis. *Science* 275(5302):964-967.
118. Timmermans F, *et al.* (2009) Endothelial progenitor cells: identity defined? *Journal of cellular and molecular medicine* 13(1):87-102.
119. Cerny J & Quesenberry PJ (2004) Chromatin remodeling and stem cell theory of relativity. *Journal of cellular physiology* 201(1):1-16.
120. Rossig L, *et al.* (2005) Histone deacetylase activity is essential for the expression of HoxA9 and for endothelial commitment of progenitor cells. *The Journal of experimental medicine* 201(11):1825-1835.
121. Spallotta F, *et al.* (2010) Nitric oxide determines mesodermic differentiation of mouse embryonic stem cells by activating class IIa histone deacetylases: potential therapeutic implications in a mouse model of hindlimb ischemia. *Stem cells* 28(3):431-442.
122. Zeng LF, *et al.* (2006) HDAC3 is crucial in shear- and VEGF-induced stem cell differentiation toward endothelial cells. *Journal of Cell Biology* 174(7):1059-1069.
123. Lu J, McKinsey TA, Zhang CL, & Olson EN (2000) Regulation of skeletal myogenesis by association of the MEF2 transcription factor with class II histone deacetylases. *Molecular cell* 6(2):233-244.
124. Cao D, *et al.* (2005) Modulation of smooth muscle gene expression by association of histone acetyltransferases and deacetylases with myocardin. *Molecular and cellular biology* 25(1):364-376.
125. Long X, Creemers EE, Wang DZ, Olson EN, & Miano JM (2007) Myocardin is a bifunctional switch for smooth versus skeletal muscle differentiation. *Proceedings of the National Academy of Sciences of the United States of America* 104(42):16570-16575.
126. Waltregny D, *et al.* (2005) Histone deacetylase HDAC8 associates with smooth muscle alpha-actin and is essential for smooth muscle cell contractility. *FASEB*

journal : official publication of the Federation of American Societies for Experimental Biology 19(8):966-968.

127. van der Veer E, *et al.* (2005) Pre-B-cell colony-enhancing factor regulates NAD+-dependent protein deacetylase activity and promotes vascular smooth muscle cell maturation. *Circulation research* 97(1):25-34.
128. Karen J, *et al.* (2011) Effects of the histone deacetylase inhibitor valproic acid on human pericytes in vitro. *PloS one* 6(9):e24954.
129. Geng H, *et al.* (2011) HDAC4 protein regulates HIF1alpha protein lysine acetylation and cancer cell response to hypoxia. *The Journal of biological chemistry* 286(44):38095-38102.
130. Isaacs JT, *et al.* (2012) Tasquinimod is an allosteric modulator of HDAC4 survival signaling within the compromised cancer microenvironment. *Cancer Res*.
131. Hu P, *et al.* (2003) Minimally invasive aortic banding in mice: effects of altered cardiomyocyte insulin signaling during pressure overload. *American journal of physiology. Heart and circulatory physiology* 285(3):H1261-1269.
132. Tsai TN, *et al.* (2012) Contribution of stem cells to neointimal formation of decellularized vessel grafts in a novel mouse model. *The American journal of pathology* 181(1):362-373.
133. Potenta S, Zeisberg E, & Kalluri R (2008) The role of endothelial-to-mesenchymal transition in cancer progression. *British journal of cancer* 99(9):1375-1379.
134. Mercado-Pimentel ME & Runyan RB (2007) Multiple transforming growth factor-beta isoforms and receptors function during epithelial-mesenchymal cell transformation in the embryonic heart. *Cells, tissues, organs* 185(1-3):146-156.
135. Meyer A, *et al.* (2012) Platelet TGF-beta1 contributions to plasma TGF-beta1, cardiac fibrosis, and systolic dysfunction in a mouse model of pressure overload. *Blood* 119(4):1064-1074.
136. Chandra M, *et al.* (2012) Nuclear translocation of type I transforming growth factor beta receptor confers a novel function in RNA processing. *Molecular and cellular biology* 32(12):2183-2195.
137. Annes JP, Munger JS, & Rifkin DB (2003) Making sense of latent TGFbeta activation. *Journal of cell science* 116(Pt 2):217-224.
138. Porter S, Clark IM, Kevorkian L, & Edwards DR (2005) The ADAMTS metalloproteinases. *The Biochemical journal* 386(Pt 1):15-27.

139. Bourd-Boittin K*, et al.* (2011) Protease profiling of liver fibrosis reveals the ADAM metallopeptidase with thrombospondin type 1 motif, 1 as a central activator of transforming growth factor beta. *Hepatology* 54(6):2173-2184.
140. Zeng L*, et al.* (2013) Histone deacetylase 3 unconventional splicing mediates endothelial-to-mesenchymal transition through transforming growth factor beta2. *The Journal of biological chemistry* 288(44):31853-31866.
141. Hinz B (2009) Tissue stiffness, latent TGF-beta1 activation, and mechanical signal transduction: implications for the pathogenesis and treatment of fibrosis. *Current rheumatology reports* 11(2):120-126.
142. Lynch KW (2007) Regulation of alternative splicing by signal transduction pathways. *Advances in experimental medicine and biology* 623:161-174.
143. Mu Y*, et al.* (2011) TRAF6 ubiquitinates TGFbeta type I receptor to promote its cleavage and nuclear translocation in cancer. *Nature communications* 2:330.
144. Kornberg LJ & Grant MB (2007) Adenoviruses increase endothelial cell proliferation, migration, and tube formation: partial reversal by the focal adhesion kinase inhibitor, FRNK. *Microvascular research* 73(3):157-162.
145. Lopez-Novoa JM & Nieto MA (2009) Inflammation and EMT: an alliance towards organ fibrosis and cancer progression. *EMBO molecular medicine* 1(6-7):303-314.
146. McKenzie JA & Ridley AJ (2007) Roles of Rho/ROCK and MLCK in TNF-alpha-induced changes in endothelial morphology and permeability. *Journal of cellular physiology* 213(1):221-228.
147. Ferreira AM, McNeil CJ, Stallaert KM, Rogers KA, & Sandig M (2005) Interleukin-1beta reduces transcellular monocyte diapedesis and compromises endothelial adherens junction integrity. *Microcirculation* 12(7):563-579.
148. Nakao A*, et al.* (1997) Identification of Smad2, a human Mad-related protein in the transforming growth factor beta signaling pathway. *The Journal of biological chemistry* 272(5):2896-2900.
149. Yamane K, Ihn H, Asano Y, Jinnin M, & Tamaki K (2003) Antagonistic effects of TNF-alpha on TGF-beta signaling through down-regulation of TGF-beta receptor type II in human dermal fibroblasts. *Journal of immunology* 171(7):3855-3862.
150. Verrecchia F, Pessah M, Atfi A, & Mauviel A (2000) Tumor necrosis factor-alpha inhibits transforming growth factor-beta /Smad signaling in human dermal fibroblasts via AP-1 activation. *The Journal of biological chemistry*

275(39):30226-30231.

151. Emmanuel C, Huynh M, Matthews J, Kelly E, & Zoellner H (2013) TNF-alpha and TGF-beta synergistically stimulate elongation of human endothelial cells without transdifferentiation to smooth muscle cell phenotype. *Cytokine* 61(1):38-40.

152. Potts JD, Dagle JM, Walder JA, Weeks DL, & Runyan RB (1991) Epithelial-mesenchymal transformation of embryonic cardiac endothelial cells is inhibited by a modified antisense oligodeoxynucleotide to transforming growth factor beta 3. *Proceedings of the National Academy of Sciences of the United States of America* 88(4):1516-1520.

153. Potts JD & Runyan RB (1989) Epithelial-mesenchymal cell transformation in the embryonic heart can be mediated, in part, by transforming growth factor beta. *Developmental biology* 134(2):392-401.

154. Ronaldson PT, Demarco KM, Sanchez-Covarrubias L, Solinsky CM, & Davis TP (2009) Transforming growth factor-beta signaling alters substrate permeability and tight junction protein expression at the blood-brain barrier during inflammatory pain. *Journal of cerebral blood flow and metabolism : official journal of the International Society of Cerebral Blood Flow and Metabolism* 29(6):1084-1098.

155. Walshe TE*, et al.* (2009) TGF-beta is required for vascular barrier function, endothelial survival and homeostasis of the adult microvasculature. *PloS one* 4(4):e5149.

156. Rieder F*, et al.* (2011) Inflammation-induced endothelial-to-mesenchymal transition: a novel mechanism of intestinal fibrosis. *The American journal of pathology* 179(5):2660-2673.

157. Maleszewska M*, et al.* (2013) IL-1beta and TGFbeta2 synergistically induce endothelial to mesenchymal transition in an NFkappaB-dependent manner. *Immunobiology* 218(4):443-454.

158. Wojciak-Stothard B, Entwistle A, Garg R, & Ridley AJ (1998) Regulation of TNF-alpha-induced reorganization of the actin cytoskeleton and cell-cell junctions by Rho, Rac, and Cdc42 in human endothelial cells. *Journal of cellular physiology* 176(1):150-165.

159. Helmke BP & Davies PF (2002) The cytoskeleton under external fluid mechanical forces: hemodynamic forces acting on the endothelium. *Ann Biomed Eng*

30(3):284-296.

160. Bentley K, Philippides A, & Ravasz Regan E (2014) Do endothelial cells dream of eclectic shape? *Developmental cell* 29(2):146-158.

161. Viemann D*, et al.* (2004) Transcriptional profiling of IKK2/NF-kappa B- and p38 MAP kinase-dependent gene expression in TNF-alpha-stimulated primary human endothelial cells. *Blood* 103(9):3365-3373.

162. Nobes CD*, et al.* (1998) A new member of the Rho family, Rnd1, promotes disassembly of actin filament structures and loss of cell adhesion. *The Journal of cell biology* 141(1):187-197.

163. Schmidt A & Hall MN (1998) Signaling to the actin cytoskeleton. *Annual review of cell and developmental biology* 14:305-338.

164. Jaffe AB & Hall A (2005) Rho GTPases: biochemistry and biology. *Annual review of cell and developmental biology* 21:247-269.

165. Uehata M*, et al.* (1997) Calcium sensitization of smooth muscle mediated by a Rho-associated protein kinase in hypertension. *Nature* 389(6654):990-994.

166. Worthylake RA & Burridge K (2003) RhoA and ROCK promote migration by limiting membrane protrusions. *The Journal of biological chemistry* 278(15):13578-13584.

167. Perkins ND (2007) Integrating cell-signalling pathways with NF-kappaB and IKK function. *Nature reviews. Molecular cell biology* 8(1):49-62.

168. Kobori M*, et al.* (2004) Wedelolactone suppresses LPS-induced caspase-11 expression by directly inhibiting the IKK complex. *Cell death and differentiation* 11(1):123-130.

169. Hotulainen P, Paunola E, Vartiainen MK, & Lappalainen P (2005) Actin-depolymerizing factor and cofilin-1 play overlapping roles in promoting rapid F-actin depolymerization in mammalian nonmuscle cells. *Molecular biology of the cell* 16(2):649-664.

170. Yang N*, et al.* (1998) Cofilin phosphorylation by LIM-kinase 1 and its role in Rac-mediated actin reorganization. *Nature* 393(6687):809-812.

171. Bernstein BW & Bamburg JR (2010) ADF/cofilin: a functional node in cell biology. *Trends in cell biology* 20(4):187-195.

172. Dejana E, Orsenigo F, & Lampugnani MG (2008) The role of adherens junctions and VE-cadherin in the control of vascular permeability. *Journal of cell science* 121(Pt 13):2115-2122.

173. Eilken HM & Adams RH (2010) Dynamics of endothelial cell behavior in sprouting angiogenesis. *Current opinion in cell biology* 22(5):617-625.
174. Arroyo AG & Iruela-Arispe ML (2010) Extracellular matrix, inflammation, and the angiogenic response. *Cardiovascular research* 86(2):226-235.
175. Sainson RC*, et al.* (2008) TNF primes endothelial cells for angiogenic sprouting by inducing a tip cell phenotype. *Blood* 111(10):4997-5007.
176. Hellstrom M*, et al.* (2007) Dll4 signalling through Notch1 regulates formation of tip cells during angiogenesis. *Nature* 445(7129):776-780.
177. Benedito R*, et al.* (2009) The notch ligands Dll4 and Jagged1 have opposing effects on angiogenesis. *Cell* 137(6):1124-1135.
178. Sobell HM (1985) Actinomycin and DNA transcription. *Proceedings of the National Academy of Sciences of the United States of America* 82(16):5328-5331.
179. Davis GE & Senger DR (2005) Endothelial extracellular matrix: biosynthesis, remodeling, and functions during vascular morphogenesis and neovessel stabilization. *Circulation research* 97(11):1093-1107.
180. Azzarelli R, Guillemot F, & Pacary E (2015) Function and regulation of Rnd proteins in cortical projection neuron migration. *Frontiers in neuroscience* 9:19.
181. Spiering D & Hodgson L (2011) Dynamics of the Rho-family small GTPases in actin regulation and motility. *Cell adhesion & migration* 5(2):170-180.
182. Mahler GJ, Farrar EJ, & Butcher JT (2013) Inflammatory cytokines promote mesenchymal transformation in embryonic and adult valve endothelial cells. *Arteriosclerosis, thrombosis, and vascular biology* 33(1):121-130.
183. Palenski TL, Sorenson CM, & Sheibani N (2013) Inflammatory cytokine-specific alterations in retinal endothelial cell function. *Microvascular research* 89:57-69.
184. Israel A (2010) The IKK complex, a central regulator of NF-kappaB activation. *Cold Spring Harbor perspectives in biology* 2(3):a000158.
185. Lee DF*, et al.* (2007) IKK beta suppression of TSC1 links inflammation and tumor angiogenesis via the mTOR pathway. *Cell* 130(3):440-455.
186. Tong L & Tergaonkar V (2014) Rho protein GTPases and their interactions with NFkappaB: crossroads of inflammation and matrix biology. *Bioscience reports* 34(3).
187. Manavski Y, Boon RA, & Dimmeler S (2014) Vascular niche controls organ regeneration. *Circulation research* 114(7):1077-1079.
188. Cao Z*, et al.* (2014) Angiocrine factors deployed by tumor vascular niche induce

B cell lymphoma invasiveness and chemoresistance. *Cancer cell* 25(3):350-365.

189. Ottone C*, et al.* (2014) Direct cell-cell contact with the vascular niche maintains quiescent neural stem cells. *Nature cell biology* 16(11):1045-1056.
190. Jones PL & Jones FS (2000) Tenascin-C in development and disease: gene regulation and cell function. *Matrix biology : journal of the International Society for Matrix Biology* 19(7):581-596.
191. Imanaka-Yoshida K, Yoshida T, & Miyagawa-Tomita S (2014) Tenascin-C in development and disease of blood vessels. *Anatomical record* 297(9):1747-1757.
192. Loomes KM*, et al.* (1999) The expression of Jagged1 in the developing mammalian heart correlates with cardiovascular disease in Alagille syndrome. *Human molecular genetics* 8(13):2443-2449.
193. Johnston DA, Dong B, & Hughes CC (2009) TNF induction of jagged-1 in endothelial cells is NFkappaB-dependent. *Gene* 435(1-2):36-44.
194. De Smet F, Segura I, De Bock K, Hohensinner PJ, & Carmeliet P (2009) Mechanisms of vessel branching: filopodia on endothelial tip cells lead the way. *Arteriosclerosis, thrombosis, and vascular biology* 29(5):639-649.
195. Welch-Reardon KM*, et al.* (2014) Angiogenic sprouting is regulated by endothelial cell expression of Slug. *Journal of cell science* 127(Pt 9):2017-2028.
196. Welch-Reardon KM, Wu N, & Hughes CC (2015) A role for partial endothelial-mesenchymal transitions in angiogenesis? *Arteriosclerosis, thrombosis, and vascular biology* 35(2):303-308.
197. Zeisberg M & Kalluri R (2013) Cellular Mechanisms of Tissue Fibrosis. 1. Common and organ-specific mechanisms associated with tissue fibrosis. *American journal of physiology. Cell physiology* 304(3):C216-225.
198. Weber KT, Sun Y, Bhattacharya SK, Ahokas RA, & Gerling IC (2013) Myofibroblast-mediated mechanisms of pathological remodelling of the heart. *Nature reviews. Cardiology* 10(1):15-26.
199. Goldsmith EC, Bradshaw AD, & Spinale FG (2013) Cellular Mechanisms of Tissue Fibrosis. 2. Contributory pathways leading to myocardial fibrosis: moving beyond collagen expression. *American journal of physiology. Cell physiology* 304(5):C393-402.
200. Seidman JG & Seidman C (2001) The genetic basis for cardiomyopathy: from mutation identification to mechanistic paradigms. *Cell* 104(4):557-567.
201. Hinz B*, et al.* (2007) The myofibroblast: one function, multiple origins. *The*

American journal of pathology 170(6):1807-1816.

202. Krenning G, Zeisberg EM, & Kalluri R (2010) The origin of fibroblasts and mechanism of cardiac fibrosis. *Journal of cellular physiology* 225(3):631-637.
203. Weber KT (1997) Monitoring tissue repair and fibrosis from a distance. *Circulation* 96(8):2488-2492.
204. Chu PY*, et al.* (2010) Bone marrow-derived cells contribute to fibrosis in the chronically failing heart. *The American journal of pathology* 176(4):1735-1742.
205. Dejana E (2004) Endothelial cell-cell junctions: happy together. *Nature reviews. Molecular cell biology* 5(4):261-270.
206. Kovacic JC, Mercader N, Torres M, Boehm M, & Fuster V (2012) Epithelial-to-mesenchymal and endothelial-to-mesenchymal transition: from cardiovascular development to disease. *Circulation* 125(14):1795-1808.
207. Medici D & Kalluri R (2012) Endothelial-mesenchymal transition and its contribution to the emergence of stem cell phenotype. *Seminars in cancer biology* 22(5-6):379-384.
208. Piera-Velazquez S, Li Z, & Jimenez SA (2011) Role of endothelial-mesenchymal transition (EndoMT) in the pathogenesis of fibrotic disorders. *The American journal of pathology* 179(3):1074-1080.
209. Maddaluno L*, et al.* (2013) EndMT contributes to the onset and progression of cerebral cavernous malformations. *Nature* 498(7455):492-496.
210. Ranchoux B*, et al.* (2015) Endothelial-to-mesenchymal transition in pulmonary hypertension. *Circulation* 131(11):1006-1018.
211. Good RB*, et al.* (2015) Endothelial to Mesenchymal Transition Contributes to Endothelial Dysfunction in Pulmonary Arterial Hypertension. *The American journal of pathology* 185(7):1850-1858.
212. Moore-Morris T*, et al.* (2014) Resident fibroblast lineages mediate pressure overload-induced cardiac fibrosis. *The Journal of clinical investigation* 124(7):2921-2934.
213. Kong P, Christia P, Saxena A, Su Y, & Frangogiannis NG (2013) Lack of specificity of fibroblast-specific protein 1 in cardiac remodeling and fibrosis. *American journal of physiology. Heart and circulatory physiology* 305(9):H1363-1372.
214. Osterreicher CH*, et al.* (2011) Fibroblast-specific protein 1 identifies an inflammatory subpopulation of macrophages in the liver. *Proceedings of the*

National Academy of Sciences of the United States of America 108(1):308-313.

215. Gustafsson E, Brakebusch C, Hietanen K, & Fassler R (2001) Tie-1-directed expression of Cre recombinase in endothelial cells of embryoid bodies and transgenic mice. *Journal of cell science* 114(Pt 4):671-676.
216. Ali SR*, et al.* (2014) Developmental heterogeneity of cardiac fibroblasts does not predict pathological proliferation and activation. *Circulation research* 115(7):625-635.
217. Duffield JS (2010) Epithelial to mesenchymal transition in injury of solid organs: fact or artifact? *Gastroenterology* 139(4):1081-1083, 1083 e1081-1085.
218. Kriz W, Kaissling B, & Le Hir M (2011) Epithelial-mesenchymal transition (EMT) in kidney fibrosis: fact or fantasy? *The Journal of clinical investigation* 121(2):468-474.
219. Wells RG (2010) The epithelial-to-mesenchymal transition in liver fibrosis: here today, gone tomorrow? *Hepatology* 51(3):737-740.
220. Tarin D, Thompson EW, & Newgreen DF (2005) The fallacy of epithelial mesenchymal transition in neoplasia. *Cancer Res* 65(14):5996-6000; discussion 6000-5991.
221. Bastid J (2012) EMT in carcinoma progression and dissemination: facts, unanswered questions, and clinical considerations. *Cancer metastasis reviews* 31(1-2):277-283.
222. Garber K (2008) Epithelial-to-mesenchymal transition is important to metastasis, but questions remain. *Journal of the National Cancer Institute* 100(4):232-233, 239.
223. Savagner P (2015) Epithelial-mesenchymal transitions: from cell plasticity to concept elasticity. *Current topics in developmental biology* 112:273-300.